Immunity-dependency of plant-microbiota dialogues

Inaugural-Dissertation

zur

Erlangung des Doktorgrades
Der Mathematicsch-Naturwissenschaftlichen Fakultät
Der Universität zu Köln

vorgelegt von

Frederickson D. Entila
aus Metro Manila, Philippinen

Köln
2023

Die vorliegende Arbeit wurde am Max-Planck-Institut für Pflanzenzüchtungsforschung in Köln in der Abteilung für Pflanzen-Mikroben Interaktionen (Direktor: Prof. Dr. Paul Schulze-Lefert), in der Arbeitsgruppe von Prof. Dr. Kenichi Tsuda angefertigt.



The dissertation has been accepted by the Faculty of Mathematics and Natural Sciences of the University of Cologne.
2023

Erstgutachter: Prof. Dr. Paul Shulze-Lefert
Zweigutachter: Prof. Dr. Stanislav Kopriva
Prüfungsvorstizende: Prof. Dr. Gunther Döhlemann
Protokollführer: Dr. Stéphane Hacquard

Tag der Prüfung: 10.08.2023

PUBLICATIONS:

Winkelmüller, T. M.*, **Entila, F**.*, Anver, S.*, Piasecka, A., Song, B., Dahms, E., Sakakibara, H., Gan, X., Kułak, K., Sawikowska, A., Krajewski, P., Tsiantis, M., Garrido-Oter, R., Fukushima, K., Schulze-Lefert, P., Laurent, S., Bednarek, P., & Tsuda, K. (2021). **Gene expression evolution in pattern-triggered immunity within Arabidopsis thaliana and across Brassicaceae species.** *The Plant cell*, *33*(6), 1863–1887. https://doi.org/10.1093/plcell/koab073

*equally contributing first co-authors

Nobori, T., Cao, Y., **Entila, F**., Dahms, E., Tsuda, Y., Garrido-Oter, R., & Tsuda, K. (2022). **Dissecting the cotranscriptome landscape of plants and their microbiota.** *EMBO reports*, *23*(12), e55380. https://doi.org/10.15252/embr.202255380

Entila, F., Han, X., Mine, A., Schulze-Lefert, P., & Tsuda, K. (2024). **Commensal lifestyle regulated by a negative feedback loop between Arabidopsis ROS and bacterial T2SS**. *Nature Communications**15*(1), 456. https://doi.org/10.1038/s41467-024-44724-2

Entila, F. and Tsuda K. **Taming of the microbial beasts: Plant immunity tethers potentially pathogenic microbiota members**. *Under preparation for Bioessay.*

ABSTRACT

Despite the beneficial effects of plant microbiota, these assemblages also comprise potentially detrimental microbes. How the plant immunity regulates its microbiota to promote plant health under these conditions remains poorly navigated. We found that commensal bacteria isolated from healthy *Arabidopsis thaliana* plants can induce varying immune responses with which is tailored in a strain-specific manner and does not coincide with their phylogeny. We have revealed that the immune output RBOHD-generated ROS selectively restricted colonization of potentially pathogenic *Xanthomonas* L148. Through random genome-wide mutagenesis, we found that the *Xanthomonas* L148 *gspE*, encoding a type II secretion system (T2SS) structural component, is essential for *Xanthomonas* L148 to elicit diseases on *rbohD* mutant plants. *In planta* bacterial transcriptomics revealed that RBOHD suppresses most carbohydrate-active enzymes (CAZymes) and T2SS gene expression including *gspE*. *Xanthomonas* L148 colonization protected plants against a foliar pathogen and its protective function is independent of its pathogenic potential. Thus, plant-derived ROS turns a potentially detrimental leaf commensal into a beneficial bacterium for the host plant by suppressing T2SS.

PREAMBLE

Part of this dissertation is from manuscripts published, submitted, or in preparation as listed above in the “PUBLICATIONS” section. Figures that have been adopted from these papers were noted in the figure legends. Some of the paragraphs were lifted from the papers mentioned above with some modifications. Most of the experiments and analyses ascribed in this thesis were conducted by myself. Those that are conducted by other people were indicated in the “AUTHOR CONTRIBUTIONS” section.

1. TABLE OF CONTENTS

2. SIGNIFICANCE

With the climate change, environmental deterioration, and population explosion, high risk for food security is imminent. The increasing pressures to mitigate food shortage had resulted to rampant and unregulated use of fertilizer and pesticides that had paradoxically aggravated the health of the people and the planet (Erisman et al, 2008; Stehle et al, 2013; Beketov et al, 2013). Likewise, the unprecedented poleward epidemic shift of pathogens and pests due to global warming further threatens food security (Bebber et al, 2013). These global issues substantiate the urgent need to enhance adaptation of agriculture crops in an ecological manner (Howden et al. 2007; Godfray et al. 2010; Foley et al. 2011). Recent studies had revealed the existence of a defined microbial communities in plants that could improve the holistic performance of crops through protective conditioning against pathogens, increased nutritional sustenance, and resilience to abiotic stresses (Ritpitakphong et al, 2016; Vogel et al, 2016; Castrillo et al, 2017; Duran et al, 2018). The direct mechanisms by which the plant host recruits and accommodates the structured microbial assemblage is still unclear. Dissecting plant-microbe interactions is quite complex and is greatly influenced by the local environment.

3. INTRODUCTION

3.1. Plant innate immunity: the supervisor and sculptor of microbiota

Plants are perpetually exposed to a plethora of microbes and have to constantly survey the environment for external threats in order to thrive and survive which is the fundamental role of immunity (Chrisholm et al, 2006). The tenet of immunity function among organisms, in this case plants, is that the organism has an evolutionary programmed capability to recognize self from non-self, and the detection of non-self signatures alarms its system to mount the protective immune responses against the potential intruder (Nurnberger et al, 2004). Plants have evolved mechanisms of recognizing well conserved microbe associated molecular patterns (MAMPs) as non-self signals through cell surface displayed pattern recognition receptors (PRRs) to constitute the pattern-triggered immunity (PTI, Jones and Dangl, 2006). The central involvement of PTI in the interaction of plant hosts with its pathogens or mutualists has been extensively described and comprehensively scrutinized (Dodds and Rathjen, 2010; Zipfel and Oldroyd, 2017; Antolin-Llovera et al, 2014; Gourion et al, 2014). In stark contrast, less is known regarding the fundamental role of PTI as the interface to its resident microbes despite its obviously conceivable participation in shaping and managing the plant microbiota.

3.1.1. Pattern-triggered immunity: surveilling among the mayhem of microbial motifs

The PTI pathway as the first layer of active defense, is initiated upon the perception of specific MAMPs by its cognate cell surface localized PRRs. For instance, the MAMP flg22, well conserved N-terminus peptide of bacterial flagellin, is perceived by the PRR leucine-rich-repeat receptor kinase (LRR-RK) FLAGELLIN SENSING 2 (FLS2) in *Arabidopsis thaliana* (Zipfel et al, 2004). The MAMP elf18, an abundant and well conserved acetylated N-terminus region of bacterial Elongation Factor Thermo-unstable (EF-Tu) is recognized by the PRR LRR-RK EF-TU RECEPTOR (EFR) which is restricted to Brassicaceae lineage (Zipfel et al, 2006). BRI1-ASSOCIATED RECEPTOR KINASE 1 (BAK1) and its close homolog BAK1-LIKE 1 (BKK1) function as co-receptors for LRR-RLK-type PRRs such as FLS2 and EFR (Roux et al, 2011). The LysM-RLK CHITIN ELICITOR RECEPTOR KINASE 1 (CERK1) is an essential co-receptor for the MAMPs fungal chitin and bacterial peptidoglycans (Miya et al, 2007). These co-receptors are prevalent and highly conserved in land plants and are crucial for PTI (Ngou et al, 2022).

The formation of MAMP-PRR complex and the subsequent oligomerization with the respective co-receptors result in a cascade of signals and a series of physiological events that comprise the PTI response which is historically characterized with a number of physiological hallmarks (Ngou et al, 2022; Boller et al, 2009) which include calcium ion influx (Blume et al, 2000), generation of reactive oxygen species (ROS, Doke et al, 1985), MITOGEN-ACTIVATED PROTEIN (MAP) kinase activation (Nühse et al, 2000; 2007), ethylene production (Spanu et al, 1994), transcriptional reprogramming (Zipfel et al, 2004; 2006; Libault et al, 2007), stomatal closure (Melotto et al, 2006), production of defense phytohormones and antimicrobials (Tierens et al, 2001; Tateda et al, 2014; Clay et al, 2009; Yi et al, 2014; Millet et al, 2010), mesophyll dehydration (Dalal et al, 2021), and callose deposition (Gomez-Gomez et al, 1999), which culminates to the restriction of microbial growth in host tissues (Zipfel et al 2004; 2006). The energetically costly appropriation to the defense program upon its activation results in the restriction of plant growth and is often interpreted as the defense-growth trade-offs (Gomez-Gomez et al, 2000).

Plants intimately associate with their microbiota which display a catalogue of MAMPs that are also exhibited by pathogens (Teixiera et al, 2019; Garrido-Oter et al, 2019). For example, genomic inspection of bacterial strains isolated from healthy *A. thaliana* leaves and roots revealed that the microbiota members harbor potentially immunogenic MAMP epitopes for flg22, elf18, nlp20, and csp22 (Teixiera et al, 2019). *In silico* analysis via sequence conservation and predictive structural modeling of potential flg22 variants within the Proteobacteria indicates a continuum of immunogenicity among the clades

suggestive of MAMP diversification. Experimentally validated, the flg22 epitopes derived from β- and γ-Proteobacteria, which contain many phytopathogenic strains, evokes very strong ROS outburst, while the flg22 epitopes from the α-, ε-, and δ-Proteobacteria elicited weak to no ROS outburst in *A. thaliana* (Cheng et al, 2021). Indeed, the *A. thaliana* microbiota members encode substantially diverse flg22 epitopes which mostly pervades PTI detection by the host and variably activates and prompts different PTI branches (Colaianni et al, 2021). Moreso, the evolution of the flg22 epitopes was strongly driven by the interaction of the microbiota members with FLS2 receptor of the plant host, wherein strains adapt by compromising bacterial motility or stalling the signaling transduction module of the host receptor, both, to purposely elude immune detection (Parys et al, 2021). Convergently, the FliC bacterial flagellins derived from most human gut microbiota strains bind to the corresponding human TOLL-LIKE RECEPTOR5 (TLR5) but weakly stimulates the downstream immune signaling which allows host tolerance to these commensals while maintaining responsiveness to potent immunostimulatory flagellins from pathogenic strains (Clasen et al, 2023). Moreso, 277 human gut microbiota derived bacterial strains evokes an array of cytokine signatures and preferentially activate different TLR innate immune branches (Spindler et al, 2022). These evidences deduce that microbes rely on a catalogue of MAMPs to consequentially activate different combinations of host immune receptors simultaneously and evoke synergized and complex immune responses. In humans, microbes can be detected via bacterial-derived RNA through host immune TOLL-LIKE RECEPTOR 7 (TLR7) and elicit host-protective interferon response (Mancuso et al, 2009). However, *E. coli* evade host detection by modifying its RNA through 2'-O-methylation, effective to inactivate human but not murine innate immunity (Rimbach et al, 2015). More so, the bacterial RNA derived from the pathogen *P. syringae* DC3000 can be perceived as MAMPs and consequentially activate PTI (Lee et al, 2016). Bacterial cGAS/DncV-like nucleotidyltransferases (CD-NTases) produces diverse types of cyclic (di- or tri-) nucleotides for the modulation of bacterial metabolism and virulence which can be perceived as MAMPs by the mammalian RECON and STING receptors (Whiteley et al, 2019). It has been recently shown that plants can also produce similar small molecules (ADPr-ATP or di-ADPr, 2'-cADPRs, 2', 3'-cGMP and 2', 3'-cAMP) upon activation of the effector-triggered immunity through intracellular TOLL/INTERLEUKIN-1 RECEPTOR nucleotide-binding, leucine-rich immune receptors (TIR-NLRs) to enhance defense stance (Yu et al, 2022; Wan et al, 2019; Huang et al, 2022; Jia et al, 2022). Nevertheless, the role of microbiota-derived nucleotide metabolites as immune-elicitor for plant innate immunity remains *terra incognito* in the plant microbiota field.

Certain members of the microbiota can be pathogenic only in conducive conditions (Jochum et al, 2020). Therefore, to allow co-existence with seemingly innocuous commensal communities, plants must control the microbiota colonization and tailor

immune responses to these diverse microorganisms (Parys et al, 2021; Colaianni et al, 2021). Though the molecular mechanism of discrimination among microbe is still a scantily navigated territory, recent advances in the field partly illuminate the processes that underly discrimination of the plant host against harmful pathogens whilst favoring accommodation of innocuous microbial partners. The requirement of the concurrent activation of both the MAMP- and damage associated molecular pattern- (DAMP) triggered immunity pathways in the roots spare the native microbiota from the hostile plant host defenses (Zhou et al, 2020). Also, the spatial distribution of MAMP receptors and the topological and biochemical features of the different root cell types are physiologically relevant to the physical containment of immune responsiveness with the interacting microbes (Zhou et al, 2020; Emonet et al 2021). Furthermore, plant innate immunity differentiates the pathogenic *Pseudomonas fluorescens* N2C3 from the beneficial *P. fluorescens* WCS365 independent of their almost indistinguishable MAMPs but through the pathogen-produced toxins or with the aftermath damages by the toxins (Thoms et al, 2023).

The MAMP repertoire of the microbes as communication signal and the plant host cognate receptor proteins, at certain circumstances dictates the fate of interaction wherein either the defense or symbiosis programs will be switched on. The co-perception of fungal chitooligosaccharides (COs, such as chitin) and lipochitooligosaccharides (LCOs, particularly nodulation [Nod] factors) by the receptors *Mt*CERK1 and *Mt*LYR4 enhances symbiosis signaling while dampening defense signaling allowing proper mycorrhizal establishment on *Medicago truncatula* roots (Feng et al; 2019). Analogously, the *Lotus japonicus* receptors of chitin and Nod factors, *Lj*CERK6 and *Lj*NFR1 respectively, transduces different programs: immunity for *Lj*CERK6 and symbiosis for *Lj*NFR1. These receptors share strikingly similar structures albeit, the LysM ectodomains define specificity to the ligands which is exclusively crucial and strictly directs the signal towards microbial extermination or accommodation (Boszoki et al, 2020).

3.1.2. Pattern-triggered immunity: commandeering the microbial occupants.

In principle, the assembly of microbiota can be explained by either stochastic or deterministic processes (Stegen et al, 2012). The growth of plants may provide unoccupied niches (eg. root or leaf exudations) which can hypothetically be exploited by any microbe with the genetic malleability to utilize these substrates, and so eventually climaxes to a manufactured microbial community via random colonization (Sieber et al, 2019; Theis et al, 2016; Chase et al, 2011). Alternatively, this process can be driven by selection pressures imposed by the plant host resulting to an active recruitment of specific set of microbes for which through time co-evolved to confirm the intimate interaction (Vellend et al, 2010; Theis et al, 2016). However, the consistently defined taxonomic

patterns of plant microbiota supports the idea that the processes responsible for the assembly of microbiota is largely deterministic (Lundberg et al, 2012; Bulgarelli et al, 2012; Thiergart et al, 2020; Hamonts et al; 2018; Edwards et al, 2015; Fitzpatrick et al, 2018).

The composition, diversity, and function of the rhizosphere and phyllosphere microbiota is to some extent determined by the host genotype and developmental stage, and is also largely influenced by environmental factors which include climate, geography, soil physico-chemistry and history (Lundberg et al, 2012; Thiergart et al, 2020; Coleman-Derr et al, 2016; Wagner et al, 2016; Dombrowski et al, 2017; Edwards et al, 2015; Mendes et al, 2011). Genome wide association studies (GWAS) using 196 natural accessions of *A. thaliana* grown in natural fields revealed plausible genetic determinants of phyllosphere and rhizosphere microbiota which are mostly involved in immunity and cell wall properties (Horton et al, 2014; Bergelson et al, 2019). These evidences put forward the notion that the holistic attribute of the host including innate immunity, is the preponderant factor in sculpting its microbiota.

Microbiota profiling of the rhizosphere compartment of PTI receptor mutants showed that root microbial diversity is conditioned by FLS2 and weakly by EFR but not with CERK1 (Fonseca et al, 2022). More so, the defense hormone salicylic acid modulates the root endosphere microbiota composition since a consistent shift in relative abundances in specific bacterial taxa is observed with SA-repleted hyperimmune mutants (*cpr5* and *cpr6*) and SA-depleted hypoimmune mutants (*sid2* and *pad4*) using natural soil and synthetic microbial communities (Lebeis et al, 2015). The ethylene defense signaling mutant *ein2* had an altered phyllosphere microbiota associated with increased proliferation of *Variovorax* strains (Bodenhausen et al, 2014).

Quite recently, a quadruple mutant *mfec* defective of PTI (co)receptors: FLS2, EFR, and CERK1; and *At*MIN7 vesicle trafficking pathway in *A. thaliana* recruited a dysbiotic phyllosphere microbiota of poor microbial diversity (Firmicutes depleted and Proteobacteria dominated) and the abnormal microbial assemblage is causative of the disease-like symptoms (Chen et al, 2020). Similarly, a dysbiotic microbiota and disease symptoms were also observed in plant with mutation in CONSTITUTIVELY ACTIVATED CELL DEATH1 (CAD1), a membrane attack complex/perforin (MACPF) domain protein which suggest a genetic framework where PTI and *At*MIN7 vesicle trafficking converge through CAD1 to control microbiota homeostasis in the phyllosphere (Chen et al, 2020). The receptor FERONIA (FER), is required for the nanoscale organization of the FLS2-BAK1 complex assembly to transduce immunity signals (Gronnier et al, 2022). FER is essential in restricting the *Pseudomonas* strains in the rhizosphere through induction and enhancement of basal ROS levels (Song et al, 2021). Moreso, the engagement of the endogenous ligand RAPID ALKANIZATION FACTOR 23 (RALF23) peptides with its cognate receptor FER allows flourishment of the beneficial *Pseudomonas fluorescens*

strain indicating its essential role in the maintenance of root microbiota and recruitment of beneficial microbes (Song et al, 2021). Similarly, the EFR-mediated ROS production is essential for the activation of auxin secretion by the beneficial microbe *Bacillus velezensis* FZB42 to neutralize the damaging effects of ROS to the bacterium consequentially allowing proper root occupation (Tzipilevich et al, 2021). In plant-pathogen interactions, the receptor-mediated activation of RESPIRATORY BURST OXIDASE HOMOLOG D (RBOHD) determines the early PTI response ROS outburst (Kadota et al, 2014). Alterations in RBOHD results in substantial aberrations to the phyllosphere microbiota, and enrichment of potentially pathogenic members in the microbiota, notably *Xanthomonas* L131, which further leads to the onset of plant disease (Pfeilmeier et al, 2021). These evidences imply the overarching influence of PTI, especially the ROS pathways, in the recruitment and maintenance of a balanced plant microbiota.

3.1.3. Microbiota and the auxiliary tiers of defense: from fortified walls to chemical armaments.

There is a myriad of host attributes that can selectively screen microbes and imminently influence the microbiota assembly. These plant host factors may include but not limited to physical barriers (eg. cell walls and cuticle), specialized secondary metabolites (eg. coumarins and glucosinolates), and anatomical structures (eg. stomata and trichomes).

The plant cell wall serves as the primary defense that physically excludes microbes. Though cell walls could serve as a potential source of nutrition by many phytopathogens via action of degradative enzymes, the subsequent release of DAMPs activates the DTI, an additional layer of active defense thus implicative of the integrated role of physical barriers with the plant innate immunity in response to pathogen attack (Bacete et al, 2018; De Lorenzo et al, 2018). Comprehensive characterization of disease resistance phenotypes of 34 *A. thaliana* cell wall mutants with varying cell wall chemistries against 3 pathogens with parasitic lifestyles ranging from necrotrophism to biotrophism revealed an enhanced resistance due to auto-activated DTI, however at the expense of plant growth and fitness (Molina et al, 2021). Metagenomic rhizosphere investigation of field cultivated wheat, cucumber, and maize showed substantial enrichment of cell wall degrading enzymes on the rhizosphere signifying that microbial activity at the root vicinity involves degradation of host barriers for source of nutrition and/or endophytic access (Ofek-Lalzar et al, 2014; Li et al, 2014).

Mutations in cuticle formation, in particular LONG-CHAIN ACYL-COENZYME A SYNTHASE 2 (LACS2) enzyme for cutin biosynthesis; and PERMEABLE CUTICLE 1 (PEC1) the transporter of cutin precursors, results to higher bacterial load on the phyllosphere as compared to wild-type Col-0 plants (Bodenhausen et al, 2014). Likewise,

the *A. thaliana eceriferum* mutant plants with abnormal cuticle having aberrations on the genes: putative very-long-chain aldehyde decarbonylase (*CER1*), β-keto-acyl-CoA-Synthase (*CER6*), and putative E3 ubiquitin ligase (*CER9*), harbored distinct phyllosphere microbial communities in comparison to the wild-type Ler plants, and were facilely inhabited by numerous bacteria due to breached cuticle, immediate leaching of nutrients, or accumulation of cutin substrates with nutritional value (Reisberg et al, 2013). The regulatory network that modulates the establishment of endodermal root diffusion barriers also affects the root microbiota assembly. Reciprocally, the rhizosphere microbiota influences the root endodermal barriers via repression of the phytohormone abscisic acid (ABA) signaling pathway enabling the plant host to cope situations of scarce mineral nutrients (Salas-Gonzalez et al, 2021). Repression of lignin biosynthesis in *Populus* trees resulted to accumulation of lignin precursor ferulic acid and significantly impacted the stem and root endosphere microbiota whereby *P. putida* capable of exploiting the lignin precursors predominate (Beckers et al, 2016). These evidences support the fundamental function of cell walls as the main gate of filtering microbes, working as a physical barricade, potential carbon source for sustenance, or potentiator of DTI.

Plant roots exude a wide-range of compounds of varying properties and activities into the surrounding soil with which mediates its interaction with the microbes, and this intentional modulation of root environment is referred as the “rhizosphere effect” (Bais et al, 2006; Jones et al, 2009; Bulgarelli et al, 2013). The MYB72/BGLU42-dependent release of the coumarin compound scopoletin selectively impacts the rhizosphere microbiota (Stringlis et al, 2018). Moreso, under iron deficient soil conditions, coumarin exudation allows the recruitment of a facilitative rhizosphere microbiota consequentially alleviating iron stress and conferring growth promotion dependent on the plant iron transport and the secretion of the coumarin fraxetin (Harbort et al, 2020). The *cyp79b2/b3* mutants impaired of tryptophan-derived specialized metabolites, which includes glucosinolates, were extremely susceptible to root fungal microbiota members, however the deleterious effects of fungi are countered by the bacterial members of the microbiota, indicating the importance of tryptophan metabolism and bacterial commensals in controlling fungal load to promote plant growth and survival (Wolinska et al, 2021). Under nitrogen deprivation, maize roots secrete flavones which enriches the root rhizosphere with Oxalobacteriaceae strains to improve plant performance (Yu et al, 2021). The exudation of flavonoids in roots globally affect the *A. thaliana* rhizosphere microbiota, and the flavonoid naringenin preferentially attracts *Aeromonas* strains which can potentially enhance plant tolerance to drought (He et al, 2022). On the other hand, the specialized metabolite triterpenes: thalianin, thalianyl fatty acid esters, and arabidin are essential for the direct recruitment and attunement of *Arabidopsis*-specific root microbiota (Huang et al, 2019).

Pathogens have been classically demonstrated to invade the plant internal tissues through natural openings such as the stomata and hydathodes (Turner et al, 1969; Mino

et al, 1987). The pathogen *P. syringae* DC3000 secretes coronatine, a molecular mimic of the phytohormone JA-Ile to forcibly re-open the stomata and enables intrusion to the apoplastic space (Melotto et al, 2006). Also, the pathogen *P. syringae* B728a uses syringolin A instead to inhibit proteolysis of the SA signaling protein NPR1 which leads to re-opening of the stomata (Schellenberg et al, 2010). Phyllosphere profiling of 24 plant species grown in gardens revealed distinct differences in the leaf microbial composition and structure between the abaxial and adaxial sides of the leaf, wherein the abaxial side housing denser stomata harbored less variable phyllosphere microbiota suggestive of a stronger host selection effect (Smets et al, 2022). This finding indicates that the stomata may act to modulate phyllosphere microbiota by affecting the micro-environment (eg. leaching nutrients, moisture) or as the main gateway to the leaf internal compartment. However, synthetic community experiment using *A. thaliana* plants with mutation in OPEN STOMATA 1 (OST1) a SNF1-related protein kinase recruited similar phyllosphere microbiota composition with the wild-type Col-0 plants (Bodenhausen et al, 2014). The pathogen *Xanthomonas campestris* pathovar *campestris* (*Xcc*) targets the hydathodes as the entry point to vascular tissue of plants (Hugouvieux et al, 1998). It was recently shown that hydathode immunity confines bacterial proliferation through the BAK1 and EDS1-PAD4-ADR1 modules preventing further spread to the vasculature (Paauw et al, 2023). Microscopic examinations of the arid-adapted resurrection plant *Myrothamnus flabellifolia* showed colonization of resident fungal species *Aspergillus* and *Penicillium* into the hydathodes, more likely allowing the fungi to feed on moisture or leaf exudates so as to persist in highly desiccated environments (Moore et al, 2011).

Trichomes are specialized epidermal appendages on the leaf characterized with the production and storage of secondary metabolites (Huchelmann et al, 2017). Recent finding revealed that trichomes operate as mechano-sensors, wherein plants perceive rain as a forecast for impending disease outbreak and correspondingly primes immunity to detect and protect against future infection (Matsumura et al, 2020). Trichomes provide a micro-niche on the leaf surface of tomato *Solanum lycopersicum* that potentially drives the general make-up or spatial distribution of the phyllosphere microbiota (Kusstatscher et al, 2020). In contrast, trichomes does not seem to shape the *A. thaliana* phyllosphere microbiota (Reisberg et al, 2012).

Altogether, it is not clear if the resident phyllosphere microbiota utilizes the same mechanisms or uses the stomata and/or hydathodes to gain entry to the endophytic leaf compartments. More so, evidence is lacking on the potential mechanisms of trichome-mediated modulation of the phyllosphere microbiota. Since the leaf is a highly heterogenous, hostile, and oligotrophic habitat (Schlechter et al, 2019), it is feasible that these leaf features may provide a more favorable niche as entry points to the nutrient-rich apoplast or access points for potential source of subsistence and in turn influence the structure and define spatial distribution of phyllosphere microbial residents. It is more

likely that these focal sites serve as colonization ground since leaf microbes tend to form aggregates (Remus-Emsermann et al, 2014).

3.2. Microbial maneuvers: eluding the plant perception and reaction

General suppression of the plant host defenses is a pre-requisite for efficient colonization of pathogens and symbionts (Dodds and Rathjen, 2010; Jacobs et al, 2011; Gourion et al, 2014). Moreso, a handful of pathogens avoid activation of the immune responses by preventing detection of their MAMPs (Wang et al, 2022), while symbionts have developed a specific set of signaling molecules (Nod factors) to inform the plant host and correspondingly dampen immunity (Antolin-Llovera et al, 2014). Microbes have evolved a multitude of mechanisms to dodge host detection or stifle host defenses. These mechanisms can be broadly categorized as PTI evasion or PTI suppression.

3.2.1. PTI evasion: MAMP diversification, decoration, and degradation

Microbes can simply elude host recognition by mutating MAMPs, for instance the bacterial pathogen *Ralstonia solanacearum* had evolve polymorphisms on its flg22 peptide sequence rendering it undetectable by various plants belonging to Brassicaceae (*A. thaliana*) and Solanaceae (tomato cultivar Moneymaker *S. lycopersicum*; tobacco *Nicotiana tabacum* and *N. benthamiana*; eggplant *Zebrina*; and pepper cultivar California Wonder *Capsicum anuum*) lineage but is recognized by soybean *Glycine max* (Wei et al, 2018; Wei et al, 2020). Similarly, phytopathogens encode varying elf18 epitopes with different ROS elicitation signatures in *A. thaliana* leaf (Lacombe et al, 2010). Genomes of the bacterial microbiota from *A. thaliana* revealed tremendous diversification of MAMPs, in particular the flg22 epitopes, with which have varying immune-elicitation properties (Teixiera et al, 2019, Cheng et al, 2021). The flg22 sequence modifications resulting to faint or no immune responses are either associated with compromised motility (indicative of antagonistic pleiotropy) or allosteric antagonism of FLS2-BAK1 oligomerization (Parys et al, 2021). Moreso, diversified flg22 epitope evokes different immune outputs (Colaianni et al, 2021). Pervasion of PTI detection of flg22 epitopes is also observed in the bacterial members of the human gut microbiota (Clasen et al, 2023). Another way of preventing host recognition is deliberately suppressing the production of MAMPs. The bacterial pathogen *P. syringae* promotes infection by AlgU-dependent suppression of flagellin fliC thus reducing PTI activation (Bao et al, 2020). In another study, the elevated cyclic-di-GMP in the pathogen *P. syringae* DC3000, potentially pathogenic *P. aeruginosa* PAO1, and commensal *P. protegens* Pf-5 suppresses flagellin synthesis to evade activation of FLS2-mediated immunity in *A. thaliana* and *N. benthamiana* (Pfeilmeier et al, 2016). The fungal pathogen *Collelotrichum graminicola* down-regulates its cell wall-derived MAMP

synthesis of β-glucans by KRE5 and KRE6 resulting to attenuated immune response of maize *Zea mays* cultivar Mikado (Oliveira-Garcia t al, 2016).

Some pathogens preclude detection by decorating their MAMPs or inhibit host-mediated pre-processing of MAMPs. The pathogen *P. syringae* DC3000 Δ*hQ* inhibits the action of *N. benthamiana* BGAL1 deglycosylation of the bacterial flagellin to liberate MAMPs disabling host detection (Buscaill et al, 2019). In contrast, *P. syringae* B728a escapes recognition by altering its flagellin glycosylation profile (Buscaill et al, 2019). The fungal tomato pathogens *Fusarium oxysporum*, *V. dahliae*, and *Botrytis cinerea* cleave host chitin-binding domain (CDB) chitinases of the host thus preventing release of fungal chitin subjugating host immune detection (Jashni et al, 2015). More so, the fungal pathogen *V. dahliae* also secretes PDA1 to deacetylates its own chitin into inactive chitosan precluding the PTI of cotton *Gossypium hirsutum* cultivar Xinluzao No.16 (Gao et al, 2019). The mutualist *Rhizobium leguminosarum* 3841 structurally modifies it lipopolysaccharide (LPS) under low oxygen conditions or in nodules displaying different immunochemical properties which might be important for evading host defenses (Kannenberg et al, 2001). Bacterial strains from the human gut microbiota display LPS of varying structural moieties with different immunomodulatory attributes (Vatanen et al, 2016).

Some pathogens can degrade or neutralize their own MAMPs to escape host recognition. The fungal pathogen *Cladosporium fulvum* releases the effector ECP6 that competitively binds to the released fungal chitin cloaking its recognition (Jonge et al, 2010). Contrastingly, the pathogen *P. syringae* DC3000 degrades its own flagellin monomers through its AprA alkaline protease (Pel et al, 2014). Moreso, timely dissociation with plant tissues through lifestyle transition from biofilm assemblage to a free-living state could repress the sustained PTI activation. The beneficial bacterium *P. fluorescens* WCS365 requires a putative diguanylate cyclase/phosphodiesterase MorA and putrescine aminotransferase SpuC, to repress biofilm formation and promotes detachment from the plant roots (Liu et al, 2018).

3.2.2. PTI suppression: secretion of immune-modulatory factors

Pathogens and mutualist have been historically documented to modulate the plant immunity in order to colonize host tissues, usually through the type-3-secretion system (T3SS) for most bacterial phytopathogens. A classic example is the pathogen *P. syringae* DC3000 which releases a concoction of type 3 effectors (T3Es) that specifically target PRRs. For example, the bacterial effector E3 ubiquitin ligase AvrPtoB cleaves the kinase cytoplasmic domains of receptors FLS2 and EFR, and to some extent, the co-receptors BAK1 and BRI1 (Göhre et al, 2008). The bacterial effector HopU1, a mono-ADP-

ribosyltransferase, binds to the FLS2 and EFR transcripts disrupting the interaction with GRP7 to form translational machinery leading to reduced FLS2 and EFR protein accumulation (Nicaise et al, 2013). The bacterial effector HopA1, a tyrosine phosphatase reduces the activated phosphorylation of EFR attenuating the subsequent immune responses (Macho et al, 2014). The bacterial mutualist *Sinorhizobium sp.* NGR234 releases the T3E NODULATION OUTER PROTEIN L (NopL) thwarting defense responses in the host by interfering with the MAP kinase cascades in beans *Phaseolus vulgaris* cultivar Tendergreen (Bartsev et al, 2004; Ge et al, 2014).

There is a growing body of evidences that the plant microbiota or its members can intercept and temper plant immunity. Around 41% of *A. thaliana* rhizosphere bacterial strains can suppress the root growth inhibition triggered by the MAMP flg22 or the endogenous DAMP *At*PEP1 indicating that the rhizosphere microbiota can modulate host immune status (Ma et al, 2021; Garrido-Oter et al, 2018). The root commensal *Dyella japonica* MF79 requires the type 2 secretion system (T2SS) components GspD and GspE to release immunomodulatory factors for effective root colonization and eventually opens the gates for other root commensals in *A. thaliana* (Teixeira et al, 2021). Nevertheless, the exact identity of the immunomodulatory effectors or compounds and their mode of action remains to be elucidated.

In plant root apoplast, the extracellular pH mediates the defense-growth balance whereby at acidic pH, the peptide ROOT GROWTH FACTOR (RGF) acquires a protonated sulfotyrosine promoting its interaction with the RGF receptor (RGFR) and eventually hetero-oligomerizes with the SERK co-receptor which culminates to encourage root meristematic growth (Liu et al, 2022). While at alkaline pH, the peptide RGF is deprotonated, disrupting the RGF-RGFR-SERK complex, and residues of PEP receptor (PEPR) gets protonated allowing binding of PEP, a DAMP which is triggered by MAMPs (Yamaguchi et al, 2010), provoking the defense machinery (Liu et al, 2022). Recent studies in rhizosphere microbiota indicate that majority of the its members can subdue immune response, potentially by altering the root pH environment (Yu et al, 2019). Various *Pseudomonas* species, including the beneficial microbe *P. capeferrum* WCS358 downplay root immune responses by gluconic-acid mediated acidification of root milieu. The bacterial lowering of pH depends on the pyrroloquinoline quinone (pqq) as co-factor for gluconic acid anabolism (Yu et al, 2019). Mutations on core pqq synthesis genes (eg. PqqF, a putative protease) and ubiquinol cytochrome b_{03} oxidase CyoB, a regulator of carbon metabolism, both important for gluconic acid synthesis, abolishes root immunity suppression (Yu et al, 2019). In contrast, the beneficial *Pseudomonas simiae* WCS417 dampens root immune response in a gluconic acid-independent manner wherein the bacteria prevent accumulation of alkaline precursors, potentially through the production of specific amino acids such as arginine by ArgF ornithine carbamoyl transferase (Liu et al, 2023). However, we still lack a clear understanding of how the plant microbiota kneads

plant immunity and so identifying the genetic mechanisms of microbiota-mediated plant immunity suppression remains a task at hand.

3.3. The functional microbiota: the host-microbiota social contract

The plant microbiota has been implicated to confer beneficial services to its host and augment holistic plant performance ranging from growth promotion, pathogen protection, nutritional provision, and abiotic stress resilience (Trivedi et al, 2020). It has also been found that under sub-optimal situations, the plant hosts actively recruit beneficial microbes, deliberately re-engineering its microbiota as needed, a phenomenon referred to as “cry-for-help” strategy (Liu et al, 2021; Pascale et al, 2020). Interestingly, the stable beneficial microbiota persists in the soil and is inherited trans-generationally as the soil legacy, such for the case of disease-suppressive soils (Raaijmakers et al, 2016).

Synthetic community experiments revealed that the bacterial components of the root microbiota alone promote plant growth and also alleviates the detrimental effects of the fungal members of the microbiota (Duran et al, 2018, Wolinska et al, 2021). Moreso, the microbiota is important for ensuing proper root developmental programs by modulating exogenous auxin levels (Finkel et al 2020, Conway et al, 2022). The root commensal *Variovorax* allows the maintenance of the stereotypical root growth by degrading auxin produced by other members of the rhizosphere microbiota (Finkel et al, 2020). The binding of MarR transcriptional regulator with bacterial auxin results to its activation and drives the expression of auxin degrading *iad*-like operons in *Variovorax* or auxin-catabolizing strains (Conway et al, 2022).

It was recently demonstrated that the *A. thaliana* rhizosphere microbiota recruited under low-light conditions alleviate the growth retardation but resulted to reduced microbiota-induced shoot defense against foliar pathogens and the microbiota-root-shoot axis modulation of the growth-defense balance depends on the plant transcription factor MYC2 (Hou et al, 2021). It is tempting to speculate that the existence of the shoot-root-microbiota circuitry is necessary for immune-training the aerial tissues against forthcoming infections. The plant conditioning of the soil in response to stress is implicative of a feed-back mechanism. It was exhibited that the transplantation of the rhizosphere microbiota recruited by the wilt-tolerant tomato *S. lycopersicum* cultivar Hawaii 7996 is sufficient to confer tolerance against the wilt pathogen *R. solanacearum* SL341 for the wilt-susceptible *S. lycopersicum* cultivar Moneymaker (Kwak et al 2018). Moreso, pathogenic *P. syringae* DC3000 infection of *A. thaliana* leaves results in the increased root exudation of L-malic acid which attracts and promotes root colonization of the beneficial *Bacillus subtilis* FB17 consequentially inducing systemic resistance against the foliar pathogen (Rudrappa et al, 2008). Poaceae species such as maize release

benzoxazinoids to alter the rhizosphere microbiota and elevates shoot JA-defense against herbivory of army worm larvae *Spodoptera frugiperda* and the protective effects of the trained soil is retained for the following planting season (Hu et al, 2018). The root endophytic fungal commensal *Colletotrichum toefieldiae* channels phosphate to the host and promote growth only under phosphate starved conditions as mediated by the host's PHOSPHATE STARVATION RESPONSE (PSR) machinery and tryptophan-derived secondary metabolism (Hiruma et al, 2016). Accordingly, a root microbial synthetic community in *A. thaliana* induces PHOSPHATE STARVATION RESPONSE 1 (PHR1) activity under phosphate-scarce conditions to prioritize nutritional augmentation over defense response (Castrillo et al, 2017). The *A. thaliana* secretion of coumarins in iron-deficient soils assembles a rhizosphere microbiota that facilitates host coumarin-dependent iron-mobilization to alleviate stress (Harbort et al, 2020; Stringlis et al, 2018). The transplantation of the flavone-conditioned microbiota enriched with Oxalobacteriaceae strains by the *Zea mays* cultivar C2 wild-type plants under nitrogen limitation promotes the growth of the flavone-deficient *Colorless2-Inhibitor diffuse* (*C2-idf*) mutant plants defective of chalcone synthase (Yu et al, 2021). The recruited *A. thaliana* rhizosphere under mineral scarce conditions modulate ABA-mediated suberization of the endodermis to improve ion import by the plant host (Salas-Gonzalez et al, 2021). These evidences support the idea that under nutrient scarce conditions, the plant host redesign its microbiota in a way to recruit specific groups of facilitative microbes that caters to ameliorate nutritional burden and assist plant growth.

There is a growing body of evidences indicating that microbiota can boost the adaptive responses of the plant host in face of environmental perturbations to facilitate survival. Microbiome profiling of 30 diverse plant species under drought stress revealed substantial enrichment of *Streptomyces* amplicon sequence variants (ASVs) belonging to Actinobacteria in the endosphere and is associated with drought acclimation response (Fitzpatrick et al, 2018). Similarly, microbiome profiling of 18 agriculturally important Poaceae lines with varying drought-tolerance showed a consistent enrichment of Actinobacteria (Naylor et al, 2017). The direct mono-inoculation of drought-enriched rhizosphere strains, in particular *Streptomyces coelicolor* Sc1 and *Streptomyces ambofaciens* Sc2 promoted modest growth advantages to *Sorghum bicolor* under drought stress (Xu et al, 2018). The artificial inoculation of a synthetic community derived from the rhizosphere microbiota of the desert legume *Indigofera argentea* confer salinity tolerance to tomato *S. lycopersicum* cultivar Moneymaker (Schmitz et al, 2022).

Microbes have an inherent capability to sequester heavy metals to bioremediate soil and potentially assist persistence of its plant hosts on polluted soils (Kour et al, 2021). Glomalin from arbuscular mycorrhizal fungi *Glomus mosseae* sequestered Cu^{2+} from copper toxic soils from *Sorghum vulgare* cultivar KS 524 roots (Gonzalez-Chavez et al, 2004). Also, the beneficial *Pseudomonas putida* KNP9 promotes growth of mung bean

Phaseolus vulgaris cultivar PM-2 and prevented host accumulation of toxic heavy metals under Cd^{2+} and Pb^{2+} toxic soils (Tripathi et al, 2005).

3.4. "Pathobionts" in dysbiosis: microbial beasts lurking within the microbiota

Plants interact with a diverse set of microorganisms from its surrounding environment and develop an intimate symbiosis along a continuum of beneficial to harmful relationships (from mutualist to commensals to pathogens) however, these interactions through the course of co-evolution could potentially oscillate indicating a dynamic transition across these lifestyles (Drew et al, 2021). Conceptually, the term "pathobiont" is defined as a symbiont that is able to cause diseases given a set of environmental conditions and due to the host genetic predisposition (Mazmanian et al 2008; Chow et al, 2010). The literature sometimes alternately used the pathobiont with opportunistic pathogens in different contexts (for example, pathobionts are "commensal-derived opportunistic pathogens", Yu et al, 2018). "Opportunistic pathogens" are microbes that can cause diseases following perturbations to the host (eg. administration of antibiotics, immune-deficiency) for which can rise from the microbiota or externally acquired from the surroundings (Brown et al, 2012). These distinctions get lost in translation and due to the lack of precision, scientific consensus, and the slack use of these terms, it causes more obscurity. More so the definition of "opportunistic pathogen" is disputed for the fact that technically every member of the microbiota can potentially become an opportunistic pathogen, as we have not exhaustively assessed the infinite sets of conditions at which this will hold true. As pointed out by Jochum and Stecher (2020) in their review, the term 'pathobionts' and also "opportunistic pathogens" attaches a negative stereotype to the microbe and ignores the possibility that in a different setting it could exert beneficial effects; for example, some previously identified "pathobionts": *Enterococcus faecalis* (Lengfelder et al, 2019), *Helicobacter hepaticus* (Danne et al, 2017), and *Mucispirillum schlaedeiri* (Caruso et al, 2019; Herp et al, 2019) were found to exert positive outcomes to their hosts in certain conditions. In plants, the strain *Rhodococcus* L278 induces blight symptoms and hyper-infection in bi-associations with the foliar pathogen *Pto* while the latter had reduced colonization, however, in a synthetic community context, *Rhodococcus* L278 protects *A. thaliana* plants against *P. syringae* DC3000 infection, and the removal of *Rhodococcus* L278 from the microbial community abolished the protective effect (Vogel et al, 2021). These examples indicate that beneficial function is an emergent community property which brings emphasis on the importance of microbe-microbe interaction within the microbiota wherein a pathogenic strain in mono-associations turns to a beneficial one in a community depending on the co-occurring strains. In this thesis we would like to adopt the term "potentially pathogenic" strain as proposed by Jochum and Stecher (2020) to

describe bona-fide members of the microbiota that can cause disease-like symptoms to the host at a given set of conditions in light of avoiding confusion.

Ecological and reductionist studies had revealed that potentially pathogenic strains populate their plant hosts in natural habitats without causing disease and are considered as bona fide constituents of the plant microbiota (Bai et al, 2015; Jakob et al, 2002; Agler et al, 2016; Duran et al, 2018; Karasov et al, 2018). These potentially detrimental strains are deleterious and in certain cases even fatal to the plant host when tested in laboratory settings in mono-associations or highly reduced functionality in microcosms (Agler e al, 2016; Duran et al, 2018; Ma et al, 2021; Shalev et al, 2022; Wolinska et al, 2021; Pfeilmeier et al, 2021). However, the adverse effects of these provisionally pathogenic microbes depend on the host status, the prevailing environment, and the concurring microbes (Shalev et al, 2011; Duran et al, 2018; Wolinska et al, 2021; Getzke et al, 2023; Vogel et al, 2021). It is an attractive thought that the potentially pathogenic members of the microbiota are evolutionarily tolerated by the plant host because they improve plant fitness in the wild.

Interestingly, there is growing evidence demonstrating that the microbiota itself jeopardizes its host to parasites (Stevens et al, 2021). For instance, the gut commensal *Lactobacillus taiwensis* heightens the regulatory T cell (Treg) production assisting infestation of the parasitic helminth *Heligmosomoides polygyros* in mice (Reynolds et al, 2014). The interaction of gut commensal (such as *E. coli*) via type 1 fimbriae FimH promotes egg hatching of the parasite whipworm *Trichuris muris* in mice leading to infestation (Hayes et al, 2010). Comparably, there are certain examples that the cost of maintaining a microbial mutualist outweighs the profits the host can acquire from the supposedly beneficial reciprocation. Though the legume host sanctions non-productive rhizobia with fitness penalties (Westhoek 2021; Kiers et al, 2003), some “cheater” strains of *Bradyrhizobium* species isolated in the wild confer no net benefit to their legume plant hosts *Acmispon stigosus*, *A. heermanii* and *Lotus strigosus* despite gaining superior *in planta* fitness as compared to other productive rhizobacteria (Gano Cohen et al, 2019; Sachs et al, 2010). Moreso, the bacterial endosymbiont *Hamiltonella defensa* protects the aphid host *Aphis fabae* from parasitoids but results to a shorter lifespan of the host (Vorburger et al, 2011). The bacterial endosymbiont *Wolbachia* confers resistance to virus infection to the fruit fly host *Drosophila simulans* but at the expense of its lifespan and fecundity (Martinez et al, 2015).

A dysbiotic microbiota is defined as a microbial community that is sufficient to confer disease onset on host and is associated with the domination of potentially pathogenic members of the microbiota, loss of key microbiota members, and poor microbial diversity (Levy et al, 2017). The observations that *A. thaliana mfec* mutant plants with defects on genes for PTI perception (PRRs *fls2, efr*, and *cerk1*) and *AtMin7* for vesicle trafficking pathway have an increased susceptibility to avirulent *P. syringae* Δ*hrcC* and an increased

endosphere bacterial load coinciding with necrotic lesion symptoms on leaves under high humidity has led to the discovery of the existence of dysbiotic microbiota in plants (Xin et al, 2016). It has been revealed that the *mfec* mutant harbored a dysbiotic microbiota with very low microbial diversity (Proteobacteria dominated and Firmicutes depleted) resulting to disease-like symptoms (Chen et al, 2020). Moreso, transplantation of the dysbiotic *mfec*-derived microbiota is sufficient to instigate disease on to the wild-type Col-0 plants indicating that the dysbiotic microbiota is causal to the disease onset.

4. THESIS OBJECTIVES

Convincing evidence from the group revealed significant variations in the alteration of the host transcriptomic terrains 6 hours post-infiltration with microbiota-derived strains, a mid PTI hallmark, concomitant to the global alterations of microbial metabolic activities at the transcript level (Nobori et al, 2022). This key finding together with the growing body of evidences in the prevalent literature, prompts us to an inquest on the fundamental contribution of PTI as the principal selection pressure in mediating the plant-microbiome communications.

This project aims to gain insight on the interconnection of the plant host immune response with the microbiota member behaviors with an auspicious and strategic prospect of underpinning specific mechanisms entailing successful microbial accommodation with emphasis on aerial tissues (Figure 1). Specifically, we aim to: ① determine the potential of the individual microbiota members to activate and evoke classical immune responses to the host, and ② determine the effects of these induced host immune responses to the individual microbiota members. With this broad objectives and the perspective of trait discovery, immune-compromised mutants, largely represented by receptor-defective genotypes (*fls2*, *efr*, *cerk1*, *fls2 efr cerk1* [fec], *bak1 bkk1 cerk1* [bbc], and *rbohD*) together with the wild-type Col-0 accession (please see Supplementary Table S1 for the plant material details) were challenged in mono-association with 20 bacterial strains derived from the AtSPHERE culture collection (please see Supplementary Table S2 for the strain details; Bai et al, 2015), a catalogue of bacterial strains isolated from seemingly healthy *A. thaliana* plants grown in wild environmental setting across Europe (Figure 1; Bai et al, 2015) and were phenotyped for PTI outputs and bacterial colonization capacities. We have revealed that the microbiota members have varying capacities to induce different PTI responses through distinct PRRs and we have shone light on to the molecular mechanisms of plant ROS mediated regulation of microbial behavior. We have revealed that plant ROS allowed co-habitation of a potentially pathogenic commensal via suppression of bacterial T2SS and CAZyme expression.

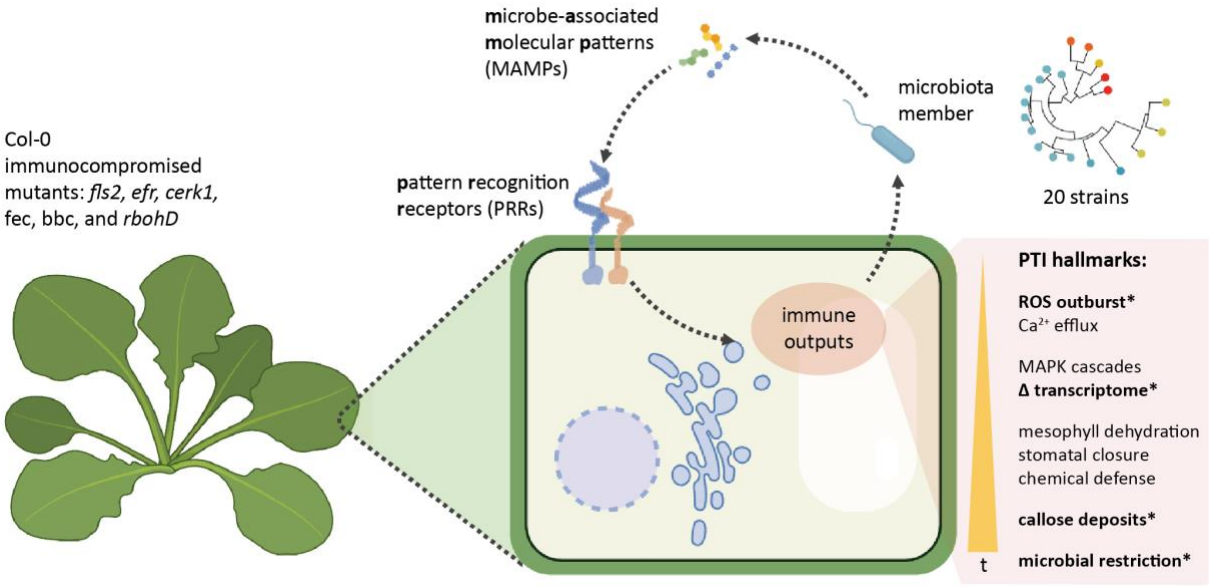

Figure 1. Pattern-triggered immunity in plants. Microbes encode a suite of well-conserved microbe associated molecular patterns (MAMPs) that can be perceived by plant host encoded, usually cell-surface bound pattern recognition receptor (PRRs) that results to a cascade of signals and a series of physiological events that constitutes the pattern-triggered immunity (PTI). It is characterized by a number of physiological responses such as ROS outburst, Ca2+ fluxes, transcriptional reprogramming, callose deposition, among others and ultimately culminates to the restriction of microbial growth. In this thesis, a nominated panel of taxonomically diverse bacteria comprising of 20 strains derived from the AtSPHERE culture collection (Bai et al, 2015) will be used as elicitors against the wild-type Col-0 plants and immune-compromised mutants *fls2*, *efr*, *cerk1*, *fec* (*fls2 efr cerk1*), *bbc* (*bak1 bkk1 cerk1*), and *rbohD* to measure PTI outputs and microbial colonization.

5. RESULTS

5.1. CHAPTER 1: Microbiota members elicits varying immunogenicity discordant with their phylogeny

We have nominated a panel of phylogenetically diverse strains that have been previously isolated from healthy-looking *Arabidopsis thaliana* leaves, roots, and its surrounding soil in wild (Bai et al, 2015) with which have been previously profiled for co-transcriptomes of plant and bacteria (Nobori et al, 2022). All of these strains despite of their isolation origins can colonize the shoot of the host plant (Figure 2e). In **CHAPTER 1**, we aimed to investigate the variations in the immune responses triggered upon mono-inoculation of these bacterial strains with the wild-type Col-0 leaves and its dependencies on immunity genes by assaying for the following read-outs: ROS outburst (early PTI response),

transcriptome reprogramming (mid PTI response, dataset from Nobori et al, 2022); callose deposition (late PTI response); and the bacterial colonization capacities.

5.1.1. Microbiota members manifest variegated immune-profiles to their plant host

ROS outburst, an early PTI response was measured *ex planta* upon triggering Col-0 leaf disks with mono-cultures of microbiota members and measurements were immediately obtained after elicitation for an hour (Figure 2a). Results showed that pure MAMPs flg22 and elf18 provoked abrupt, strong, and pronounced ROS peaks in Col-0 as compared to chitinDP7 elicitor indicative that the different MAMPs elicit varying degrees of ROS outputs and the host plants have inherently different amplitude of response to these motifs and the signal was lost depending on the absence of their cognate receptors and the *rbohD* gene (Supplementary Figure S1).

Upon elicitation with microbiome members, ROS outbursts assume different signatures and dynamics revealing variations in the capacities among microbiome members to induce immediate PTI responses in Col-0 leaves (Figure 2e, Supplementary Figure S2). Among the microbiome members that activate ROS, *Pseudomonas* strains L127 and L15 elicited the strongest response in Col-0 leaves. Likewise, *Xanthomonas* L148 elicited ROS response in a relatively subdued but persistent fashion. Surprisingly, some strains such as *Flavobacterium* R935 and *Erwinia* L53, did not induce any detectable ROS signals (Figure 2e, Supplementary Figure S2). These observed variations in ROS outbursts can be plausibly explained by the MAMP polymorphisms or the rate at which MAMPs are liberated to be accessible for plant host detection, nevertheless the use of intact live cells as elicitors cannot capture the full immunogenic profile of these strains due to immuno-latency from potential evasion and/or suppression mechanisms.

To have a closer inspection of the potential immunogenicity profile of these strains, harshly heat-killed cells were used as inputs for ROS outburst bioassay. This was done with the presumption that upon heat treatment of bacterial cells, MAMPs which are thermo-stable will then be fully released. Most strains that were initially not inducing ROS outburst with live intact cells, elicited very strong and distinct ROS peaks in the context of heat-treated cells (resembling ROS outputs with MAMP elicitors) for instance, members of Gammaproteobacteria: *Erwinia* L53, *Pseudomonas* L48, *Bulkholderia* L177, and *Xanthomonas* L70 (Figure 2e, Supplementary Figure S2). These results imply that microbiome members encode considerably immunogenic MAMP repertoire and the disparity on the outputs from live intact cells and heat-treated cells strongly suggests deterrence of ROS responses through evasion or suppression mechanisms. Conversely, *Flavobacterium* R935 consistently did not induce ROS outburst in both live and heat-treated versions, indicative that its MAMP repertoire is weakly or not immunogenic at all.

Likewise, *Pedobacter* L176 which considerably activated ROS outburst with live cells, failed so upon heat-treatment, implicating that its MAMP repertoire (or majority of it) is thermo-labile.

To gain insight on the potential evasion mechanisms deployed by microbiota members to escape immune detection of self-derived MAMPs, we hypothesized that a considerable reduction of ROS outputs induced by heat-killed cells in the presence of live cells could be interpreted as a signature for an active interference of ROS outburst by the live bacterial strains. We then performed similar ROS bioassays in different doses of bacterial cells and in combination of live and heat-killed cells. Interestingly, we were able to granularize the potential ROS evasion strategies being implemented by some of the microbiota members. Some of the strains directly suppress ROS outburst elicited by their self-derived MAMPs: ROS outburst is only observed with heat-killed cells but this response is significantly dampened in the presence of live cells, as for the case of *Erwinia* L53 and *Burkholderia* L177 (Supplementary Figure S3). These clearly suggest an evasive mechanism (here we categorized as "immune-evasive[1]"). Other strains that can only trigger ROS outburst in heat-killed form, such as *Microbacterium* L1 and *Xanthomonas* L70 (Supplementary Figure S3) convincingly supports evasion of host recognition via preclusion or delayed release of self-derived MAMPs (here we categorized as "immune-evasive[2]").

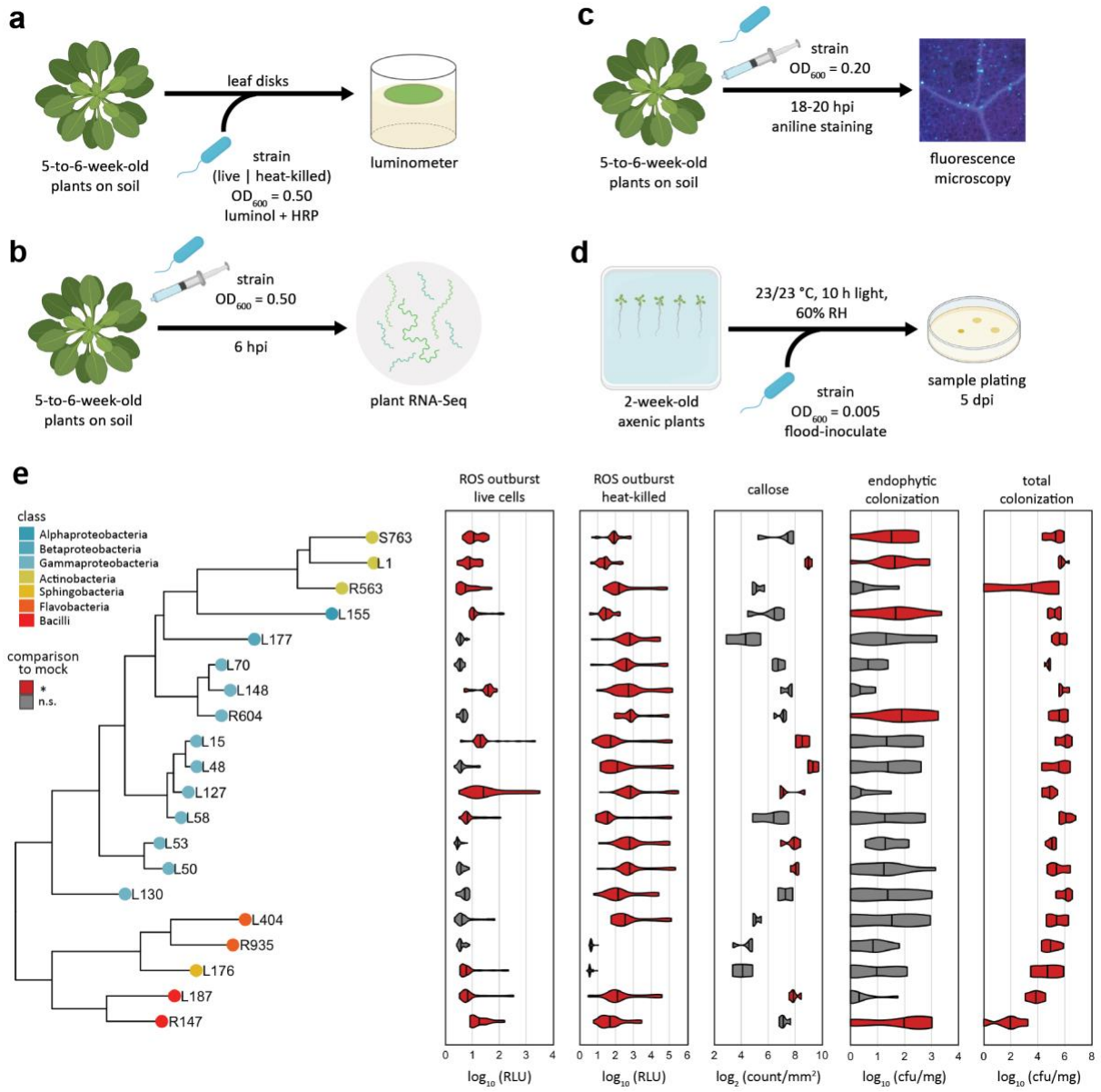

Figure 2. **Microbiota members manifest varying immunogenic potential to the wild-type Col-0 plants. a-d,** schematic diagram of PTI hallmarks induced by the selected microbiota members. **a**, ROS outburst, an early PTI event was assayed *ex planta*; leaf disks were cored from mature Col-0 plants and were triggered with either live or heat-treated microbiota-derived strains (OD_{600}=0.50), measurements were immediately obtained for an hour. **b**, transcriptional reprogramming, a mid PTI event was profiled *in planta*, leaves of mature Col-0 plants were infiltrated with monocultures of microbiota-derived strains (OD_{600}=0.50) and were harvested after 6 hpi wherein bacterial cell populations remain similar across all strains, and were profiled for RNA-Seq, data were published in Nobori et al, 2022. **c**, callose deposition, a late PTI event was assessed *in vivo*, leaves of mature Col-0 plants were infiltrated with monocultures of microbiota members (OD_{600}=0.20) and were cored and stained with aniline blue to visualize callose structures with the aid of a fluorescence microscope. **d**, colonization capacities of the microbiota members were determined by flood-inoculating axenic 2-week-old Col-0 plants with monocultures (OD_{600}=0.005) and plated for leaf total and endophytic compartments 5 dpi. **e**, phylogenetic relationship of the selected microbiota members and the

violin plots of their corresponding ROS burst profiles using live and heat-killed cells, callose deposition, and their respective colonization capacities in leaves of Col-0. Colors of the tips in the phylogenetic tree represent the taxonomic classes. Experiments were repeated at least two times each with 8 biological replicates for ROS assay, 2-3 biological replicates for callose deposition, and 3–4 biological replicates for colonization assays (See Supplementary Figures S2, S5, and S7 for the full ROS outburst, callose production, and colonization profiles, respectively; see Supplementary Table S2 for detailed descriptions of the strains included). Red violins indicate significantly different from the mock treated samples while grey violins indicate no significance (ANOVA with *post hoc* Tukey's test, $P \leq 0.05$). Some illustrations were created with BioRender.

Plant transcriptome reprogramming, a mid PTI event was profiled by hand infiltrating Col-0 leaves with the microbiota members in mono-association context and were harvested 6 hpi (Figure 2b, Dataset from Tatsuya et al, 2022). The foliar pathogen *Pto* induced a distinct plant transcriptomic profile, wherein surprisingly, the avirulent *Pto* D36E prompts an extensive plant transcriptional terrain closely resembling some of the leaf commensals, in particular *Xanthomonas* strains L148, L70; and *Pseudomonas* strains L127, L48, and L58 (Figure 3a). Principal component (PC) analysis revealed that PC1 and PC2 can explain 91.3% of the variations in the plant transcriptome (Figure 3). It also subscribed with the observation that some of the commensals elicit strong transcriptional reprogramming which is reminiscent of the plant transcriptome induced by the *Pto* strains (Figure 3). It is also interesting that some of the commensals induced very weak plant transcriptomic remodeling like for the case of *Agrobacterium* L155, *Acinetobacter* L130, *Chryseobacterium* L404, and *Flavobacterium* R935 (Figure 3a). Moreover, these expression profiles coincide with the transcriptomic changes upon elicitation with a MAMP flg22 (Nobori et al, 2022; Hillmer et al, 2017) which indicates that these commensals induce the PTI pathway at the transcript level. With these, we then rationalized to use the transcriptome PC1 and PC2 values as a proxy for transcriptional reprogramming with which low PC1 values or high PC2 values indicate strong transcriptional reprogramming. The transcriptional reprogramming reflects some degree of phylogeny since most of the Gammaproteobacteria induced stronger transcriptional changes perhaps due to overrepresentation of the clade in the panel (Figure 3b). Nevertheless, due to this observed pattern, we then investigated the conservation of the MAMPs flg22 and elf18 and interrogated the concordance with the transcriptional reprogramming. Indeed, a significant correlation exists between the conservation of these canonical MAMPs with the alterations in the plant transcriptional terrains (Figure 3c-d), implicative that the variations in the MAMPs harbored by these commensals drive the transcriptional response of the plant host upon encounter (Nobori et al, 2022).

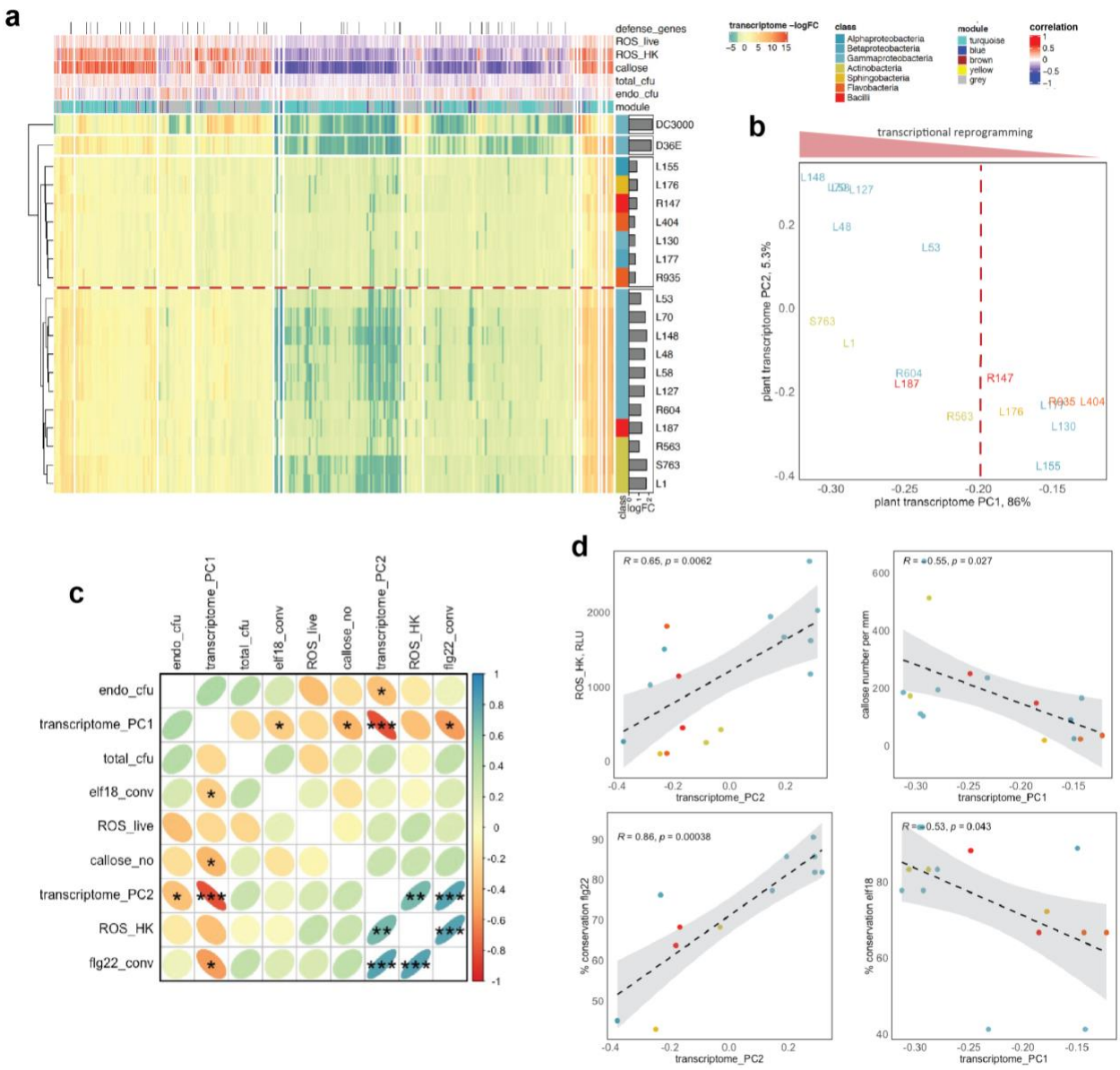

Figure 3. Microbiota members induced transcriptional reprogramming to Col-0 and correlates significantly with either early or late PTI outputs. a, heatmap representation of the Col-0 leaf transcriptomic profile upon infiltration with microbiota-derived strains (OD_{600}=0.50) 6 hpi. Module memberships of the genes were calculated using WGCNA. Gene expressions were correlated with the PTI read-outs, ROS outburst for live and heat-killed cells (ROS_live and ROS_HK), callose number (callose_no), and colonization capacities on the total and endophytic leaf compartments (total_cfu and endo_cfu, respectively) were represented as color bars. The annotated defense genes are marked. Color side bars indicate phylogenetic affiliations of the strains. Side-bar plots represent the mean of the absolute values for log_2 fold-changes (logFC, strain vs. mock) for each of the strain tested with the pathogenic *Pto* DC3000 and avirulent *Pto* D36E as controls. **b**, principal component (PC) analysis of the transcriptomic responses of Col-0 to the microbiota-derived strains, wherein the PC values reflects the degree of host transcriptional re-modelling (transcriptome_PC1 and PC2). **c-d**, correlational analysis among the PTI read-outs and the sequence conservation of the classical MAMPs flg22 and elf18 peptides (flg22_conv and elf18_conv, respectively, *R* is the coefficient of determination, $p \leq 0.05$).

Callose deposition, a late PTI response was measured *in planta* upon challenging Col-0 leaves with mono-cultures of microbiota members and sampled after 18-20 hpi (Figure 2c). Results for the controls showed that Col-0 formed callose deposits upon leaf infiltration with MAMP elicitors and in a greater extent for the avirulent *Pto* strains (*D36E*, deficient of 36 effectors; *ΔhrcC*, lacks functional T3SS), which are in agreement with previous publications (Supplementary Figure S4). Moreover, the receptor mutants did not form significant amount of callose structures in response to their corresponding MAMPs. The triple mutants *fec* and *bbc* exhibited less callose formation for all of the MAMPs (Supplementary Figure S4).

Significant variations in the callose structure induction were observed upon Col-0 leaf infiltration with the microbiota members wherein *Pseudomonas* strains L48, L15, L127; *Erwinia* L53, *Microbacterium* L1, and *Exiguobacterium* L187 stimulated significant callose formation, some of which were far more intense than the avirulent *Pto* versions suggesting intense activation of defense by these commensal strains (Figure 2, Supplementary Figure S5). Intriguingly, a number of strains, such as *Pedobacter* L176, *Flavobacterium* R935, and *Burkholderia* L177 induced virtually no callose deposits supporting the notion of their weak immunogenic nature (Figure 2e). Moreover, upon comparison of the distribution of callose sizes as stimulated by the microbiota members with that of avirulent *Pto* D36E (Kolmogorov-Smirnov statistics, D; Supplementary Figure S6), all of the strains induced significantly distinct callose profiles. Though many of the strains prompted production of callose structures, only few strains can induce considerable amount of larger callose deposits comparable to *Pto* D36E (arbitrary threshold callose area of 8.3μm^2), namely *Microbacterium* L15, and *Pseudomonas* strains L1 and L48 (Supplementary Figure S6). This callose profile is reminiscent of basal defense response mounted against non-host adapted *Pseudomonas* pathogens (Ham et al, 2007).

Summing up these findings, microbiota members can be categorized into four distinct classes of immunogenicity on the basis of the intensity, degree, and tempo of the PTI outputs being elicited to their native host. First, immuno-active strains can induce robust PTI responses for both live and heat-killed cells, for instance *Pseudomonas* L127 induces strong ROS outburst with live and dead bacteria, substantially triggers callose formation, and significantly reprograms plant transcriptome landscape. Second, immuno-evasive^1 strains can induce immune responses only when heat-killed and can seemingly subdue in an active fashion the immune outputs when live cells are present like for the case of *Burkholderia* L177 which dampens ROS outputs of dead cells in the presence of live cells. These suggest that the strains belonging to this category can either neutralize or digest their self-derived immunogens to cloak recognition or release factors that directly target and suppress plant immunity sectors. Third, immuno-evasive^2 strains can also induce immune response only when heat-killed and the addition of live cells does not result to

the attenuation of the PTI response such as for *Xanthomonas* L70 which only induces ROS when heat-killed and also weakly stimulates callose formation. This signature indicates that these strains evade detection via preclusion or delayed liberation of MAMPs. And lastly, immuno-quiescent strains do not induce any observable immune outputs in both live or dead cell context for all the PTI read-outs measured as represented by *Flavobacterium* R935.

5.1.2. Microbiota members differentially occupy distinct leaf compartments

Since PTI pathway eventually culminates to the restriction of microbial growth, it is imperative to determine the colonization behaviors of these strains (Figure 2d). Results revealed that all of the strains were able to colonize the leaf albeit few strains can occur in considerable population sizes in the apoplast. The strains *Acinetobacter* L130, *Chryseobacterium* L404, and *Burkholderia* L177 can effectively colonize and persist on the surface of the leaf and into some extent the endophytic compartments in mono-associations indicative of their efficient general colonization capacities (Figure 2e, Supplementary Figure S7). This finding is in agreement with the previous publication wherein the phyllosphere strains *Burkholderia* had been found to colonize the leaf consistently while *Chryseobacterium* served as a keystone species since its absence resulted to drastic changes in composition and structure of the leaf synthetic bacterial communities (Carlström et al, 2019). More so, strains *Agrobacterium* L155, *Microbacterium* L1, *Arthrobacter* S763, and Xanthomonadaceae R604 can subsist substantially in the apoplast and also on the surface of the leaf, indicative that these strains adapted to both endophytic and epiphytic habits (Figure 2e, Supplementary Figure S7). However, there are strains that have preferential colonization of the leaf surface as for the case of *Pseudomonas* L15, L58, and *Acinetobacter* L130, suggestive of their epiphytic lifestyle (Figure 2e).

5.1.3. Plant gene expression networks upon microbiota elicitation are tightly regulated and are pertinent to PTI responses

With the plant transcriptomic data, we then ventured onto dissecting the gene expression networks that govern the transcriptional reprogramming upon commensal interaction and to address this, the **w**eighted **g**ene **c**o-expression **n**etwork **a**nalysis (WGCNA) was conducted to discover modules of highly correlated plant host genes and relate these expression profiles to the corresponding phenotypic responses, in this case PTI read-outs. The resulting modules usually comprised of genes involved in the same biological pathways, and more likely to share regulatory factors (Langfelder and Horvath, 2008).

Module content pathway analysis could uncover specific and even novel processes and functions condensed within modules (Farber, 2013).

Network analysis revealed 4 distinct gene modules: M1 turquoise with 5934 genes; M2 blue with 1569 genes; M3 brown with 78 genes; and M4 yellow with 60 genes (Figure 4a-c, please see Supplementary Dataset S1 for details). M1 turquoise and M3 brown clustered with the traits ROS with live cells and bacterial colonization capacities; M2 blue groups closely with ROS heat-killed and colonization capacities, while M4 yellow clusters with callose deposition (Figure 4d). Remarkable enrichments were revealed upon module content characterizations. The genes in M1 turquoise are substantially enriched for functions related to defense, response to biotic stimulus, and photosynthesis. The M2 blue module is significantly associated with regulation of transcription and translation. The M4 yellow module is mostly involved in protein transport and localization. Lastly, M3 brown module is mostly composed of genes with unknown functions (Figure 4e, please see Supplementary Dataset S2 for the list of GO terms for each module). Correlation of the **g**ene **s**ignificance parameter for the PTI outputs (GS, correlation of the gene expression within the module with the PTI trait in question) with the module membership were substantial (except for M4 yellow with ROS HK trait) indicating that these modules were pertinent to the PTI response (Supplementary Figure S8).

Next**, s**upport **v**ector **m**achine classifier with **r**ecursive **f**eature **e**limination (SVM-RFE) was implemented on the expression profiles within the identified modules to nominate genes that predict the PTI read-outs upon interaction with microbiota members. Profoundly, a number of WRKY transcription factors in modules M1 turquoise and M2 blue appeared to have expression signatures that concur with PTI responses, *WRKY53* for ROS outburst; *WRKY39*, *WRKY48*, and *WRKY66* for transcriptional reprogramming; and *WRKY30* for callose (Supplementary Dataset S3). Many of these WRKY transcription factors (specifically WRKY39, 48 and 53) are immediately induced upon flg22 treatment (Birkenbihl et al, 2018). More so, expression profiles of MAPK genes *MAPKKK1* and *MPK10* within the M1 turquoise module and *MPK8* in M2 blue module also predicts callose deposition, endophytic colonization, ROS outburst, respectively (Supplementary Dataset S3). *MPK8* has been implicated in the negative regulation of *RBOHD*-mediated ROS (Takahashi et al, 2011). Similarly, *MAPKKK δ-1* is required for full immunity against bacterial and fungal pathogens (Asano et al, 2020). The genes implicated in cell-death pathways *NCA1* and *BAG6* belonging to modules M2 blue and M3 brown were predictive of bacterial colonization (Hackenberg et al, 2013; Li et al, 2016). The expression profile of *IBS1* in M4 yellow module, a gene involved in priming defenses was also prognostic of ROS outburst (Ton et al, 2005). These genes could be potentially host genetic modulators of the PTI-dependent plant-microbiota dialogues and thus warrants future validation and investigation (See Supplementary Dataset S3 for the list of genes relevant to PTI responses identified through machine learning).

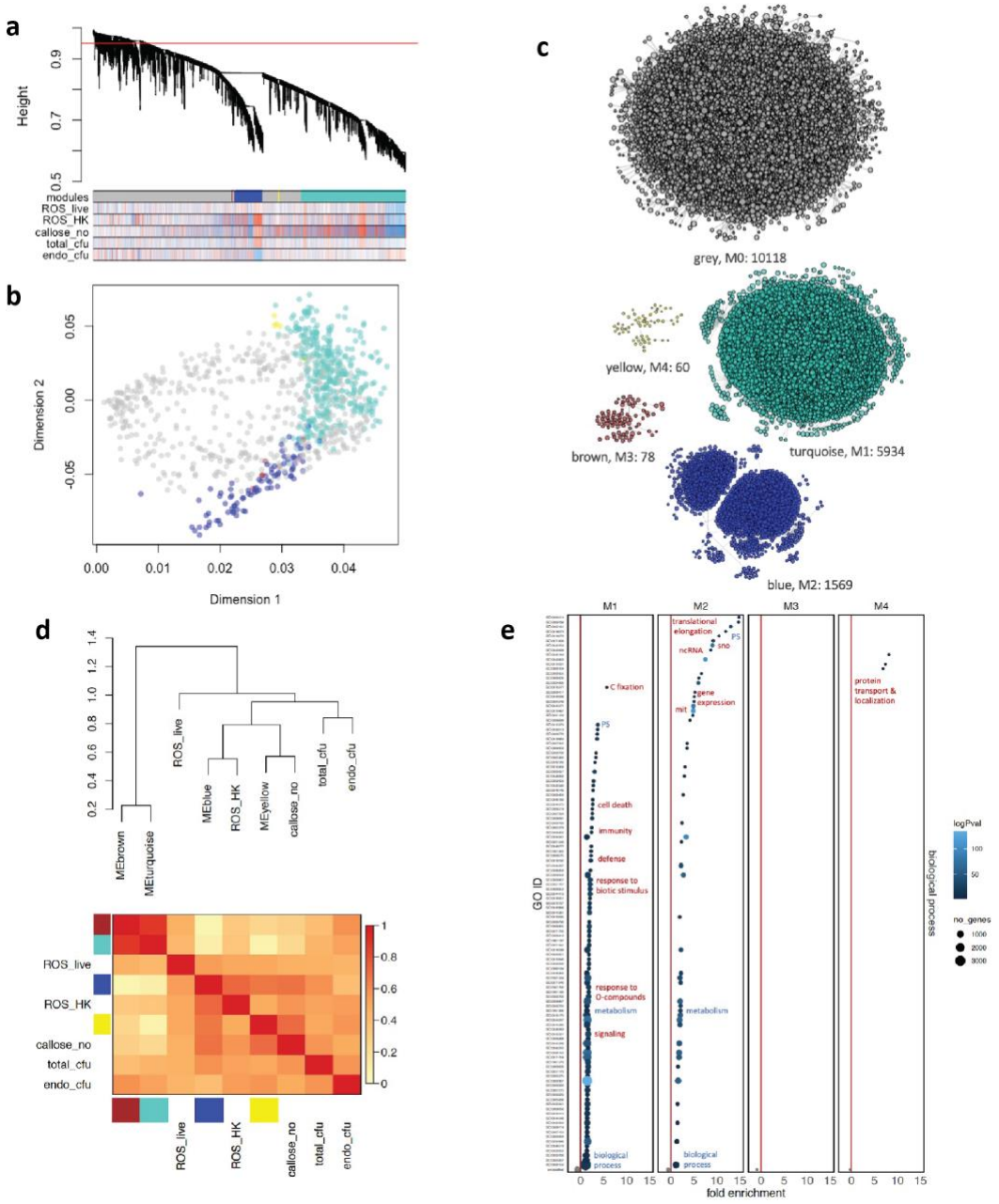

Figure 4. Weighted gene co-expression network analysis (WGCNA) reveals distinct and tightly connected gene modules associated to specific biological functions and pathways. a-d, WGCNA results for the Col-0 transcriptomic profiles upon microbiota mono-associations. **a**, hierarchical clustering and **b**, multi-dimensional scaling revealed 4 distinct modules: M1 turquoise, M2 blue, M3 brown, and M4 yellow. M0 grey module contains genes that are generally poorly connected. **c**, gene network connectivity within the modules and their corresponding network sizes. **d**, eigengene dendrogram and network heatmap representing adjacencies of the gene modules with the PTI traits: ROS outburst with live and heat-killed cells (ROS_live and ROS_HK, respectively), callose production (callose_no), and bacterial colonization of the total and endophytic leaf compartments (total_cfu and endo_cfu, respectively). **e**, pathway enrichment analysis within the modules (hypergeometric test, p-values ≤ 0.05).

5.1.4. Immunogenicity is dissonant with phylogeny and is strain-specific

With the PTI readouts (including colonization behaviors), correlational analysis reflected very poor association among traits (Figure 3c). The early heat-killed cell induced ROS outburst significantly correlates with the mid-response plant transcriptome reprogramming PC2 (R= 0.65**, Figure 3c). Conversely, the late callose deposition response correlates significantly with the mid response transcriptome reprogramming PC1 (R=0.55*, Figure 3c). The substantial association of the host transcriptional landscape re-modelling with the early and the late PTI responses argues a fundamental link that connects these temporally separated distinct PTI events. Conversely, microbiota colonization, in particular in the leaf endophytic compartment only substantively correlates with transcriptome reprogramming PC2 (Figure 3c). The lack of response-wide correlation of PTI responses signifies that physiological consequences and the fate of the host-microbiota interaction are far more complicated and further highlights that the perception of the nuanced compendium of stimuli, triggering the cascade of signals, and the eventual reactions are at a certain degree, differentially fine-tuned and tailored for each strain. Also, our understanding of the interdependencies of these PTI outputs were pathogen- or symbiont-focused, lacks clear definition or refinement (eg. one being a prerequisite to other thus occur in a sequence or a separate branch), and remains fragmented (Bigeard et al, 2015). However, one cannot exclude the possibility that these results could also be partially attributed to the inherent limitations of the experimental features (eg. timing of the response, age of samples, nature of assay, different experimental systems). Previous findings have revealed substantial correlation in the MAMP conservations with the gene clusters functionally associated with defense response, indicative of corollary dependence of transcriptional reprogramming to MAMP immune-potency (Nobori et al, 2022). Only the ROS outburst as induced by heat-killed cells, the transcriptome PC1 and PC2 had a significantly positive correlation with percent conservation of the classical MAMPs flg22 and elf18, which implicates that other MAMP epitopes might explain the variations observed in the PTI read-outs ($R \geq |0.53|$**, Figure 3c).

To gain insights on the evolution of immunogenicity of the microbiota members, **p**hylogenetic **P**rincipal **C**omponent (pPC) analysis was conducted. Results revealed that though pPC1 entirely explains the variations existing among the PTI traits (99.9%, generally positive scores for colonization and negative scores for immunogenicity, Figure 5a-b), there was no clear emerging pattern that coincides with the kinship, which further supports the notion of strain-specificity of the responses

Since evidence points out the possibility that PTI responses towards the microbiota are under stabilizing selection (Colaianni et al, 2021; Parys et al, 2021), l1ou analysis, a model-based approach was performed. This method follows the Ornstein-Uhlenbeck process which assumes that traits are phylogenetically correlated and selection pressure simultaneously acts upon these traits; likewise, anomalies on these assumptions are

detected as “adaptive shifts” (Bastide et al, 2018, Khabazzian et al, 2016). Results revealed lineage-specific patterns and evolutionary shifts were detected in the Gammaproteobacteria clade for *Acinetobacter* L130; and the *Pseudomonas* strains L15, L48, L58, and L127 (Figure 5c). Moreover, the α scores (adaptation rate) for ROS outburst with dead cells and callose number are relatively low indicating low selection pressure (deviates largely from the optima) allowing diversity on these phenotypes which puts forward the notion that the plant hosts have a variegated defense program depending on the strain (Figure 5c). However, δ^2 scores (variance rate) for phyllosphere colonization were high implying high stochasticity and/or plasticity for this trait which can be attributable to external factors (eg. environmental condition). With the weak concordance among PTI responses and with the phylogenetic relationship, these results support the idea that the evolutionary trajectory of the underlying processes governing PTI responses to microbiota members is shaped in a strain-specific manner.

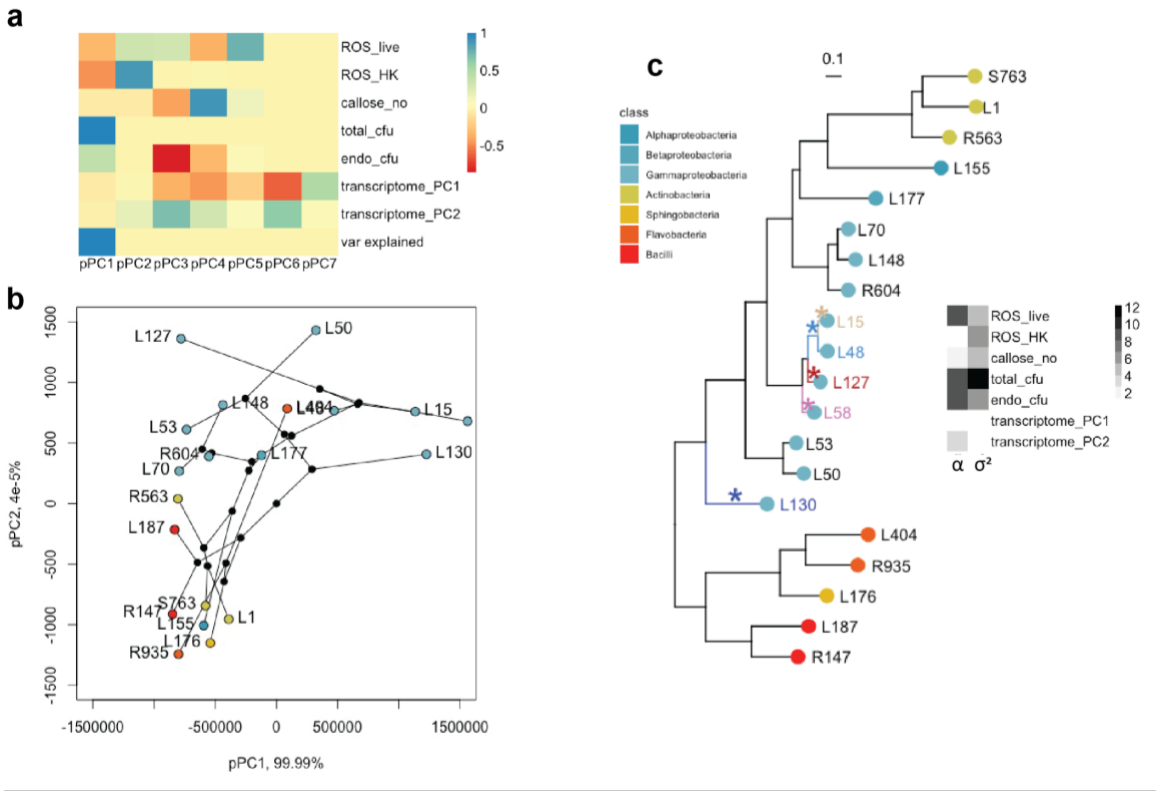

Figure 5. PTI traits are phylogenetically discordant and strain-specific. a-b, phylogenetic principal component analysis (pPCA) of the PTI traits: ROS outburst for live and heat-killed cells (ROS_live and ROS_HK); callose deposition (callose_no); transcriptional reprogramming (transcriptome _PC1 and transcriptome_PC2); and bacterial leaf colonization of the total and endophytic compartments (total_cfu and endo_cfu, respectively). a, heatmap representation of the eigenvalues for each PTI traits and the variance explained (var explained) by each of the pPCs. **b**, pPCA plot of pPC1 and pPC2 which explains the variations in the PTI traits accounting for the phylogenetic relationships among the tested microbiota-derived strains. **c**, l1ou analysis of the PTI traits revealed 5 evolutionary shifts for immune responses had occured, marked in * on the phylogenetic tree. The adaptation rate α, and variance rate δ^2 are represented in a heatmap for each of the PTI read-out.

5.1.5. Immuno-compromised mutants have attenuated immune responses towards microbiota members

Since the focus of this research is to understand the quantitative contribution of PTI pathways, with emphasis on pattern-recognition-receptors and ROS, the microbiome members were profiled for PTI readouts using the mutants *fls2*, *efr*, *cerk1*, *fec*, *bbc*, and *rbohD*. Results showed that most of these strains elicited subdued ROS outbursts from these mutants, particularly in a greater extent for the higher order mutants *fec* and *bbc*, (Figure 6, Supplementary Figure S2). As expected, all of the strains were not able to induce ROS efflux in *rbohD*, for both living or dead cells as stimulants (Supplementary Figure S2). Different dependencies of commensal bacteria-induced ROS were noted for

the MAMP (co)receptors. For instance, ROS production by both live and heat-killed *Exiguobacterium* L187 and *Janibacter* R563 were dependent on *EFR* but not on *FLS2* and *CERK1* (Figure 6, Supplementary Figure S2). This *EFR* dependency for commensal bacteria-induced ROS production was observed for most of the strains, but we detected no or only weak effects of mutations in *FLS2* and *CERK1* alone (Figure 6, Supplementary Figure S2). These results suggest that the recognition of EF-Tu-derived peptides via EFR is the prevalent mechanism for ROS production by commensal bacteria in *A. thaliana* leaves. However, there were commensal bacteria such as *Pseudomonas* L127 that triggered ROS in higher order *fec* and *bbc* mutant plants (Supplementary Figure S2), indicating that MAMPs other than flg22, elf18, and peptidoglycans are responsible for ROS production upon host detection. Profoundly, no detectable ROS efflux was consistently observed for *Flavobacterium* R935 upon challenging all the mutants indicative of its very weak immunogenicity (Figure 6, Supplementary Figure S2).

In general, all the (co)receptor mutants induced attenuated deposition of callose structures upon elicitation with the microbiota members. A significant reduction of callose formation was observed for strains *Pseudomonas* L15, *Pseudomonas* L48, and Enterobacteriaceae L50 for all the single receptor mutants, *fls2*, *efr*, and *cerk1* indicating that callose formation upon detection of these strains rely on these receptors (Figure 6, Supplementary Figure S5). Consistently, many of the strains have a substantial decrease in callose induction, in particular *Acinetobacter* L130, *Agrobacterium* L155, *Janibacter* R563, and *Arthrobacter* S763 only for *efr* mutant plants indicating that elf18 MAMPs served as the primary epitope for callose formation (Figure 6, Supplementary Figure S5). Seemingly, the flg22 peptide is the main callose elicitor for *Xanthomonas* L148 due to a significant subdual of callose production in *fls2* mutant leaves. Moreover, induction with strains *Pseudomonas* L58 and Bacillaceae R147 did not result to a pronounced change in the callose response (Figure 6, Supplementary Figure S5).

The bacterial titers of different commensals in leaves of mutant plants were also assessed. To our surprise, while we observed increased colonization of some commensal bacteria in some of the MAMP (co)receptor mutants compared with Col-0 wild-type plants, we mostly did not see effects of *rbohD* mutation on either total or endophytic commensal colonization (Figure 6 and Supplementary Figure S7). This suggests that plants recognize commensal bacteria and produce ROS that do not have detectable effects on most commensal bacterial colonization. Consistently, the *efr* mutant harbored higher populations of the strains *Burkholderia* L177, *Acinetobacter* L130, *Agrobacterium* L155, *Erwinia* L53, and *Pseudomonas* L58 on the total leaf compartment as compared to the wild-type Col-0 leaves (Figure 6 and Supplementary Figure S7). Furthermore, only *Acinetobacter* L130 and *Agrobacterium* L155 significantly colonized the apoplast of *efr* mutants as compared to Col-0, indicative that *efr* recognition of the elf epitopes from these strains are vital for restricting microbial proliferation on the surface and in the internal leaf

tissues (Figure 6 and Supplementary Figure S7). In sharp contrast, however, both total and endophytic colonization of *Xanthomonas* L148 was dramatically increased in the *rbohD* mutant compared with Col-0 wild-type plants (Figure 6 and Supplementary Figure S7), suggesting that RBOHD-mediated ROS suppress *Xanthomonas* L148 colonization, which is consistent with a recent finding (Pfeilmeier et al, 2019).

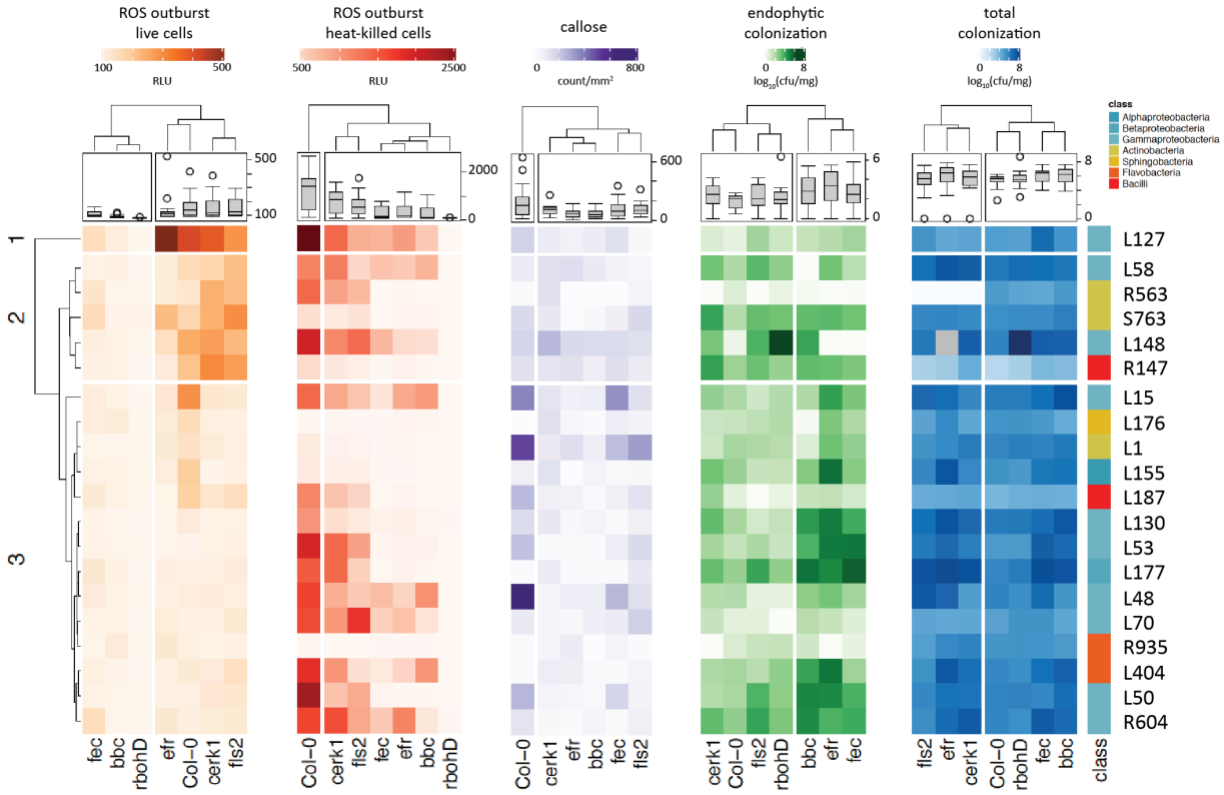

Figure 6. Immunocompromised mutants have attenuated immune response to the microbiota members. Heatmap representation of the PTI responses of the immune-compromised mutants: *fls2* lacks the receptor recognizing flg22, *efr* lacks the receptor for elf18, and *cerk1* lacks the co-receptor for chitinDP7; *fec* (*fls2 efr, cerk1*) and *bbc* (*bak1 bkk1 cerk1*) are triple mutants lacking the MAMP (co) receptor; *rbohD* lacks a functional NADPH oxidase for ROS. Experiments were repeated at least two times each with 8 biological replicates for ROS assay, 2-3 biological replicates for callose deposition, and 3–4 biological replicates for colonization assays (See Supplementary Figures S2, S5, and S7 for the full ROS outburst, callose production, and colonization profiles, respectively; see Supplementary Table S2 for detailed descriptions of the strains included). Data used for ANOVA with *post hoc* Tukey's test, $P \leq 0.05$. Side color bars indicate phylogenetic affiliations of the microbiota-derived strains. Boxplot represent mean PTI responsiveness of the plant genotypes for each of the PTI traits with the boxes spanning the interquartile range (IQR, 25th to 75th percentiles), the mid-line indicates the median, and the whiskers cover the minimum and maximum values not extending beyond 1.5x of the IQR.

5.2. CHAPTER 2: Plant reactive oxygen species licenses co-habitation with a potentially pathogenic leaf commensal

We have revealed that among the microbiota-derived strains tested, the rampant colonization capacity and pathogenicity of the leaf commensal *Xanthomonas* L148 is linked with the PTI output ROS outburst as mediated by the NADPH oxidase gene *RBOHD*. In **CHAPTER 2**, we aimed to comprehensively and systematically dissect the ROS-dependency of the interaction with *Xanthomonas* L148 in light of determining the genetic and molecular mechanisms that govern this process. We also aspire to gain insight on how plant-derived ROS modulate the behavior of a potentially detrimental commensal and tame it and eventually confer beneficial services to the plant host.

5.2.1. *Xanthomonas* L148 is detrimental to *rbohD* mutant but not Col-0 wild-type plants

Leaf colonization of *rbohD* mutants with live *Xanthomonas* L148 leads to mortality within 5 dpi and this visual observation did not occur with the wildtype Col-0 plants (Figure 7a and c). In an orthogonal system, we infiltrated leaves with *Xanthomonas* L148 and observed disease-like symptoms only in *rbohD* inoculated leaves at 3 dpi (Figure 7b and d). It is important to note that *Xanthomonas* L148 activated ROS outburst in Col-0 leaves but not in *rbohD*, linking restriction of *Xanthomonas* L148 pathogenicity by ROS pathway (Figure 7e). Furthermore, *Xanthomonas* L148 does not only persisted on the leaf surface but aggressively colonized the apoplast of the *rbohD* mutants as compared to Col-0 at 3 dpi (Figure 7f). These evidences support the impression that *Xanthomonas* L148 is potentially pathogenic and its deleterious effect depends on the absence of *RBOHD* gene.

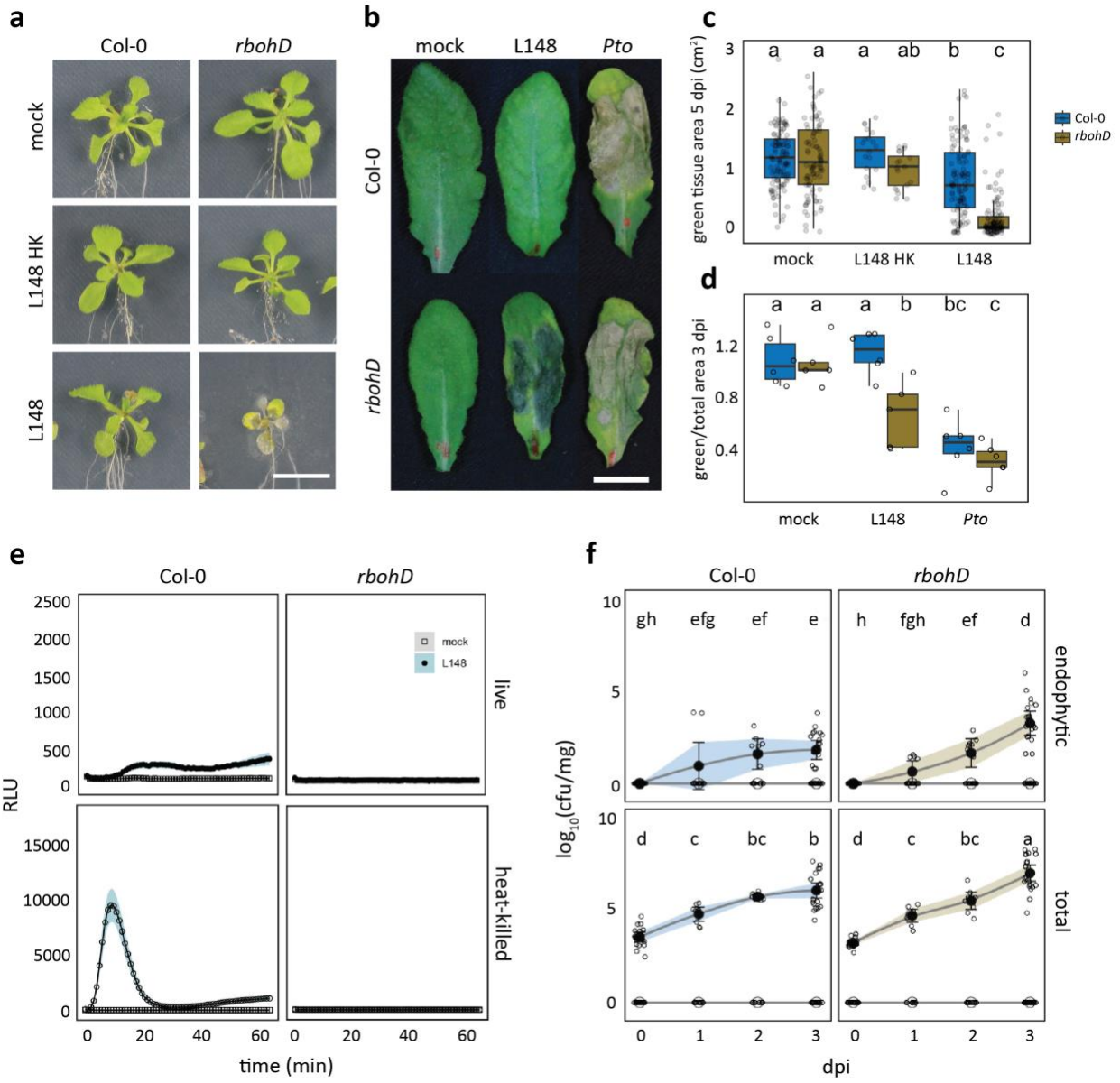

Figure 7. *Xanthomonas* L148 is detrimental to *rbohD* mutant but not to Col-0 wild-type plants. **a**, **c**. Representative images (**a**) and quantification of green tissue area (**c**) as the plant health parameter. 14-day-old Col-0 and *rbohD* plants grown on agar plates were flood-inoculated with mock and live and heat-killed (HK) *Xanthomonas* L148 (OD_{600}=0.005). Samples were taken at 5 dpi (4 independent experiments each with at least 5 biological replicates). **b, d.** Representative images **(b)** and quantitation of percentage green tissue of leaves **(d)** hand-infiltrated with mock, *Xanthomonas* L148 and *Pto* (OD_{600}=0.2). Samples were taken at 3 dpi (2 independent experiments each with 3-4 biological replicates). **e,** ROS burst profile of leaf discs of 5-to-6-week-old Col-0 and *rbohD* plants treated with live and heat-killed *Xanthomonas* L148 (OD_{600}=0.5) (at least 4 independent experiments each with 8 biological replicates). **f,** Infection dynamics of *Xanthomonas* L148 upon flood-inoculation of 14-day-old Col-0 and *rbohD* plants grown in agar plates (OD_{600}=0.005). Leaf samples were harvested at 0 to 3 dpi for total and endophytic compartments (2 independent experiments each with 3-4 biological replicates). Results in **c** and **d** are depicted as box plots with the boxes spanning the interquartile range (IQR, 25^{th} to 75^{th} percentiles), the mid-line indicates the median, and the whiskers cover the minimum and maximum values not extending beyond 1.5x of the IQR.

Results in **f** are shown as line graphs using Locally Estimated Scatter plot Smoothing (LOESS) with error bars and shadows indicating the standard errors of the mean. **c,d,f**, ANOVA with *post hoc* Tukey's test. Different letters indicate statistically significant differences ($P \leq 0.05$). This figure was adopted from Entila et al, (*in preparation*).

5.2.2. *Xanthomonas* L148 is largely insensitive to radicals

ROS, due to its highly reactive nature could directly oxidize bacterial components resulting to extensive cellular injuries which could possibly explain the observed phenomenon in Col-0 but not in *rbohD* plants. We then tested the sensitivity of *Xanthomonas* L148 to ROS compounds via H_2O_2 or O_2^{-1} instantaneous *in vitro* exposures. As opposed to our hypothesis, *Xanthomonas* L148 seemingly tolerates acute treatments with ROS compounds due to its retained viability (Figure 8a-b). More so, the same findings were obtained when a ROS generating compound, paraquat (PQ, Figure 8c) was used. It can be argued that the adverse effects of ROS compounds can only be observed upon prolonged ROS treatment. Convincingly, results showed no significant effects on the growth rates of *Xanthomonas* L148 upon chronic contact with PQ in liquid medium (Figure 8d). This plainly suggests that the rampant proliferation of *Xanthomonas* L148 in *rbohD* plants is not due to the direct microbiocidal effects of ROS but possibly by other mechanisms.

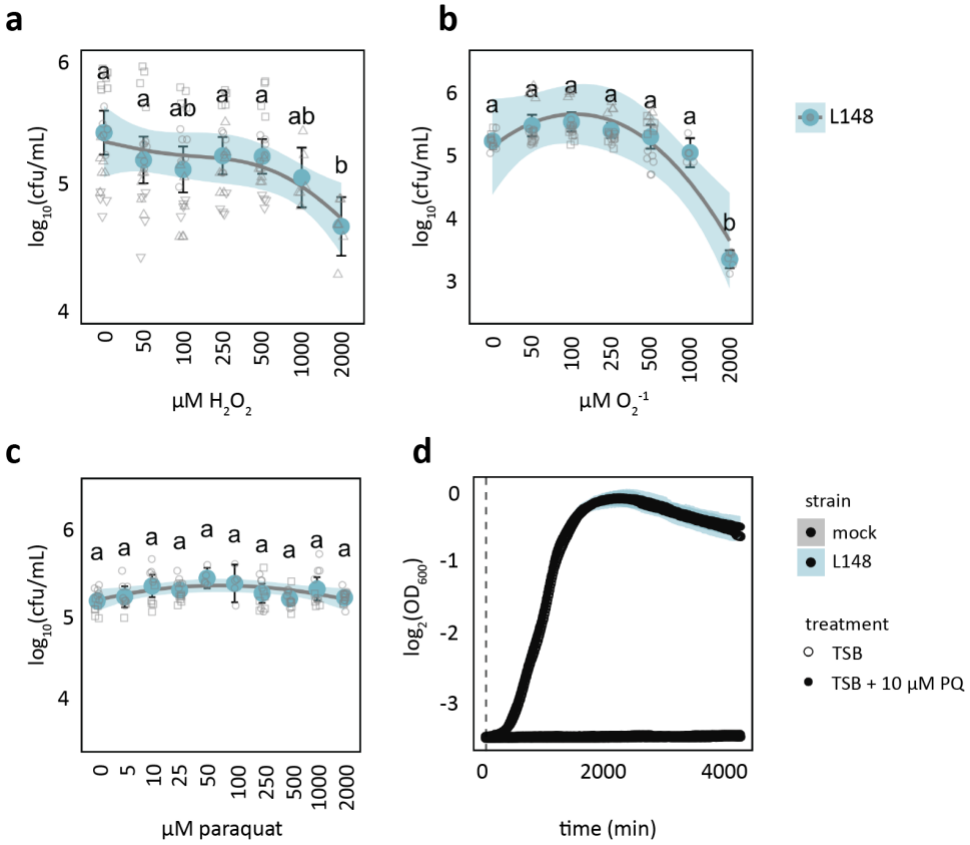

Figure 8. *Xanthomonas* L148 is not sensitive to *in vitro* exposure to ROS compounds. **a-c,** Recovery of *Xanthomonas* L148 bacterial cells (initial inoculum OD_{600}=0.02) upon acute exposure with ROS compounds H_2O_2 (**a**), O_2^{-1} (**b**), and PQ (**c**) in different concentrations (0-2000 µM). H_2O_2 treatments of different doses were done for 30 min. With 1 mol of xanthine is converted to 1 mol O_2^{-1} with 1 U xanthine oxidase at pH 7.5 at 25 °C in 1 min, O_2^{-1} treatment was done by commencing the reactions and sampling for bacterial cells for different time points: 0, 2, 4, 10, 20, 60, and 80 min to produce 0, 50, 100, 250, 500, 1000, and 2000 µM O_2^{-1} , respectively. **d,** Growth curves of *Xanthomonas* L148 in TSB upon chronic exposure of 0 or 10 µM PQ for 4000 min. **a-d**, Data were from at least 2 independent experiments each with 3-4 biological replicates. Different letters indicate statistically significant differences (ANOVA with *post hoc* Tukey's test, $P \leq 0.05$). This figure was adopted from Entila et al, (*in preparation*).

5.2.3. *Xanthomonas* L148 pathogenic potential was dampened by the presence of other leaf microbiota members

It is with intrigue and dissonance to note that a potentially pathogenic *Xanthomonas* L148 was isolated from healthy-looking *Arabidopsis* plants grown in its natural habitat indicating that it is a genuine constituent of its natural leaf microbiota. It could be postulated that in a microbial community setting, *Xanthomonas* L148 is disarmed and so *rbohD* plants will become asymptomatic. To test this, we have constructed a synthetic bacterial community which consists of nine leaf-derived isolates that were found to be robust leaf colonizers, important keystone species, were prevalent, and covers the major phyla in the natural

microbiota (Carlström et al, 2019; Thorsten et al, 2019) with which we refer as LeafSC (Figure 9a, please see Supplementary Table S2 for the list of strains). We also assessed the dose-dependence of the disease onset by using different proportions of *Xanthomonas* L148 in relation to the composition of the entire LeafSC with $L148_{P1}$ as a dose equivalent to that of each synthetic community member (L148/LeafSC, 1:9) while $L148_{P9}$ is a dosage that is the same with the entire bacterial load of the synthetic community (L148/LeafSC, 9:9). Results showed that flood inoculation of plants with the LeafSC does not result to any observable onset of disease symptoms nor conspicuously different with the mock treatment. As expected, *rbohD* plants inoculated with *Xanthomonas* L148 resulted to substantial mortality, on the other hand Col-0 plants still subsist though with lighter shoot tissues and this decline corresponds with the elevated *Xanthomonas* L148 population density in the initial inoculum (Figure 9b-c). To some extent, the killing effects of *Xanthomonas* L148 is reduced or maybe delayed in *rbohD* plants when other functional microbiota strains are present but this counter-effect is overcome when *Xanthomonas* L148 exists in higher populations (Figure 9b-c). These findings imply that the functional leaf microbiota contributes to the partial subdual of the disease symptoms caused by *Xanthomonas* L148 in *rbohD* plants potentially through niche occupancy, resource competition, or antibiosis.

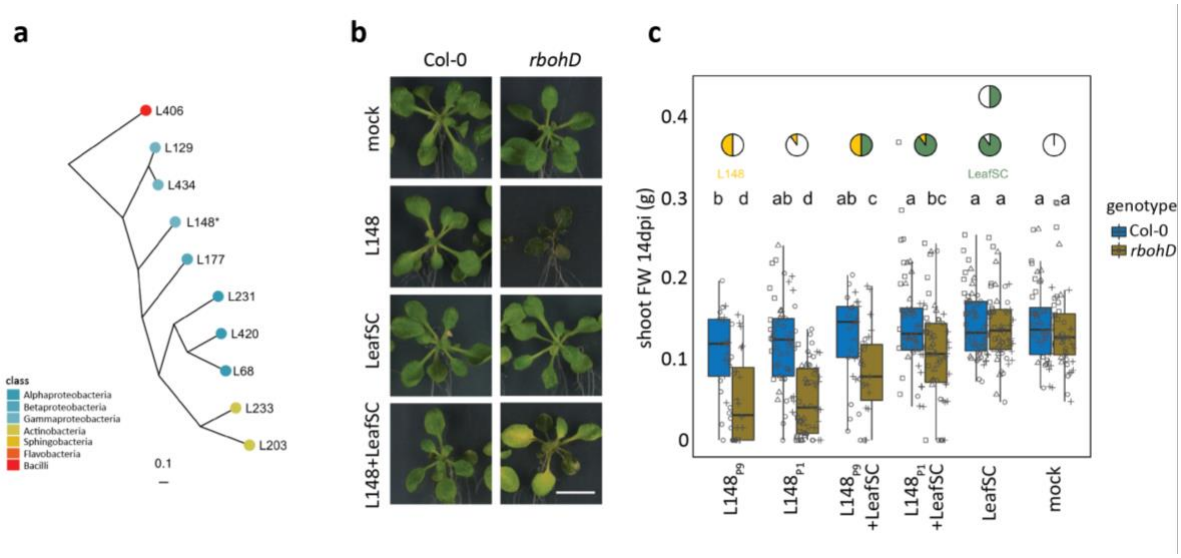

Figure 9. *Xanthomonas* L148 pathogenic potential was partially suppressed by the presence of other leaf commensal. a, Phylogenetic relationship of the strains comprising the leaf-derived synthetic community (LeafSC) which consists of strains that are robust and prevalent leaf colonizers, and taxonomically represents diverse members of the leaf microbiota. **b, c,** Representative image (**b**) and the measured shoot fresh weights (**c**) of Col-0 and *rbohD* plants flood-inoculated with mock, LeafSC, $L148_{P1}$ + LeafSC (equal portions of *Xanthomonas* L148 with each strain: L148/LeafSC, 1:9, final OD_{600}=0.01), $L148_{P9}$ + LeafSC (portion of *Xanthomonas* L148 equals the bacterial load of the all strains: L148/LeafSC, 9:9, final OD_{600}=0.01), and the equivalent doses of *Xanthomonas* L148 ($L148_{P1}$ and $L148_{P9}$, P9 is 9 times the dose

of P1). The pies indicate the relative proportion of the *Xanthomonas* L148 = yellow and LeafSC = green. Data from 2 independent experiments each with 3-4 replicates were used. Different letters indicate statistically significant differences (ANOVA with *post hoc* Tukey's test, $P \leq 0.05$). The white horizontal bar = 1cm. This figure was adopted from Entila et al, (*in preparation*).

5.2.4. *Xanthomonas* L148::Tn5 mutant screening unveils plausible genetic determinants of pathogenic potential

It is clear that *Xanthomonas* L148 is a conditional pathogen and its virulence is unlocked in the absence of functional *rbohD* gene in plants. With this, we aimed to identify the bacterial genetic determinants of this trait through a genome-wide mutant screening. In order to carry out the forward genetic study, we developed and optimized a robust high-throughput screening protocol (Supplementary Figure S9a-c) and generated and validated a *Xanthomonas* L148 Tn5 mutant library (Supplementary Figure S9d-f). This Tn5 mutant compendium was phenotyped for the loss-of-*rbohD* mortality using the developed high-scale system. From 6,862 transposon insertional mutants, 214 candidate strains consistently not decimated *rbohD* mutant plants (Figure 10a, See Supplementary Dataset S4 for the complete list of the candidate mutant strains). Most of the 214 strains did not exhibit significant defects in their *in vitro* growth parameters (growth rate, biofilm formation, and motility) in rich TSB medium or minimal XVM2 medium (Figure 10b). We found that out of the 214 strains, only 124 had transposon insertions on genes with functional annotations. Moving forward, these strains were re-tested in the typical square plate agar format and found that 18 bacterial mutants exhibited consistent loss-of-*rbohD* mortality. Out of the 18 strains, three showed very strong phenotypes namely *gspE*::Tn5, *alaA*::Tn5, and *rpfF*::Tn5 (Figure 10c and e). The candidate gene *gspE* encodes a core ATPase component of the type II secretion system (T2SS); *alaA* encodes an alanine-synthesizing transaminase involved in amino acid metabolism; and *rpfF* encodes synthase for diffusible signaling factor (DSF) constituting the quorum sensing machinery in bacteria (Figure 10d).

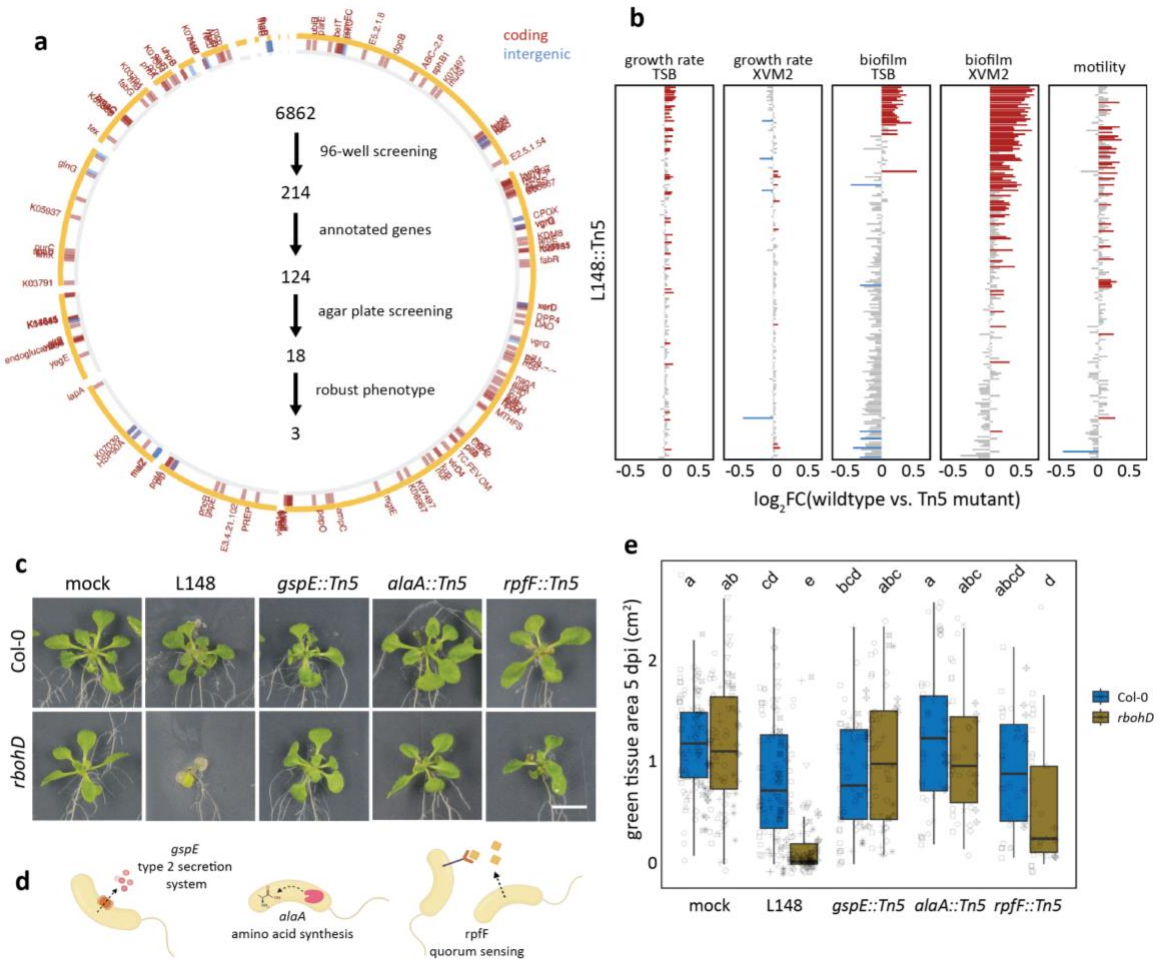

Figure 10. *Xanthomonas* L148::Tn5 mutant screening unveils genetic determinants of its pathogenic potential. a, Schematic diagram of the optimized high-throughput genetic screening for the *Xanthomonas* L148::Tn5 mutant library. Bacterial strains were inoculated onto 2-week-old *rbohD* plants followed by phenotyping at 5 dpi. **b**, Genomic coordinates of genes disrupted in the 214 *Xanthomonas* L148::Tn5 candidate strains. Total of 6862 *Xanthomonas* L148::Tn5 strains were screened for no *rbohD* killing activity in a 96-well high-throughput format (2 independent experiments). 124 strains had functional annotations and were subsequently screened using the agar plate format, which resulted in 18 strains with robust phenotypes. Finally, 3 strains were selected as the best-performing candidate strains. **c**, *In vitro* phenotypes of the 214 candidate strains: growth rates, biofilm production, and motility in rich TSB medium; growth rates and biofilm production in a minimal XVM2 medium. Data from 2 independent experiments each with 2-3 biological replicates were used for ANOVA with *post hoc* Least Significant Difference (LSD) test. Red and blue bars indicate significantly higher or lower than the wild-type *Xanthomonas* L148 ($P \leq 0.05$), respectively. **d**, **f**. Representative images **(d)** and quantification of green tissue area **(f)** as plant health parameter of Col-0 and *rbohD* plants flood mono-inoculated with *Xanthomonas* L148::Tn5 strains (OD_{600}=0.005). Samples were harvested at 5 dpi. Data from at least 4 independent experiments each with 3-4 biological replicates were used for ANOVA with *post hoc* Tukey's test. Different letters indicate statistically significant differences ($P \leq 0.05$). **e,** Graphical representation of the functions of the candidate genes. Results in **f** are depicted as box plots with the boxes spanning the interquartile range (IQR, 25th to 75th percentiles), the mid-line indicates the median, and the whiskers cover the minimum and maximum

values not extending beyond 1.5x of the IQR. Some of the illustrations created using BioRender. This figure was adopted from Entila et al, (*in preparation*).

5.2.5. Secretion, amino acid metabolism, and quorum sensing underpin conditional pathogenicity of *Xanthomonas* L148

We re-evaluated the candidate mutant strains using leaf-infiltration assays. Results showed that the disease progression required live *Xanthomonas* L148 as heat-killed bacteria did not elicit the same response, excluding the possibility of hypersensitive response (Figure 11a). Concurring with the previous systems (high-throughput and square plate set-ups), the mutant strains lost their capacity to cause disease symptoms in *rbohD* mutant plants (Figure 11a). It can be postulated that the absence of symptoms in *rbohD* plants is due to the aberration in the colonization capacities of these mutant strains. As shown before, wild-type *Xanthomonas* L148 exhibited increased colonization in both total and endophytic compartments of *rbohD* leaves. In contrast, *gspE*::Tn5 mutant exhibited colonization capacities comparable to *Xanthomonas* L148 wild-type in Col-0 leaves however failed to establish on the same levels in *rbohD* plants (Figure 11b). On the other hand, *alaA*::Tn5 mutants had a compromised colonization capacity in Col-0 plants while *rpfF*::Tn5 mutant strains colonized *rbohD* leaves similar to the wildtype *Xanthomonas* L148. Nonetheless, all of the mutant strains did not just persist but were able to actively colonize in the leaf endosphere (Figure 11b). These indicate that the *gspE*::Tn5 mutant retained its general colonization ability but specifically compromised its capability to efficiently colonize *rbohD* plants as compared to the wild-type *Xanthomonas* L148. Additionally, the mutant strains have retained the ability to induce ROS outburst on Col-0 leaves though in an attenuated manner using live cells. However, the mutant strains, except *alaA*::Tn5, have comparable ROS outburst induction in Col-0 leaves using heat-killed cells as trigger (Figure 11c). All of the strains did not elicit any detectable ROS outburst signal for *rbohD* leaves. Correlation analysis revealed a negative association between colonization and plant health indicating that the observed leaf symptoms can be explained by the aggressive colonization of the strains (Figure 11d).

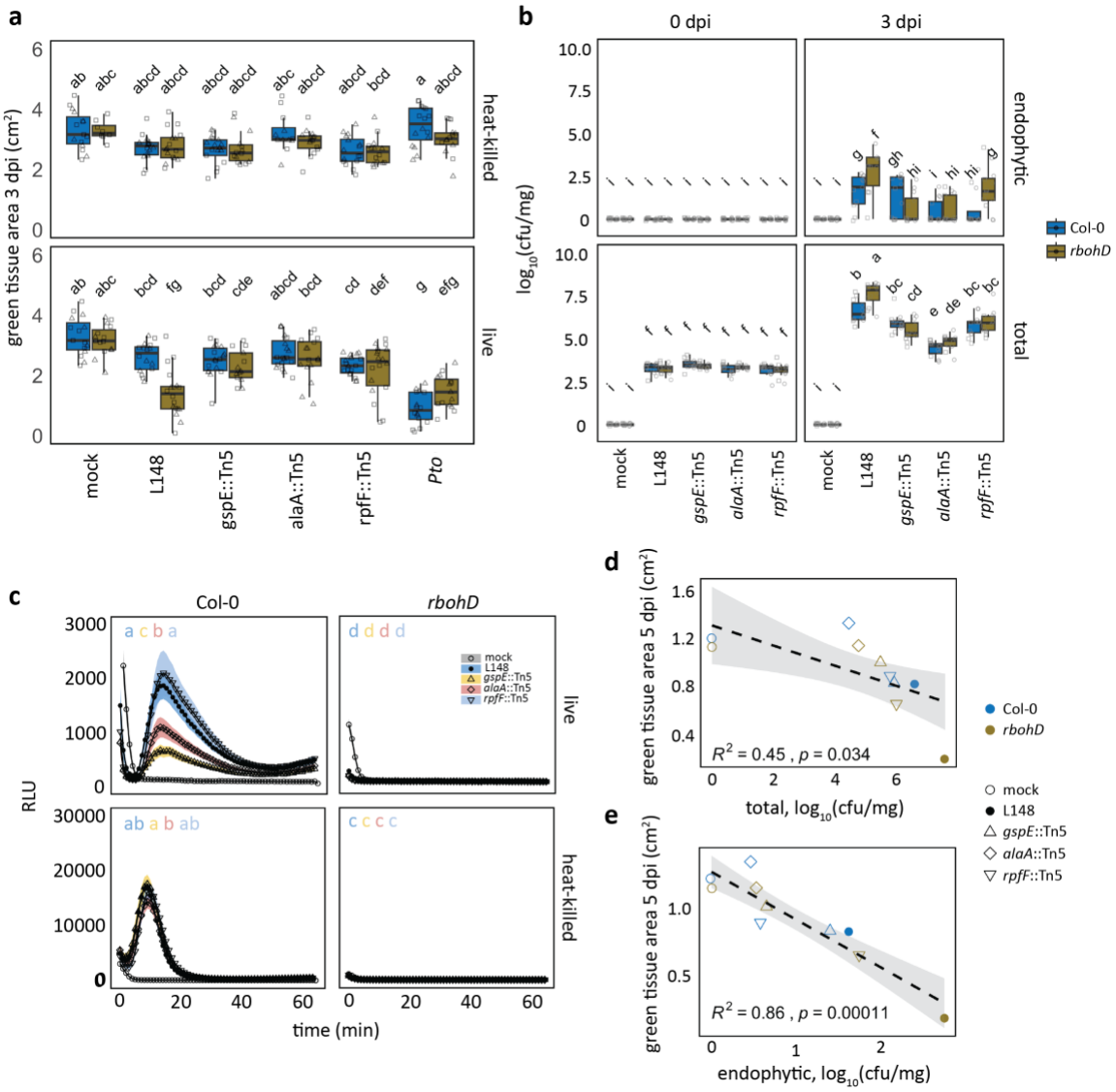

Figure 11. T2SS, amino acid metabolism, and quorum sensing underpin conditional pathogenicity of *Xanthomonas* L148 in *rbohD* plants. a, Quantification of green tissue area of hand-infiltrated 5 to 6-week-old Col-0 and *rbohD* leaves with *Xanthomonas* L148::Tn5 mutant strains using live and heat-killed cells as inoculum (OD_{600}=0.2). Samples were collected at 3 dpi (2 independent experiments each with 3-4 biological replicates). **b**, Infection dynamics in axenic Col-0 and *rbohD* plants flood-inoculated with *Xanthomonas* L148::Tn5 mutant strains (OD_{600}=0.005). Samples harvested at 0 to 3 dpi for total and endophytic leaf compartments (2 independent experiments each with 3-4 biological replicates). **a,b,** ANOVA with *post hoc* Tukey's test. Different letters indicate statistically significant differences ($P \leq 0.05$). Results in **a** and **b** are depicted as box plots with the boxes spanning the interquartile range (IQR, 25th to 75th percentiles), the mid-line indicates the median, and the whiskers cover the minimum and maximum values not extending beyond 1.5x of the IQR. **c**,**d,** Pearson correlational analyses of plant health performance measured as green tissue area against bacterial colonization capacities in the total **(c)** and endophytic **(d)** compartments (R^2, coefficient of determination). This figure was adopted from Entila et al, (*in preparation*).

All of the three mutant strains were not defective in growth, biofilm production, and motility in rich TSB medium (Figure 12a-c). Also, the mutant strains remained insensitive to PQ treatment, indicating retained tolerance to chronic ROS exposure (Figure 12a-b). *In vitro* growth phenotypes were also unchanged in minimal XVM2 medium apart from an increase in biofilm production for *gspE*::Tn5 and *alaA*::Tn5 mutant strains (Figure 12d). The Xanthomonas L148::Tn5 mutants were also assessed for auxotrophy in a minimal XVM2 medium for amino acids involved in *alaA* function: alanine, glutamic acid, and arginine. Though there were no significant changes in the growth rates among the L148::Tn5 mutants with the wild-type strain in general, *alaA::*Tn5 mutant seem to approach the death phase in a rapid fashion in the presence of glutamic acid indicating that *alaA::*Tn5 is sensitive to or is unable to utilize this amino acid (Supplementary Figure S10).

Secretion of extracellular enzymes acting on plant cell walls is a canonical feature of plant pathogens to breach the host physical barriers (Salmond, 1994). Bacterial pathogens often utilize T2SS to deliver these enzymes to their plant host (Cianciotto et al, 2005). We conducted enzyme secretion plate assays to test the proficiency of these strains to degrade different substrates (carbohydrates, protein, and lipids). The wildtype *Xanthomonas* L148 was able to secrete extracellular enzymes that can degrade the proteinaceous substrates gelatin and milk; and the carbohydrates pectin and carboxymethyl-cellulose. Notably, the *gspE*::Tn5 mutant unsuccessfully degrade these substrates as compared to the wild-type and other mutant strains, indicative of ineffectual secretion activities (Figure 12e-f). This insinuates the possibility that the lack of disease progression in *rbohD* plants with the *gspE*::Tn5 mutant strain can also be explained by its inability to extracellularly secrete enzymes via T2SS to degrade the host plant cell walls.

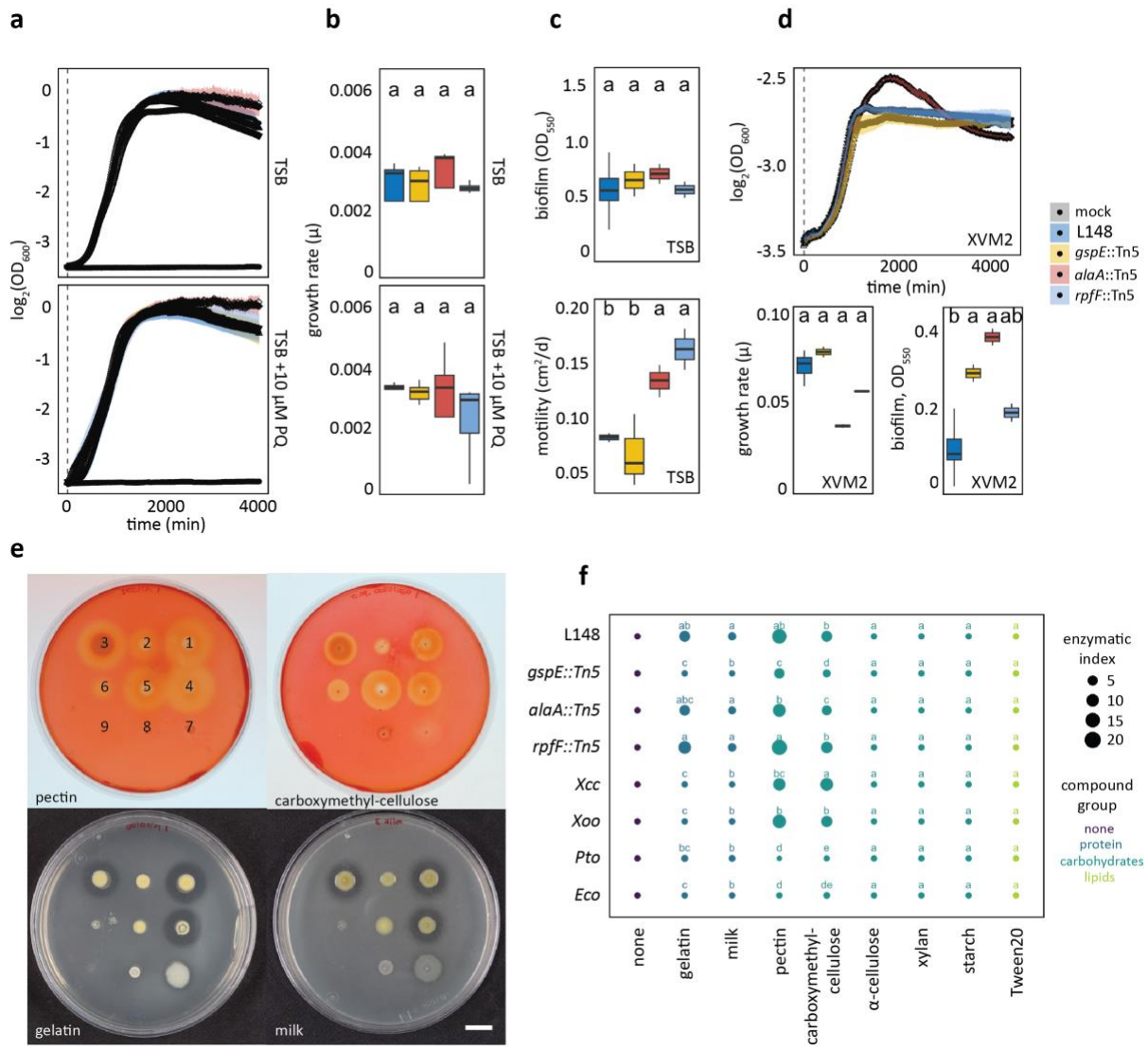

Figure 12. The *Xanthomonas* L148 *gspE*::Tn5 mutant compromises extracellular secretion activities. a,b, Growth curves (**a**) and rates (**b**) of *Xanthomonas* L148::Tn5 candidate mutant strains in TSB upon chronic exposure to 0 or 10µM PQ for 4000 min (2 independent experiments each with 3 biological replicates). **c,** Biofilm production and motility of *Xanthomonas* L148::Tn5 candidate mutant strains in TSB medium (2 independent experiments each with 2-3 biological replicates). **d**, Growth curves, growth rates, and biofilm production of *Xanthomonas* L148::Tn5 candidate mutants in XVM2 (2 independent experiments each with 2-3 biological replicates). **e**, Exemplary images of plate assays for secretion activities of bacterial strains (1 = wildtype *Xanthomonas* L148; 2 = *gspE*::Tn5; 3 = *alaA*::Tn5; 4 = *rpfF*::Tn5; 5 = *Xanthomonas campestris* pv. *campestris* [*Xcc*]; 6 = *X. oryzae* pv. *oryzae* [*Xoo*]; 7 = *P. syringae* pv. *tomato* DC3000 [*Pto*]; 8 = *E. coli* HB101 [*Eco*]; and 9 = mock) for the carbohydrates pectin and carboxymethylcellulose, and the proteins gelatin and milk. **f**, Enzymatic indices for bacterial strains grown on TSB supplemented with 0.1 % substrates (proteins: gelatin and milk; carbohydrates: pectin, carboxymethyl-cellulose, α-cellulose, xylan, and starch; lipids: Tween20) after 2 day-incubation at 28 °C (3 biological replicates). The enzymatic indices were calculated by subtracting the size of the colony with the zone of clearance, indicative of substrate degradation by the strain after 2-3 d. **b,d,** the growth rate, µ was calculated by running rolling regression with a window of 5 h along the growth curves to determine the maximum slope. **b-d, f**, Different letters indicate statistically significant differences (ANOVA with *post hoc*

Tukey's test, $P \leq 0.05$). Results in **b**, **c** and **d** are depicted as box plots with the boxes spanning the interquartile range (IQR, 25th to 75th percentiles), the mid-line indicates the median, and the whiskers cover the minimum and maximum values not extending beyond 1.5x of the IQR. This figure was adopted from Entila et al, (*in preparation*).

With the *in planta, ex planta*, and *in vitro* evidences, emphasis and comprehensive characterization was placed over the *gspE*::Tn5 mutant. To unrefutably show genetic causality that *gspE* determines *rbohD*-dependent pathogenicity, we generated two independent *gspE* deletion mutant strains (***ΔgspE***_1 and ***ΔgspE***_2) via homologous recombination. Both of the *gspE* deletion mutants as the *gspE*::Tn5 mutant, showed loss of secretion activities and failed to cause disease in *rbohD* plants (Figure 13a-b). Taken together, *gspE*, an integral component of T2SS, is conclusively required to deploy *Xanthomonas* L148 pathogenicity in *rbohD* mutant plants.

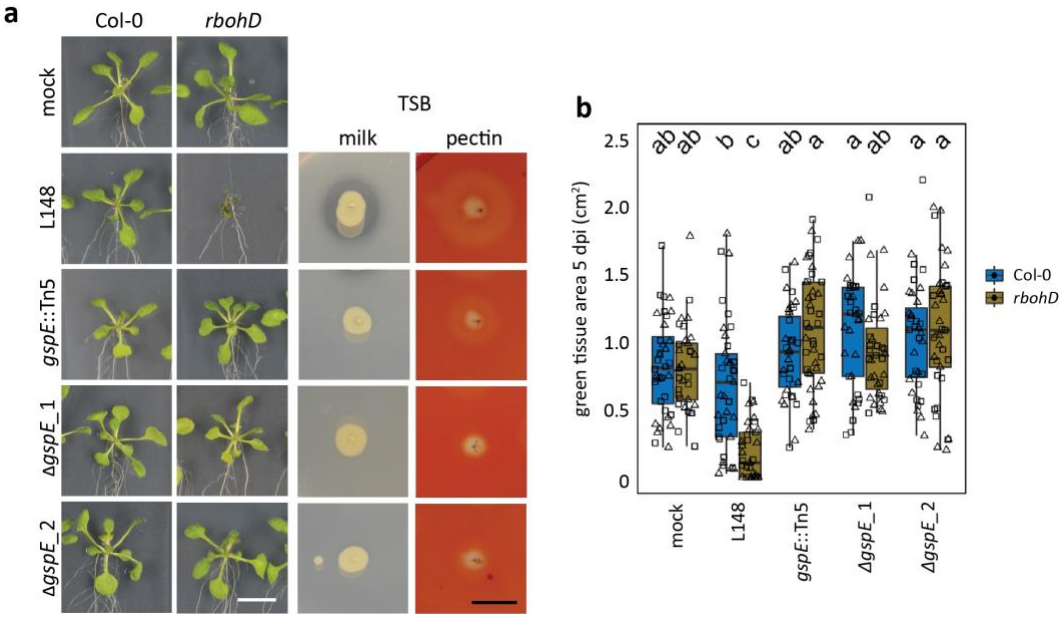

Figure 13. The T2SS component *gspE* gene is a genetic determinant for the loss of the *rbohd*-dependent pathogenicity of *Xanthomonas* L148. a, Images of axenic Col-0 and *rbohD* plants flood-inoculated (OD_{600}=0.005) with the wildtype *Xanthomonas* L148, *gspE*::Tn5 mutant and 2 ***ΔgspE*** lines at 5 dpi. Plate images of secretion activities of the bacterial strains grown on TSB with either milk or pectin as substrate after 2-3 days. **b**, Measured green tissue area as the plant health parameter for Col-0 and *rbohD* plants flood-inoculated with the bacterial strains at 5 dpi (2 independent experiments each with 3-5 biological replicates). Different letters indicate statistically significant differences (ANOVA with *post hoc* Tukey's test, $P \leq 0.05$). Results in **b** are depicted as box plots with the boxes spanning the interquartile range (IQR, 25th to 75th percentiles), the mid-line indicates the median, and the whiskers cover the minimum and maximum values not extending beyond 1.5x of the IQR. This figure was adopted from Entila et al, (*in preparation*).

5.2.6. Plant reactive oxygen species modulates cooperative behavior of *Xanthomonas* L148

Since *Xanthomonas* L148 pathogenicity is provisionally exerted in the absence of ROS through RBOHD and that *in vitro* results dispute against the general cellular toxicity of ROS, it can be posited that *RBOHD*-mediated ROS production suppresses virulence of *Xanthomonas* L148 (Figure 7 and 8). To gain insight into this, we conducted *in planta Xanthomonas* L148 bacterial transcriptome profiling for Col-0 and *rbohD* plants (Nobori et al, 2018a). Plants were flood-inoculated with *Xanthomonas* L148 and shoots were sampled at 2 dpi wherein bacterial titers were still indistinguishable at this time point but later became significantly different between Col-0 and *rbohD* leaves at 3 dpi (Figure 7f). Thus, with the bacterial transcriptomes observed at this time window, one can exclude the expression differences attributable to the different bacterial population densities, known to affect bacterial transcriptome (Nobori et al, 2018b).

Principal component (PC) analysis revealed that *in planta Xanthomonas* L148 transcriptomes were distinct in Col-0 and *rbohD* plants (Figure 15b). Statistical analysis revealed 2946 differentially expressed genes (DEGs) upon comparing *in planta* bacterial transcriptomes in Col-0 with *rbohD* leaves (threshold: q-values ≤ 0.05), with which 546 genes were up-regulated and 2400 genes were down-regulated in Col-0 compared with *rbohD* plants (Figure 14a, See Supplementary Dataset S5 for the details on DEGs). Strikingly, most T2SS apparatus genes were down-regulated in Col-0 as compared to *rbohD*, specially *gspE* (Figure 14c-e). The DEGs were significantly enriched for the candidate genes detected from the *Xanthomonas* L148::Tn5 mutant screening (29 up-regulated and 73 down-regulated out of 214 genes in Col-0 as compared to *rbohD* inoculated plants, hypergeometric test, p-value = 1.00E-10***), which further strengthens the concurrence of the genetic evidence with the obtained bacterial transcriptomic profiles *in planta* (Figure 14a). The DEGs were also significantly over-represented for carbohydrate-active enzymes (CAZyme, 4 up-regulated, 49 down-regulated out of 135 in Col-0 as compared to *rbohD* colonized plants, hypergeometric test, p-value = 9.54E-8***, Figure 14a), which is consistent with the notion that CAZymes function in virulence. More so, 6 *Xanthomonas* L148::Tn5 mutants have insertion in genes annotated as CAZymes, 5 of which are significantly down-regulated in Col-0 as compared with *rbohD* inoculated plants. The significantly down-regulated CAZymes in Col-0 plants can potentially degrade plant cell wall components cellulose, pectin, arabinan, α-glucan, β-glucan, and β-mannan (Figure 14c, Supplementary Figure S11). Pathway enrichment analysis revealed that upregulated gene clusters such as clusters 3, 9, and 14 are enriched for biological functions related to chemotaxis and attachment (K15125, K13924, and K05874), while gene clusters down-regulated in Col-0 such as clusters 8, 10, and 12 are enriched for pathways involved in transport and detoxification processes (K02014 and K00799, Figure

14f, See Supplementary Dataset S6 for the clustering membership and the enriched GO terms).

With a closer look, the identified candidate genes *gspE* and *alaA* were substantially repressed while *rpfF* was marginally subdued in Col-0 juxtaposed to *rbohD*, which supports the hypothesis that these genes are required and thus tightly regulated by the immune-competent wild-type Col-0 plants to prevent disease progression (Figure 14g). These findings were re-confirmed in independent experiments using qRT-PCR where all the candidate genes were suppressed in Col-0 compared to *rbohD* plants (Figure 14h). It can be postulated that ROS directly regulate the expression of these genes. Therefore, *Xanthomonas* L148 bacterial cells were grown *in vitro* in the presence of PQ and conducted gene expression analysis. We found that the expression of the candidate genes *gspE, alaA*, and *rpfF* is suppressed in *Xanthomonas* L148 upon chronic exposure to ROS (Figure 14i). Taken together, these findings suggest that *Xanthomonas* L148 colonization triggers RBOHD-mediated ROS production which directly inhibits the expression of genes related to virulence, in particular the components of T2SS in Col-0 plants. Contrastingly, the absence of ROS production in *rbohD* mutant plants switches on the pathogenicity of *Xanthomonas* L148 leading to disease onset.

To gain insight on the evolution of the pathogenicity of *Xanthomonas* L148, available genomes of other Xanthomonadales members, including the potentially pathogenic close-relative *Xanthomonas* L131 (Pfeilmeier et al, 2021) and the commensal *Xanthomonas* L70 in the AtSPHERE culture collection, together with some pathogenic *Xanthomonas* strains (except *X. massiliensis*, an isolate from human feces) were interrogated for the occurrence of secretion systems and their potential CAZyme catalogues. In general, all Xanthomonadales strains encode both T1SS and T2SS genes but the latter have increased copies for the pathogenic and potentially pathogenic strains (Supplemental Figure S12a). Moreso, the pathogenic and potentially pathogenic Xanthomonadales strains have expanded its CAZyme repertoire with proclivities for plant cell wall components: α-, β-glucans, β-mannans, arabinan, cellulose, and pectin (Supplemental Figure S12b-c). These indicate that though secretion systems are prevalent among the Xanthomonadales members, CAZyme repertoire expansion is key feature of pathogenic and potentially pathogenic strains.

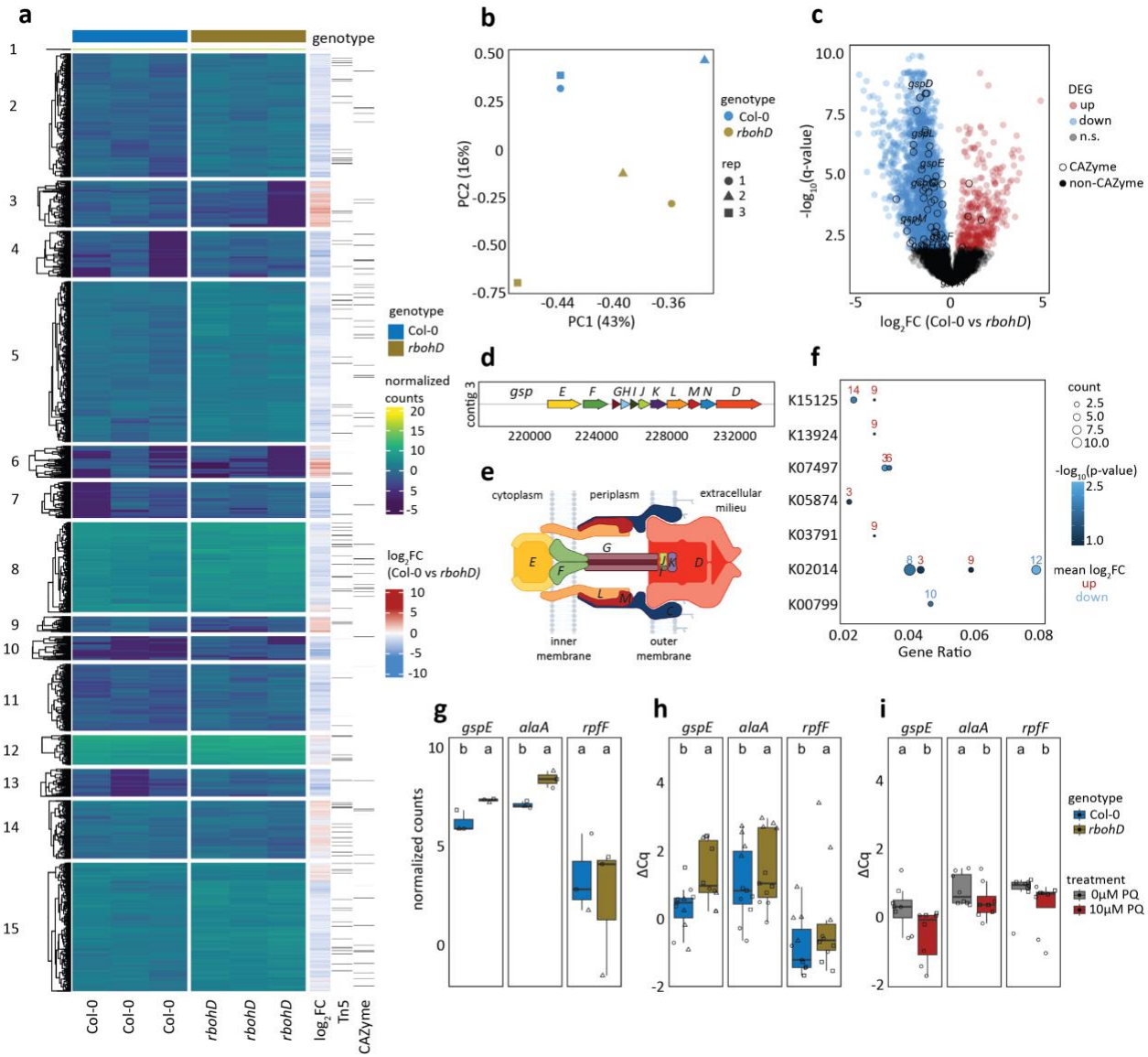

Figure 14. Plant ROS suppress T2SS genes including *gspE* of *Xanthomonas* L148. a, Heatmap representation of *in planta* bacterial transcriptome landscape of the wildtype *Xanthomonas* L148 in Col-0 and *rbohD* plants. Leaves of 2-week-old plants were flood-inoculated with L148 and samples were taken at 2 dpi. Gene clusters were based on k-means clustering of the normalized read counts. DEGs were defined based on $|\log_2 FC > 1|$ and q-value < 0.05. Sidebars indicate the $\log_2$ fold changes of Col-0 compared with *rbohD*, *Xanthomonas* L148::Tn5 candidate genes (the 214 candidates), and the genes annotated as CAZyme. **b**, Principal component (PC) analysis of the *in planta Xanthomonas* L148 transcriptome for DEGs in Col-0 and *rbohD* plants. **c**, Volcano plot of the DEGs with which T2SS component genes were labelled and CAZymes highlighted. **d**, Genomic architecture of the T2SS genes. **e**, Graphical representation of T2SS assembly. **f**, KEGG pathway enrichment analysis of the gene clusters (indicated in numbers) in **a**. **g**, RNA-Seq normalized counts of *gspE*, *alaA*, and *rpfF*. **h**, Independent qRT-PCR experiments for *in planta* expression profiling of *gspE*, *alaA*, and *rpfF*. Experiments were performed as in RNA-seq with 2 independent experiments each with 3–4 biological replicates. **i**, qRT-PCR *in vitro* expression profiling of *gspE*, *alaA*, and *rpfF* in *Xanthomonas* L148 wildtype strain grown in TSB ± 10 μM PQ for 24 h (2 independent experiments each with 3–4 biological replicates). **h,i,** Gene expression was

normalized against the housekeeping gene *gyrA*. Different letters indicate statistically significant differences (ANOVA with *post hoc* Tukey's test, $P \leq 0.05$). Results in **g–i** are depicted as box plots with the boxes spanning the interquartile range (IQR, 25th to 75th percentiles), the mid-line indicates the median, and the whiskers cover the minimum and maximum values not extending beyond 1.5x of the IQR. Some illustrations were created with BioRender. This figure was adopted from Entila et al, (*in preparation*).

5.2.7. Protective function of *Xanthomonas* L148 is genetically uncoupled to its pathogenic potential

Core members of the phyllosphere microbiota are known to confer protective function against foliar pathogens (Vogel et al, 2021) and it is attractive to assess if a conditionally pathogenic microbiota member can offer beneficial services to its plant host. To address this question, Col-0 and *rbohD* plants were pre-colonized with the *Xanthomonas* L148 or *gspE*::Tn5 mutant strain for five days and then were challenged with the bacterial pathogen *Pto*. Bacterial titers of *Xanthomonas* L148 and *Pto* were determined for the endophytic and total leaf compartments at 0 and 3 dpi. As *Xanthomonas* L148 killed *rbohD* mutant plants, we were not able to measure *Pto* titers in this condition. Pre-colonized Col-0 plants with either the wildtype *Xanthomonas* L148 or *gspE*::Tn5 mutant had increased resistance against *Pto* (Figure 15a). Interestingly, *rbohD* mutant plants pre-colonized with *gspE*::Tn5 strains showed increased resistance against *Pto*, mimicking *Xanthomonas* L148 pre-colonized Col-0 plants (Figure 15a). More so, Col-0 and *rbohD* plants pre-colonized with *gspE*::Tn5 had marginally better plant performance as compared with the non-inoculated plants after *Pto* challenge (Figure 15c-d), suggesting that the strain promotes plant fitness in pathogen encounter. This also indicates that the protective role of *Xanthomonas* L148 is genetically uncoupled from the *gspE*-dependent pathogenic potential, even so that protection by this strain is not reliant on the *RBOHD* gene. Invasion by *Pto* did not result in a significant decline in *Xanthomonas* L148 and *gspE*::Tn5 populations (Figure 15b), denoting a strong colonization competence and resistance of the commensal *Xanthomonas* L148 against pathogen invasion. In summary, these results revealed that RBOHD-produced ROS turn the potentially harmful *Xanthomonas* L148 into a beneficial bacterium, thereby protecting the plant from the aggressive pathogen colonization.

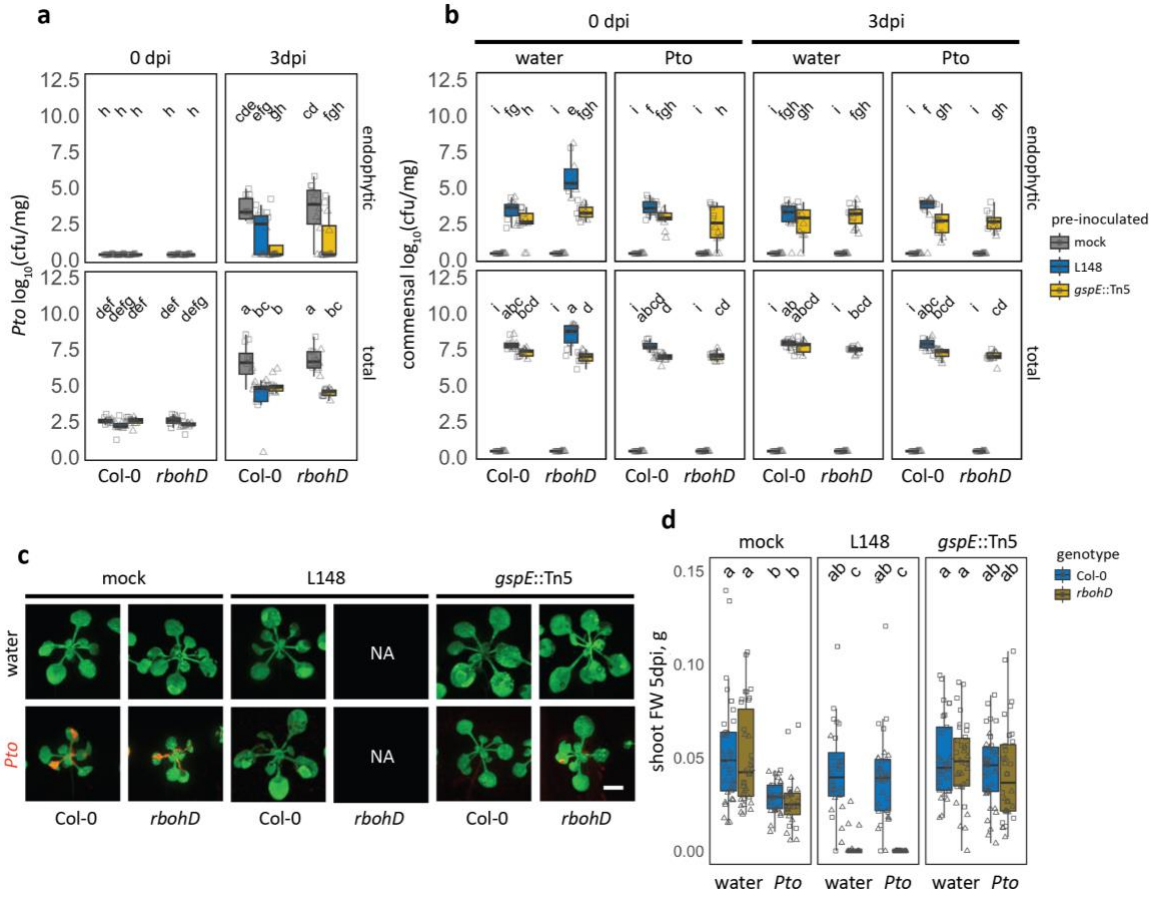

Figure 15. RBOHD-mediated ROS turn *Xanthomonas* L148 into a beneficial bacterium. a, b, 14-day-old Col-0 and *rbohD* plants grown on agar plates were flood-inoculated with wildtype *Xanthomonas* L148 and *gspE*::Tn5 (OD_{600}=0.005) for 5 days followed by spray infection with *Pto*. Bacterial titers were determined at 0 and 3 dpi (**a**, *Pto*; **b**, L148) (2 independent experiments each with 6 (**a**) or 3-5 (**b**) biological replicates). **c, d,** Representative images (**c**) and quantification of shoot fresh weight as a plant health parameter (**d**). 14-day-old Col-0 and *rbohD* plants grown on agar plates were flood-inoculated with wildtype *Xanthomonas* L148 and *gspE*::Tn5 (OD_{600}=0.005) for 5 days followed by spray infection with *Pto*. Samples were taken at 5 dpi (2 independent experiments each with 3–5 biological replicates). Different letters indicate statistically significant differences (ANOVA with *post hoc* Tukey's test, $P \leq 0.05$). Results in **a**-**b, d** are depicted as box plots with the boxes spanning the interquartile range (IQR, 25th to 75th percentiles), the mid-line indicates the median, and the whiskers cover the minimum and maximum values not extending beyond 1.5x of the IQR. This figure was adopted from Entila et al, (*in preparation*).

6. DISCUSSION

6.1. CHAPTER 1: Microbiota members elicits varying immunogenicity discordant with their phylogeny

In this study we have profiled a handful of taxonomically diverse strains for their potential to trigger PTI responses, in particular ROS outburst, transcriptional reprogramming, and callose deposition, and also microbial growth. We have shown that the microbiota members can induce varying PTI outputs and can also colonize the leaf compartments though in varying extents. Based on the immune responses, in particular ROS burst profiles, most plant microbiota members can elicit ROS effluxes especially when MAMPs are heat released indicating their immunogenicity although intriguingly few strains did not induce any response (Figure 2; Supplementary Figures S2 and S3). These strains can be broadly categorized onto 4 classes of immune reactivity (summarized in Figure 16): **immune-active** strains can immediately elicit immune responses with intact cells (eg. *Pseudomonas* L15); **immune-evasive[1]** strains only induce immune outputs when MAMPs are released but the presence of live cells can dampen the immune response indicative of active interception by the commensal potentially through release of factors that degrade self-derived MAMPs or halt immune-signaling (eg. *Burkholderia* L177); **immune-evasive[2]** strains can only evoke immune response with heat-killed cells indicating that these microbes escape recognition by precluding release of MAMPs (eg. *Xanthomonas* L70); and **immune-quiescent** strains which do not elicit observable immune responses even when the MAMPs are liberated (eg. *Flavobacterium* R935). We propose the term “quiescent” as opposed to “silent” since Gauthier et al (2021) had used “silent” in a context that connotes no intention for the microbe to adapt to the target host immunity, to describe immunogenicity of MAMPs from microbes isolated from extreme environments (eg. deep sea) against unnatural hosts (eg. mice or human) from which neither have overlapping ecologies, share the same habitats, nor the microbe virtually encounter these hosts. Quiescent indicates dormancy and contingently suggests the potential to become immunogenic as the microbiota member and the host hitherto co-evolve.

We have revealed that these immune responses are attuned in a strain-specific manner as indicated with the poor association of PTI outputs with microbial colonization in general and the detected “adaptive shifts” across the lineages (Figure 5a-c). These signify that physiological consequences and the fate of the host-microbiota interaction are far more complicated and further highlights that the perception of the nuanced compendium of stimuli, triggering the cascade of immune signals, and the eventual restriction of microbial colonization or reconfiguration of host physiology are distinct events that to a certain degree, differentially or autonomously fine-tuned and tailored for each strain. Previous findings have revealed a substantial correlation in the MAMP conservations with the gene clusters functionally associated with defense response, indicative of corollary

dependence of transcriptional reprogramming to MAMP immune-potency (Nobori et al, 2022). A number of studies had dissected host responses with a single MAMP peptide derived from the microbiota members (Parys et al, 2021; Colaianni et al, 2021; Clasen et al, 2023; Vatanen et al, 2016) which might dismiss the possibility that the combination of MAMPs has synergistic effects or some components of the microbe act as an adjuvant to amplify immune reactivity. Moreso, MAMP responsiveness does not necessarily ensue changes in plant host phenotype (such as susceptibility or resistance to diseases) nor the type of interaction (beneficial or detrimental) since MAMPs derived from pathogenic or mutualistic bacterium can induce the same PTI responses (Veluchamy et al, 2014; Stringlis et al, 2018). Also, different types of MAMPs or its variants can elicit quantitatively different intensities of immune responses and detection of these molecular patterns might not essentially result to the same immune outputs, indicative of different underlying gene networks, and each immune readouts are tailored to the MAMP epitope or to the catalogue of MAMPs a particular microbe possesses (Parys et al, 2021; Colaianni et al, 2021; Clasen et al, 2023; Spindler et al; Hacquard et al, 2017). For instance, *Xanthomonas* L148 activates ROS burst mainly via FLS2 while EFR for callose production, on the other hand *Acinetobacter* L130 activates both ROS burst and callose deposition through EFR perception (Supplementary Figure S2 and S5). As we have also revealed, some strains, in particular *Pseudomonas* L127 still elicit immune responses despite the absence of critical co-receptors indicating that there are other yet-to-be-characterized MAMP-PRR partners involved in the microbiota recognition (Supplementary Figure S2).

We have also revealed potential host regulators of the PTI response through implementation of combined gene network analysis and machine learning approach to our plant transcriptomic data (Supplementary Figure S8, Supplementary Dataset S3). We have uncovered the potential link of WRKY transcription factors, MAP kinases, and cell-death pathways in the modulation of PTI responses with the resident microbiota and have extended its fundamental role of immunity against pathogens. In agreement with our findings, *WRKY30* has been identified to be induced by a wide range of phyllosphere microbiota members as part of the general non-self response and by the rhizosphere microbiota (Maier et al, 2021; Ma et al, 2021). Likewise, it has been recently shown that the microbiota or its metabolite modulate ROS and cell-death in mammals (Castillo-Ruiz et al, 2018; Tintelnot et al, 2023). Nevertheless, these candidate genes need to be further assessed and experimentally validated.

Here, we observed that generally, most microbiota members of *A. thaliana* are perceived through the EFR receptor (Supplementary Figures S2 and S5), indicative that EF-Tu peptides serve as the main motif of recognition to elicit appropriate defense programs upon recognition of the resident microbiota. So much so, a number of strains have

increased colonization in *efr* mutants which emphasizes the fundamental link of microbial perception with bacterial colonization (Supplementary Figure S7). This observation also coincides with the GWAS finding that *efr* (and also *rbohD*) is a plausible genetic determinant for response to varying MAMP epitopes in *A. thaliana* natural populations (Vetter et al 2016). Although EFR is a Brassicaceae lineage specific innovation (Zipfel et al, 2006), other fragments of the EF-Tu peptide seem to be recognized by yet-unknown receptors and were immunogenic to some rice cultivars (Furukawa et al, 2014). Also, the interfamily transfer of the EFR to Solanaceous species is sufficient to confer broad spectrum resistance to pathogens indicating that the downstream genetic components of EFR is evolutionarily conserved (Lacombe et al, 2010). These findings suggest that EF-Tu peptides might be a prevalent microbial motif for host detection across the plant kingdom.

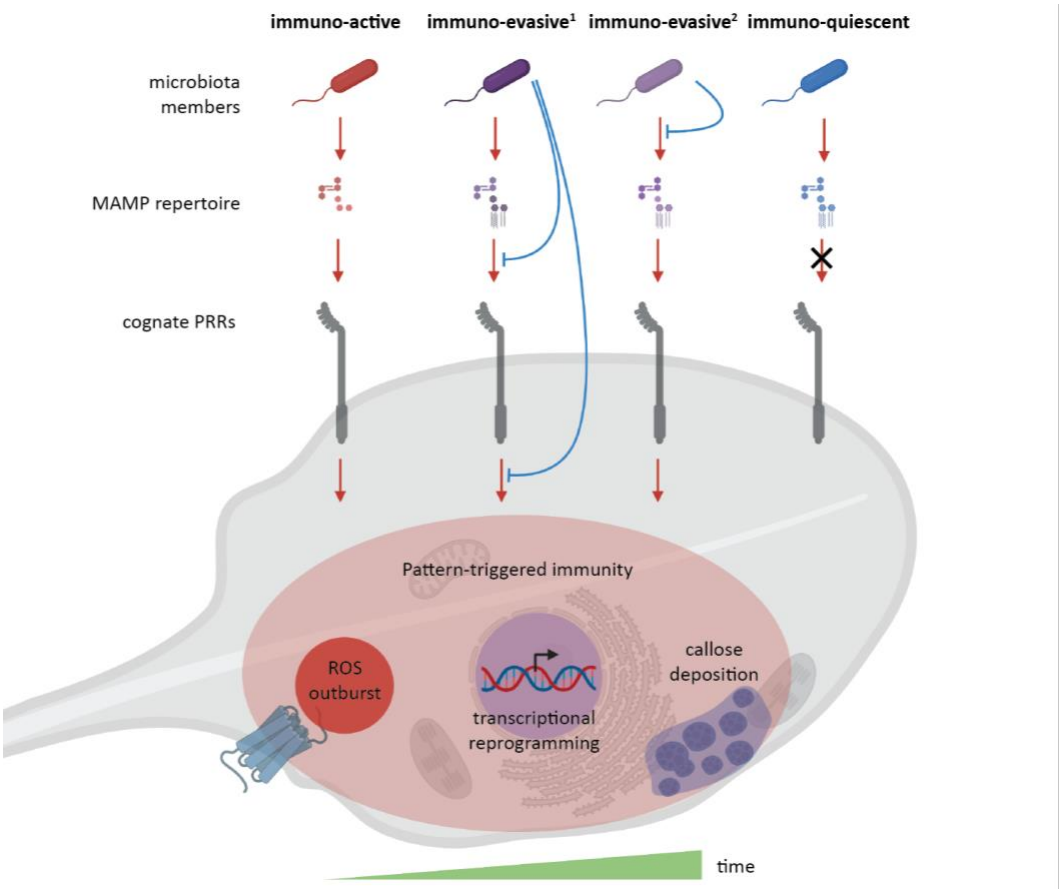

Figure 16. Immunological model of microbiota members. Microbiota members can be classified into 4 classes of immunogenicity: immune-active strains can induce PTI with live intact cells; immune-evasive[1] strains only induces PTI with heat-killed cells and the live cells actively reduce the immune response suggestive of mechanisms involving sequestration or degradation of self-derived MAMPs and/or release of factors dampening immune responses; immune-active[2] only induces PTI with heat-killed cells indicative of evasion via preclusion of MAMP release; and immune-quiescent strains do not induce observable PTI responses.

6.2. CHAPTER 2: Plant reactive oxygen species licenses co-habitation with a potentially pathogenic leaf commensal

We have identified from our screening *Xanthomonas* L148 as a potentially pathogenic member of the phyllosphere microbiota, and its deleterious effect depends on the plant host RBOHD function (Figures 7a-d) wherein the plant ROS licenses co-habitation with the conditional pathogenic microbiota member. Our results strongly entail that the plant host "domesticates" and instructs its microbial members by means of ROS as a molecular message and harness it for its own benefits. The stringent control of the host over the potentially pathogenic members of their microbiota has been currently exemplified in animal systems. For example, the host secreted intestinal immunoglobulin T (sIgT) maintains microbiota homeostasis. The depletion of sIgT results in expansion of potentially pathogenic microbiota members, tissue inflammation, and susceptibility to pathogens (Xu et al, 2020). Likewise, the intestinal immunoglobulin IgA arm of adaptive immunity favorably targets and suppresses the pathogenic filamentous morphotypes of *Candida albicans*, thus encouraging mutualism and improving its competitive fitness in the gut (Ost et al, 2021).

It has been demonstrated that pathogens and beneficial microbes manipulate the PTI responses of the host to allow successful colonization. However, we have limited information on how the triggered PTI readouts affect pathogenic microbes as well as the members of the plant microbiota. In this study, we have provided a molecular mechanism by which the immune output RBOHD-mediated ROS acts as a signaling cue to selectively control the potentially harmful *Xanthomonas* leaf commensal, thereby helping accommodate a potential foe and turn it into a friend. Our *in vitro* experiments support the notion that ROS as produced by RBOHD modulates the behavior of the *Xanthomonas* L148, however it can't be excluded that other functions of plant RBOHD apart from its role in defense (Torres et al, 2002), for instance cell wall fortification (Denness et al, 2011; Fujita et al, 2020), host signaling (Miller et al, 2009), and stomatal responses (Kwak et al, 2003; Sierla et al, 2016) might contribute to the restriction of the pathogenicity of the microbial partner. In mice, depreciation in the mitochondria-derived ROS due to senescence or pharmacological intervention, is associated with the increased gut microbiota diversity (Yardeni et al, 2019). Also, ROS produced via NOX1 pathway in the colon is consumed by *Citrobacter rodentium* to drive anaerobic growth and in turn remodels the epithelial milieu (Miller et al, 2020). In plants, ROS induces auxin secretion of a beneficial bacterium *Bacillus velezensis* FZB42 to sequester the damaging effects of ROS in the bacteria and allows efficient root occupation (Tzipilevich et al, 2021). Similarly, FER up-regulates ROP2-mediated ROS production in roots which preferentially constrains *Pseudomonas* establishment in the rhizosphere (Song et al, 2021). It has also been genetically shown that the plant NADPH oxidase *RBOHD* for ROS production is integral in maintaining microbiota homeostasis by keeping opportunistic bacterial

members at bay (Pfeilmeier et al, 2021). Though it appears to be a universal pattern across multicellular organisms that ROS as the component of immunity or an intrinsic developmental feature, modulates the structure, composition, and function of microbiota, little is known regarding the actual machineries that underly these processes.

We have revealed that apart from the strong effect of the plant host, other members of the phyllosphere microbiota can partially contribute onto the alleviation of the deleterious effects of *Xanthomonas* L148. It has been shown that close-kin innocuous strains within the plant microbiota out-competes or antagonizes it potentially pathogenic counterparts preventing disease progression but allowing persistence and co-existence among the strains in nature (Karasov et al 2018; Shalev et al, 2022). The microbe-microbe interactions somehow explain the rarity of plant microbiota dysbiosis in the wild. However, this phenomenon is accession and strain specific as these commensal-mediated protection is lost in some plant genotypes and a particular harmful *Pseudomonas* strain predominates the microbial community (Shalev et al, 2022). The existence of potentially pathogenic members within the natural *A. thaliana* microbiota has been recently documented and the list is continually growing, such examples are *Xanthomonas* L131, *Pseudomonas* R401, Streptomycetaceae R107 and R187, *P. viridiflava* OTU5 strains (P1-P7), *Serratia* L50, *Williamsia* L354, *Rhodococcus* L278, *Arthrobacter* L145, *Bacillus* L49, and *Bacillus* L75 (Pfeilmeier et al, 2021; Ma et al, 2021; Shalev et al, 2022, Vogel et al, 2021).

We have demonstrated in this study that the pathogenic potential of *Xanthomonas* L148 depends on the T2SS component *gspE* gene. The loss of killing effect to *rbohD* mutant plants of the *gspE*::Tn5 mutants strains can be explained by its compromised secretion activities and hampered colonization of *rbohD* leaf tissues (Figure 10c, e, and Figure 12e-f). T2SS is often utilized by plant pathogens to deliver CAZymes which degrade plant cell walls allowing intrusion of barriers so as to efficiently colonize the host and promote disease (Cianciotto et al, 2005). In addition, T2SS allows a human pathogen *Shiga*-toxigenic *E. coli* and the root commensal *Dyella japonica* MF79 to efficiently colonize roots and is also required for the virulence of leaf pathogen Dickeya *dadantii* (Teixiera et al, 2021; Holmes et al, 2020; Expert et al, 2018). These findings suggest a paramount role of T2SS in the establishment of microbial residence in the host tissues, making it conceivable that it is targeted by the host to manipulate microbial behavior. The secreted CAZymes could also trigger immune responses such as ROS burst via direct recognition of the CAZyme as a MAMP or the release of recognized plant-derived DAMPs due to its enzymatic action (Expert et al, 2018; Ma et al, 2015; Wang et al, 2018; Gui et al, 2017). Indeed, we have shown that live T2SS-deficient *gspE*::Tn5 L148 mutant triggers less ROS as compared with wild-type L148 while heat-killed wild-type L148 and *gspE*::Tn5 mutant triggered undistinguishable ROS burst, implying that T2SS-mediated CAZymes secretion might further enhance ROS response (Figure 11c). Plant ROS might act as a

counter-defense to curb L148 invasion via CAZymes by suppressing the T2SS expression (Figure 11c, Supplementary Figure 8a-b). Considering that the wild-type *Xanthomonas* L148 and the *gspE*::Tn5 mutant had similar leaf colonization patterns in wild-type Col-0 plants (Figure 4b), this retaliation likely functions to dampen T2SS activity and makes *Xanthomonas* L148 a commensal bacterium in wild-type Col-0 plants. We propose a model that the interaction of *Xanthomonas* L148 and the Col-0 plants lies in a delicate balance driven by the host ROS levels resulting in a negative feedback loop to control the potentially pathogenic commensal (Figure 17).

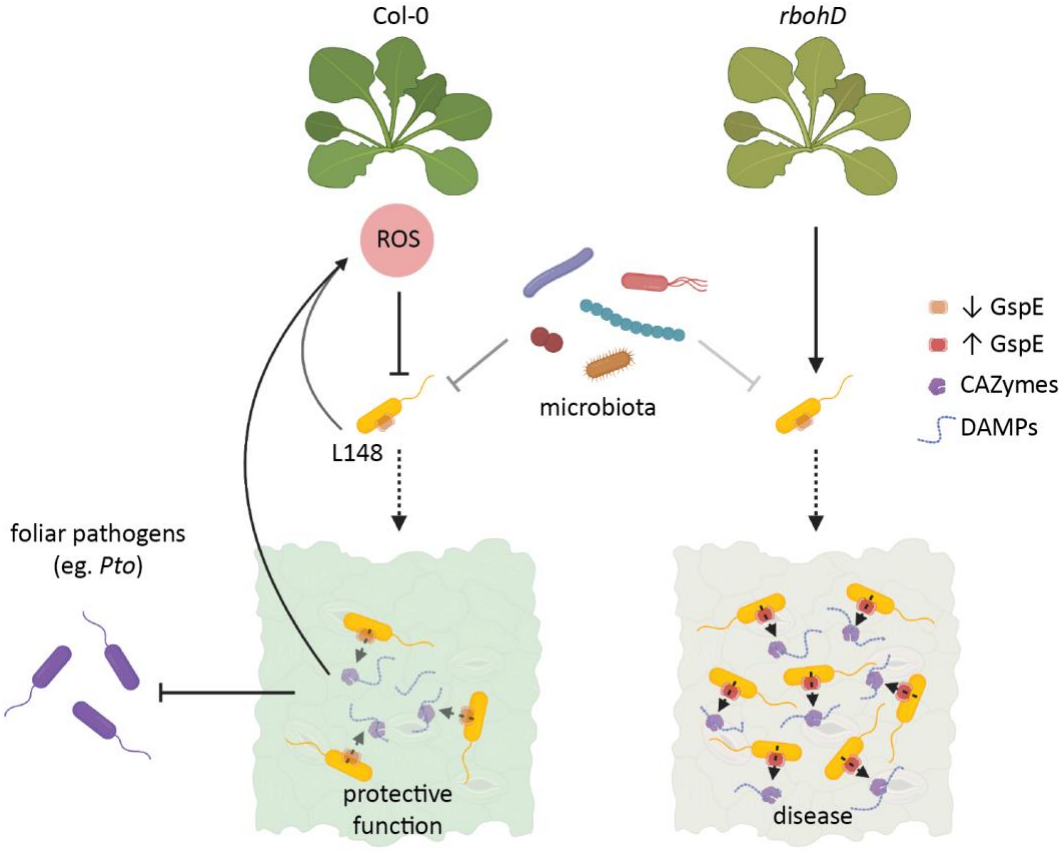

Figure 17. Mechanistic model for plant ROS licensing of co-habitation with a potentially pathogenic *Xanthomonas* L148 commensal. The *Xanthomonas* L148 releases MAMPs that are perceived by plants and trigger ROS production. The T2SS delivers CAZymes to the host to degrade cell wall liberating DAMPs and/or the CAZymes act as a MAMP, which both can potentially bolster ROS generation. The ROS then acts as a molecular beacon for *Xanthomonas* L148 to suppress its pathogenicity, in particular by dampening the activity of T2SS resulting in a negative feedback regulation of the bacterial activity by the plant host. We propose that in wild-type Col-0 plants, the ROS- and the microbiota-mediated suppression of *Xanthomonas* L148 promotes the cooperative behavior of L148 with the host plant and in turn confers protective function against subsequent invasion by foliar pathogens. In the case of *rbohD* mutant plants wherein plant ROS is absent, *Xanthomonas* L148 virulence is unlocked, resulting in disease. Some illustrations were created with BioRender. This figure was adopted from Entila et al, (*in preparation*).

We have also shown evidences that a significant portion of the *Xanthomonas* L148 CAZyme repertoire is also down-regulated by plant ROS indicating that the host also targets the expression of these microbial effectors to disable its virulence (Figure 14a, c, and Supplementary Figures S11a-b). The ROS-responsive CAZyme families can possibly utilize canonical components of the plant cell wall, in particular cellulose, pectin, arabinan, glucans, and mannans (Zablackis et al, 1995; Cosgrove et al, 2005). Five of the significantly down-regulated CAZymes were also identified in the forward genetic screening: 3 copies of *malZ* (maltodextrin glucosidase), CBH2 (cellobiohydrolase), and a hypothetical protein (Supplementary Figure S11b). Nonetheless, it remains to be investigated if the amplification of the plant ROS response is due to the perception of these CAZymes as MAMPs increasing PTI, its function to degrade host barriers releasing DAMPs activating DTI, or both. Interestingly, the CAZyme endoglucanase which potentially degrades glycan components of plant cell wall is up-regulated in Col-0 which might indicate its importance in general colonization and epiphytic persistence. Also, CAZymes have been also important for microbial fitness outside the host during saprophytic phase (Gamez-Arjona et al, 2022).

We observed that despite the prevalence of the T2SS in Xanthomonadales regardless of lifestyle (Supplementary Figure S12a), the CAZyme repertoire of pathogenic and potentially pathogenic strains have greatly diversified and increased enabling these strains to degrade host cell walls to promote infection. The types of CAZymes does not seem to distinguish potential pathogens from full-pledged pathogens (Supplemental Figure S12b-c), however the regulation of CAZyme expression might demarcate the two groups. The fundamental role of CAZymes in the virulence of *Xanthomonas* has been extensively documented (Giuseppe et al, 2023). Comparative analysis of 49 fungal genomes revealed wide variety of CAZymes but fungal pathogens tend to encode copious CAZyme genes (Zhao et al, 2013). More so, a distinct set of CAZymes were upregulated in fungal members of the *A. thaliana* rhizosphere microbiota upon engagement with the plant roots, and the CAZyme gene family PL1_7 pectate lyase are essential for aggressive root colonization of detrimental fungi (Mesny et al, 2021). Moreso, though CAZymes are enriched for both symbiotic and pathogenic fungi, there is an increased representation of CBM18, chitin-binding CAZyme modules in the genomes of mutualistic fungi *Colletotrichum toefildae*, *Piriformospora indica*, and *Harpophora oryzae* which might be essential to sequester fungal chitin and evade plant host immunity (Hacquard et al, 2017).

Emerging evidence suggests that plant immunity modulates microbial processes required for virulence in addition to its effects on general microbial metabolism including protein translation (Nobori et al, 2018; 2020). For instance, the secreted aspartic protease SAP1 inhibits *Pto* growth by cleaving the *Pto* protein MucD in *A. thaliana* leaves (Wang et al,

2019). Plants target the iron acquisition system of *Pto* to inhibit *Pto* growth during effector-triggered immunity (Nobori et al, 2020). The defense phytohormone salicylic acid and the specialized metabolite sulforaphane inhibit the type III secretion system (T3SS) in the pathogenic *Pto* (Nobori et al, 2018; Wang et al, 2020). Our finding that RBOHD-mediated ROS targets *Xanthomonas* T2SS adds an additional mechanism and proposes an extended concept that plant immunity supervises members of the plant microbiota from pathogens to potentially detrimental commensals.

The impression that a potentially pathogenic strain is maintained in the plant microbiota is paradoxical, nonetheless they serve some ecological function. We have shown evidences that *Xanthomonas* L148 confers protection against a foliar pathogen *Pto*, which suggest that the host interaction with this potentially pathogenic commensal is retained due to its offered benefits and its behavior is then tightly modulated by the plant-derived ROS keeping it on leash (Figure 15). Moreover, the plant protective function against the pathogen is genetically uncoupled with *gspE*-dependent pathogenic potential since the *gspE*::Tn5 mutant can still confer significant resistance against *Pto* in both Col-0 and *rbohD* mutant plants (Figure 15a, c-d). The mechanisms by which the ROS-tamed *Xanthomonas* L148 confers pathogen protection, via direct antagonism or through host immune-training warrants further investigation. Taken together, our findings have advanced our understanding of plant-microbiota dialogues in the context of plant immunity and have provided a mechanistic framework for plant ROS-mediated strict control of potentially pathogenic members of the microbiota, converting it to a commensal with beneficial service to the plant host.

7. MATERIALS AND METHODS

Plant materials and growth conditions

The *A. thaliana* Col-0 accession was the wild-type and the genetic background of all the mutants utilized in this study. The mutants *fls2* (SAIL_691C4*,* Zipfel et al, 2004), *efr* (SALK_068675, Zipfel et al, 2006), *cerk1* (GABI_096F09, Miya et al, 2007), *fec* (Xin ete al, 2016), *bbc* (Xin et al, 2016), and *rbohD* (*atrbohD D3,* Torres et al, 2002) were previously described. For agar plate assays, seeds were sterilized with Cl_2 gas for 2 h (Lindsey et al, 2017). Seeds were then stratified for 2-3 days at 4 °C on 0.5x Murashige and Skoogs (MS) medium agar with 1% sucrose, germinated for 5 days, and subsequently transplanted to 0.5x MS plates without sucrose. Plants were grown in a chamber at 23 °C / 23 °C (day/night) with 10 h of light. Then, 14-day-old seedlings were inoculated with bacterial strains and were harvested or phenotyped at the indicated time points. For ROS burst and infiltration patho-assays, plants were grown in greenhouse soil

for 5-6 weeks in a chamber at 23 °C / 23 °C (day/night) with 10 h of light and 60% relative humidity (See Supplementary Table S1 for details of the plant genotypes used).

Bacterial strains and growth conditions

All the bacterial strains derived from the AtSPHERE were previously described[20]. *Pseudomonas syringae* pv. *tomato* DC3000 (*Pto*), *D36E* (Wei et al, 2018), *ΔhrcC* (Morello et al, 2009), and *Pto* lux (Matsumoto et al, 2022) were described previously. All bacterial strains were grown in 0.5x Tryptic Soy Broth (TSB) for 24 h, harvested through centrifugation, washed twice with sterile water, and diluted to the appropriate OD_{600} (See Supplementary Table S2 for the list of bacterial strains used).

ROS burst measurement

ROS burst was determined as in Smith and Heese (2014) with slight modifications. Concisely, bacterial strains were grown in TSB at 28 °C for 16-18 h with shaking at 200 rpm. Cells were harvested, washed twice with sterile water, and diluted to OD_{600}=0.50 in sterile water. Heat-killing of the bacterial cells was done by incubating the suspension at 99 °C for 1 h. The day before the assay, leaf discs (4 mm) from leaves of the same physiological state and size from 5-to-6-week-old plants grown in a chamber at 23 °C / 23 °C (day/night) with 10 h of light were harvested, washed twice with sterile water every 30 min, immersed on sterile water in 96-well plates, and incubated in the same growth chamber for 20 h. Prior to the assay, the elicitation solution was prepared by adding 5 µL 500x horseradish peroxidase (HRP, P6782-10MG, Sigma-Aldrich) and 5 µL 500x luminol (A8511-5G, Sigma-Aldrich) in 2.5 mL of bacterial suspension, 1 µM MAMP solutions (flg22 [ZBiolab inc.], elf18 [Eurofins], chitinDP7 [N-acetylchitoheptaose, GN7, Elicityl]), or sterile nanopure water as mock. During the assay, the water was carefully removed from the 96 well-plate and 100 µL of the elicitation solution was added into the 96-well plate. With minimal delay, the luminescence readings were obtained for 60 min using a luminometer (TrisStar2 Multimode Reader, Berthold).

Callose deposition assay

Callose deposition, a late PTI readout, was determined *in planta* following Jin and Mackey (2017) with slight modifications. Briefly, bacterial strains were grown in TSB for 16-18 h at 22 °C, 200 rpm shaking, and cells were harvested and washed twice with sterile water and finally diluted to OD_{600}=0.20 in sterile water. Leaves of the same physiological state and size from 5-to-6-week-old plants were hand-infiltrated with needleless syringe on the

abaxial side with the resulting bacterial suspensions (20 strains, in mono-association) or controls (mock, 1 µM flg22, 1 µM elf18, 1mg mL^{-1} chitin; and *Pto* strains DC3000, D36E, and *ΔhrcC* at OD_{600}=0.20). Leaf discs (6mm diameter) were cored out from the inoculated leaves after 18-20 h and were decolorized and fixed in 1:4 (v/v) glacial acetic acid (A6283, Sigma-Aldrich): ethanol (20821.321, VWR) for 24 h. The cleared leaf discs were washed with water twice then 1mM MES buffer (M1503.1000, Duchefa Biochemie) pH 9.5 for 30 min, stained with 0.01% aniline blue (415049-50G, Sigma-Aldrich) in 1 mM MES buffer pH 9.5 for at least 2 h with initial vacuum infiltration of 5min. The stained leaf discs were mounted in 50% glycerol (7530.1, Roth), and were stored at 4°C temporarily. Micrographs were taken using epifluorescence microscope (Zeiss, AxioImager A2) with UV light and DAPI filter at 10x objective, with 3 frames for each disc. The images were processed and analyzed using ImageJ software and callose deposition was expressed as counts mm^{-2} or percent area.

Commensal bacterial colonization assay

To prepare the bacterial inoculum, all bacterial strains were grown in 0.5x TSB for 24 h, harvested through centrifugation, washed twice with sterile water, and suspended in sterile water (final OD_{600}=0.005). Two-week-old seedlings grown on 0.5x MS medium agar in a chamber at 23 °C / 23 °C (day/night) with 10 h of light were flood-inoculated with these bacterial suspensions and incubated in the same growth chamber. Leaf samples were aseptically harvested at 3 to 5 dpi, weighed, and plated for two compartments: for the total compartment, leaves were directly homogenized in 10 mM $MgCl_2$ with a homogenizer (TissueLyser III, Qiagen), serially diluted with 10 mM $MgCl_2$, and plated on 0.5x TSB agar; for the endophytic compartment, leaves were surface-sterilized with 70% ethanol for 1 min, washed twice with sterile water, homogenized, serially diluted, and then plated as for the total compartment. Colonies were allowed to grow at 28 °C, and photographs were taken for 1 to 3 days. Colonization was expressed as cfu mg^{-1} sample.

Gene network analysis and machine learning

Network analysis was performed using WGCNA package (weighted gene co-expression network analysis, Langfelder and Horvath, 2008) in R environment. A WGCNA network for the DEGs was constructed with manual module. The optimal soft threshold of 5 was implemented as fitting index to assess scale-free network constructed upon gene-gene correlation from RNA-Seq samples. Genes were clustered based on topological overlap of their connectivity through average linkage hierarchical clustering followed by dynamic tree cutting to define network modules. Gene Significance (GS) for each gene network was defined as the Pearson correlation with trait while Module Significance (MS) is the

mean of absolute GS values of the genes in the module. Module Membership (MM) was computed as the Pearson correlation between each gene's expression and its module eigengene. The network depictions were visualized using igraph package (Csardi et al, 2006). Pathway enrichment analysis was done using the PANTHER database with hypergeometric test (Mi et al, 2013). The **s**upport **v**ector **m**achine classifier with **r**ecursive **f**eature **e**limination (SVM-RFE) was implemented using the caret package (Kuhn, 2008). The machine learning pipeline was applied on training the expression profiles of genes for each of the modules to identify genes predictive of the PTI outputs.

Leaf infiltration patho-assay

Briefly, bacterial strains were grown in TSB for 16-18 h at 22 °C, 200 rpm shaking, and cells were harvested and washed twice with sterile water and finally diluted to OD_{600}=0.20 in sterile water. Heat-killing of the bacterial cells was done by incubating the suspension at 99 °C for 1 h. Leaves of the same physiological state and size from 5-to-6-week-old plants were hand-infiltrated with needleless syringe on the abaxial side with the resulting bacterial suspensions of *Xanthomonas* L148(::Tn5) or *Pto* strain DC3000, at OD_{600}=0.20. Plants were incubated for 3 to 5 days in the same climate chambers till symptoms were observed. Photographs of the infiltrated leaves were taken and green tissue area was obtained using ImageJ software.

Generation of bacterial mutants

Xanthomonas L148::Tn5 library was constructed via conjugation of *Xanthomonas* L148 with *E. coli* SM10*λpir* harboring puTn5TmKm2 (Merrel et al, 2002) in which both strains were mixed in equal portions (OD_{600}=0.10), spot plated on TSB medium, and incubated for 2 d at 28 °C. The resulting mating plaques were diluted and plated on TSB with kanamycin and nitrofurantoin for selection for L148 transformants and counter-selection against *E. coli*, respectively. To constitute the entire library, around 7000 individual colonies were picked, re-grown in 0.5x TSB, aliquoted for glycerol stocks, and stored at -80 °C. Around 20 strains from this *Xanthomonas* L148::Tn5 library were randomly selected for confirmation of Tn5 insertion in the genome via nested PCR (first PCR with primers FDE117 and FDE118; second PCR with primers FDE119 and mTn5AC) and the final amplicons were Sanger-sequenced (see Supplementary Table S3 for details). For the generation of targeted deletion mutants for *gspE*, the pK18mobsacB suicide plasmid (GenBank accession: FJ437239, Kvitko et al, 2011) was PCR linearized (primers FDE234 and FDE235) with Phusion Taq polymerase (F-5305, ThermoScientific); 750 bp of upstream (primers FDE278 and FDE279) and downstream (primers FDE280 and FDE281) flanking regions of *gspE* coding sequence with terminal sequences overlapping

with the linearized pK18mobsacB were amplified using Phusion Taq polymerase (F-5305, ThermoScientific) and were sequence verified. The plasmid construct was assembled using Gibson cloning (E5510S, New England Biolabs; Gibson et al, 2009) following the manufacturer's instructions. The plasmid construct was transformed into *E. coli* cells (DH5α strain) and then delivered to *Xanthomonas* L148 via triparental mating with the helper strain pRK600 (Kessler et al, 1992). Transformants were selected using kanamycin and nitrofurantoin and the second homologous recombination was induced with sucrose in 0.5x TSB. The deletion mutants were individually picked and stored at -80°C in glycerol stocks and were verified by PCRs (using primers FDE196 and FDE197 for the presence of the plasmid with the inserts; primers FDE125 and FDE126 for the presence of *gspE* gene in the genome; and primers FDE279 and FDE280 for the removal of *gspE* gene in the genome) and Sanger-sequencing, and were plated on 0.5x TSB containing 10 µg/mL kanamycin. True deletion mutants should not contain the plasmid, lose the *gspE* gene, and be sensitive to kanamycin (See Supplementary Table S3 for list of primers and PCR profile used).

L148::Tn5 library 96-well screening

Seedlings of *rbohD* were grown in 96-well plates with 0.5x MS agar with 1% sucrose for 14 days. Concomitantly, the Tn5 insertion mutants (~7000 individually picked colonies) were grown in 96-well plates with TSB at 28 °C for 3 days with 200 rpm agitation till saturation. The resulting bacterial suspension was diluted 6 times (resulting in a concentration of approximately $6x10^9$ bacterial cells per mL) and 20 µL aliquots were inoculated onto the seedlings. Plants were phenotyped for survival after 5 days. The resulting 214 *Xanthomonas* L148::Tn5 candidate strains which showed the loss of the *rbohD* killing activity from the two independent 96-well plate screenings were genotyped to identify Tn5 insertion locus in the genome via nested PCR (first PCR with primers FDE117 and FDE118; second PCR with primers FDE119 and mTn5AC) and the final amplicons were Sanger-sequenced (see Supplementary Table S3 for list of primers and PCR profile used and Supplementary Figure S9). The 124 *Xanthomonas* L148::Tn5 candidate mutants which have insertions on genes with functional annotations (please see Supplementary Dataset S4 for the list) were further screened using plants grown in agar plates to re-evaluate the phenotypes as described in commensal bacterial colonization assay.

***In vitro* assays**

For instantaneous ROS treatment, *Xanthomonas* L148 was grown for 24 h, pelleted, and diluted to OD_{600} = 0.02. A 500 µL of the bacterial suspension was mixed with H_2O_2

(H10009-500ML, Sigma-Aldrich) at final concentrations of 0-2000 µM, incubated for 30 min, and plated for colony counts. Similarly, 500 µL of the bacterial suspension was mixed with 1 mM xanthine (X7375-10G, Sigma-Aldrich) and 10 U/mL xanthine oxidase from bovine milk (X4875-10UN ,Sigma-Aldrich) to generate O_2^{-1}, and samples were plated at different time points (1 mol of xanthine is converted to 1 mol O_2^{-1} with 1 U xanthine oxidase at pH 7.5 at 25 °C in a min, thus 0, 2, 4, 10, 20, 40, 60, and 80 min incubations should have produced O_2^{-1} equivalent to 0, 50, 100, 250, 500, 1000, 2000 µM respectively) for colony counts. Chronic exposure to ROS was implemented by growing the strains in TSB ± 10 µM paraquat (856177-1G, Sigma-Aldrich), a ROS-generating compound, for 3 days while obtaining OD_{600} readings using spectrophotometer (Tecan Infinite Microplate reader M200 Pro) to calculate growth curves and rates. The candidate *Xanthomonas* L148::Tn5 mutants were phenotyped *in vitro* via growing bacterial culture with an initial inoculum of 10 µL OD_{600}=0.1 in 96-well plates supplicated with 140 µL TSB or XVM2 (a minimal medium designed for *Xanthomonas* strains; Wengelnik et al, 1996) for 3 days while obtaining absorbance readings at OD_{600} using a spectrophotometer (Tecan Infinite Microplate reader M200 Pro) to calculate growth curves and rates. The resulting cultures were gently and briefly washed with water and cells adhering on the plates were stained with 0.1% crystal violet (27335.01, Serva) for 15 min. The staining was solubilized with 125 µL 30% acetic acid (A6283, Sigma-Aldrich) to quantify biofilm formation at OD_{550} using a spectrophotometer (Tecan Infinite Microplate reader M200 Pro). Motility was assayed by point inoculating bacterial cultures (OD_{600}=0.1) on 0.5x TSB with 0.8% agar and colony sizes were measured after 2 to 3 days. Secretion activities were profiled via point inoculating (1 µL culture, OD_{600}=0.1) bacterial strains on 0.5x TSB agar with 0.1% substrate-of-interest (carbohydrates: pectin, carboxymethyl-cellulose, α-cellulose, xylan, starch; protein: milk and gelatin; lipid: Tween 20), incubated at 28 °C for 2 days. For gelatin, halo of degradation was visualized by incubating the plates in saturated ammonium persulfate for 15 min. For carbohydrates, clearance zones were visualized by staining the plates with 0.1% congo red (C-6767, Sigma-Aldrich) for 15 min followed by washing with 6 ppm NaCl solution (0601.1, Roth). All plates were photographed before and after the staining procedures. The enzymatic indices were calculated by dividing the zones of clearing by the colony size. Amino acid auxotrophy test was conducted by following the growth of *Xanthomonas* L148::Tn5 mutants in minimal XVM2 supplied with single or combinations of the amino acids alanine (A7267, Sigma-Aldrich), arginine (A5006, Sigma-Aldrich), and glutamic acid (G8415, Sigma-Aldrich) with a final concentration of 3 mM while obtaining absorbance readings at OD_{600} using a spectrophotometer (Tecan Infinite Microplate reader M200 Pro) for 3 days.

In planta bacterial RNA-Seq

The *in planta Xanthomonas* L148 RNA-Seq was done in accordance to Nobori et al (2018). Briefly, two-week-old plants grown in agar plates were flood-inoculated with *Xanthomonas* L148 (OD_{600}=0.005 in 10 mM $MgCl_2$) and approximately shoots of 150 plants were harvested and pooled per sample at 2 dpi when bacterial populations were similar between Col-0 and *rbohD* plants. Samples were harvested, snap-frozen in liquid N_2, and stored at -80 °C until RNA extraction. The whole experiment was repeated three times. Samples were crushed with metal beads and incubated for 24 h at 4 °C with the isolation buffer[64]. Bacterial cells were separated from the plant tissue via centrifugation. The RNA was isolated from the bacterial pellets using TRIzol (15596026, Invitrogen) and were treated with Turbo DNase (AM1907, Invitrogen) prior sending to the Max-Planck Genome-Center Cologne for RNA Sequencing with plant ribo-depletion and cDNA library construction (Universal Prokaryotic RNA-Seq Library Preparation Kit, Tecan) using Illumina HiSeq 3000 system with 150 bp strand-specific single-end reads resulting in approximately 10 million reads per sample. The resulting reads were mapped to *Xanthomonas* L148 genome (Bai et al, 2015) using the align() function with the default parameters in Rsubread package to generate BAM files (Liao et al, 2019). Mapping rates ranged from 20-46% which is within the expected values (Nobori et al, 2018). Mapped reads were counted using DESeq2 using the function featureCounts() from the BAM files and were normalized using the voom() function in limma package prior analysis (Love et al, 2014; Ritchie et al, 2015). RNA-Seq raw reads and processed data were deposited in NCBI GEO repository with accession number GSE226583.

Upon passing quality checks (assessing batch effects through PCA and MA plots for data dispersion), differentially expressed genes were determined using a linear model (gene expression ~ 0 + genotype + rep; contrast = Col-0 - *rbohD*) and Empirical Bayes statistics with eBayes() function in limma (Ritchie et al, 2015). False discovery rates were accounted for p-values using qvalue (Storey et al, 2022). The threshold for significantly differentially expressed genes was |log2 fold change| > 1 and q-value < 0.05. Principal component analysis was done using the prcomp function (R Core Team, 2013); the optimal number of clusters was determined using NbClust() function in NbClust package (Charrad et al, 2014), cluster memberships were computed with the k-means algorithm (Struyf et al, 1997), heatmaps were generated using Heatmap() function in ComplexHeatmap package (Gu, 2022), and pathway enrichment analysis was done for each of the identified gene clusters using enricher() function in clusterProfiler package in R (Wu et al, 2021).

Synthetic community experiment

Two-week-old plants grown in agar plates in a chamber at 23 °C / 23°C (day/night) with 10 h of light were flood-inoculated with *Xanthomonas* L148 with or without the leaf-derived synthetic communities (LeafSC, 9 leaf prevalent and functional leaf isolates) in two different doses: $L148_{P1}$ + LeafSC contains equal portions of each strain including L148 in the inoculum (Xanthomonas L148/LeafSC, 1:9, each strain would have a final OD_{600}=0.01 totaling to OD_{600}=0.09 for LeafSC) and $L148_{P9}$ + Leaf SC contains a population of *Xanthomonas* L148 that equals the entire bacterial load of the LeafSC (Xanthomonas L148/LeafSC, 9:9, L148 and the LeafSC at OD_{600}=0.09); and were incubated in the same growth chamber. Plants were phenotyped for shoot fresh weights at 14 dpi (See Supplementary Table S2 for list of bacterial strains).

Protective function experiment

Two-week-old plants grown in agar plates in a chamber at 23 °C / 23 °C (day/night) with 10 h of light were flood-inoculated with *Xanthomonas* L148 strains (OD_{600}=0.005) and incubated for 5 days. *Pto* lux (OD=0.005) or water was aseptically spray-inoculated (approximately 200 µL per plate) onto the pre-colonized plants. Samples were collected at 0 and 3 dpi to count L148 and *Pto* colonies for different leaf compartments. For the total compartment, leaves were directly homogenized, serially diluted, and plated; for the endophytic compartment, leaves were surface-sterilized with 70% ethanol for 1 min, washed twice with sterile water, homogenized, serially diluted, and then plated. Colonies were allowed to grow on 0.5x TSB agar at 28 °C, and photographs were taken for 1 to 3 days. Colonies were differentiated via their color and chemiluminescence and colonization was expressed as cfu mg^{-1} leaf sample.

Genomic interrogation for CAZyme functions

Genomes for *Xanthomonas* L148 and other Xanthomonadales strains within the AtSPHERE culture collection (Bai et al, 2015) and known *Xanthomonas* pathogens (downloaded from NCBI; Sayers, et al, 2022) were annotated for CAZymes functions (http://www.cazy.org/; Drula et al, 2022) using the eggnog mapper (http://eggnog-mapper.embl.de/; Cantalapiedra et al, 2021) to determine the CAZyme repertoire of the bacterial strains and their potential substrates.

qPCR analysis

The bacterial RNA was isolated from plant samples inoculated with *Xanthomonas* L148 2 dpi or from bacterial pellets from *Xanthomonas* L148 grown in 0.5x TSB with or without 10 µM PQ using TRIzol (15596026, Invitrogen) followed by treatment with Turbo DNase (AM1907, Invitrogen). The cDNA libraries were synthesized with 1 µg RNA input using SuperScript II reverse transcriptase (18064-014, Invitrogen) and random hexamers as primers following the manufacturer's instructions. An input of 50 ng of cDNA was used for qPCR analyses (CFX Connect Real-Time System, Biorad) of the bacterial genes (please see Supplementary Table S3 for the list of primers and genes tested). The *Δ*Cq was computed by subtracting Cq of the gene-of-interest from Cq of *gyrA* gene from *Xanthomonas* L148.

Statistical analysis

The R programming environment (R version 4.2.2) was used for data analysis and visualization (R Core Team, 2013). The data were inspected for the assumptions of the linear model (homodescacity, independence, and normality) and were normalized, if necessary, prior to statistical analysis through ANOVA with *post hoc* Tukey's HSD test or Lest Significant Difference (LSD) test using the package agricolae (Mendiburu et al, 2020). The corresponding figures were created using the ggplot2 package (Wickham, 2016).

Data deposition

The plant RNA-Seq data reported in this thesis was part of the publication (Nobori et al, 2022), and the corresponding raw data were deposited in the Gene Expression Omnibus (GEO) database https://www.ncbi.nlm.nih.gov/geo (accession no. GSE150422).

The *in planta Xanthomonas* L148 RNA-Seq data reported in this thesis have been deposited in the GEO database, https://www.ncbi.nlm.nih.gov/geo (accession no. GSE226583).

Code availability

There is no custom code generated for this study.

8. SUPPLEMENTARY FIGURES AND LEGENDS

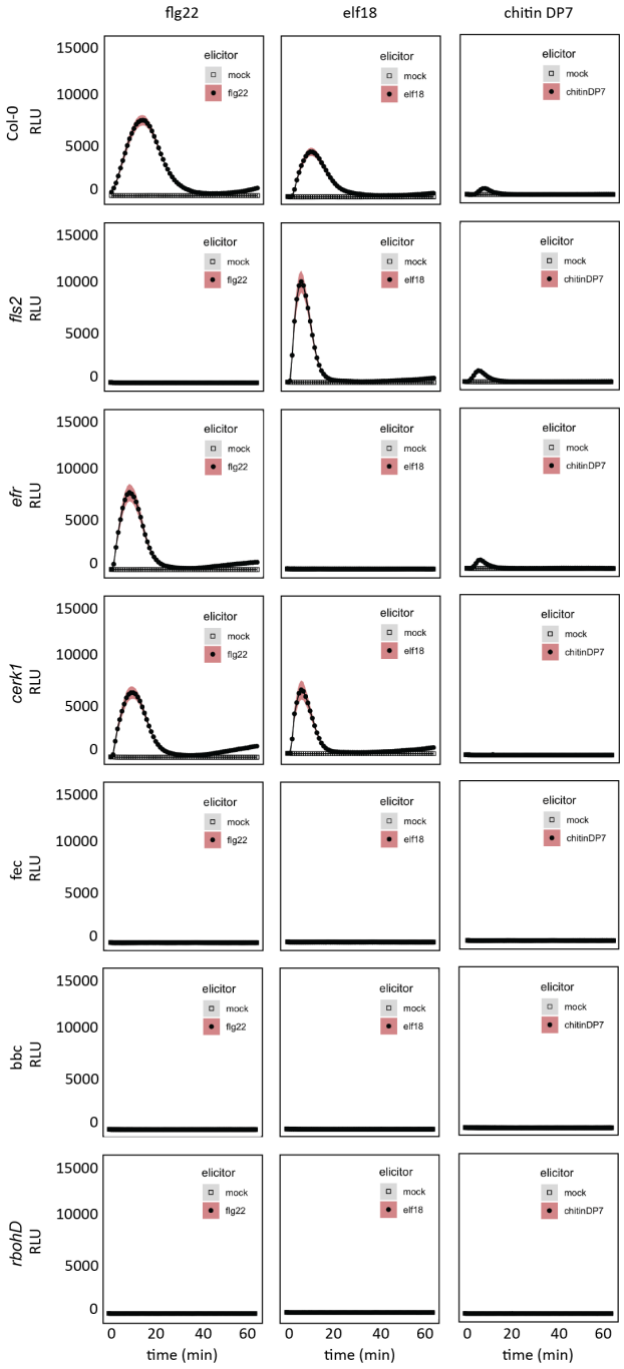

Supplementary Figure S1. ROS burst profile of immune-compromised mutants and Col-0 wildtype plants with MAMPs and foliar pathogens. Leaf discs from 5-to-6-week-old plants were treated with 1 µM of MAMPs, flg22, elf18, and chitinDP7. The immune-compromised mutant *fls2* lacks the receptor recognizing flg22, *efr* lacks the receptor for elf18, and *cerk1* lacks the co-receptor for chitinDP7; *fec* (*fls2 efr, cerk1*) and *bbc* (*bak1 bkk1 cerk1*) are triple mutants lacking the MAMP (co) receptor. Data from at least 2 independent experiments each with 8 biological replicates were used. This figure was adopted from Entila et al, (*in preparation*).

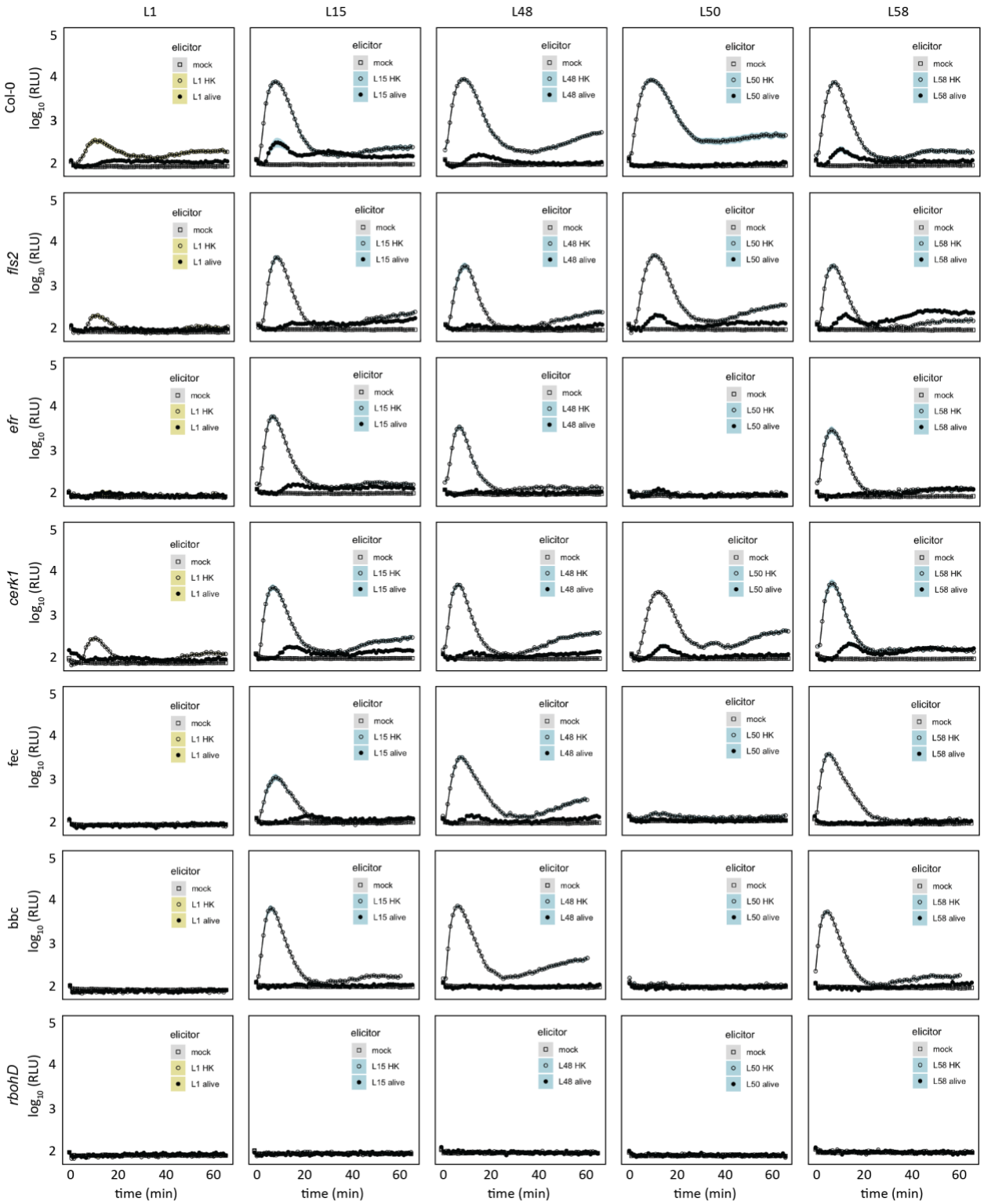
L1
L15
L48
L50
L58
Col-0
fls2
efr
cerk1
fec
bbc
rbohD
log10 (RLU)
time (min)
elicitor
mock
L1 HK
L1 alive
L15 HK
L15 alive
L48 HK
L48 alive
L50 HK
L50 alive
L58 HK
L58 alive

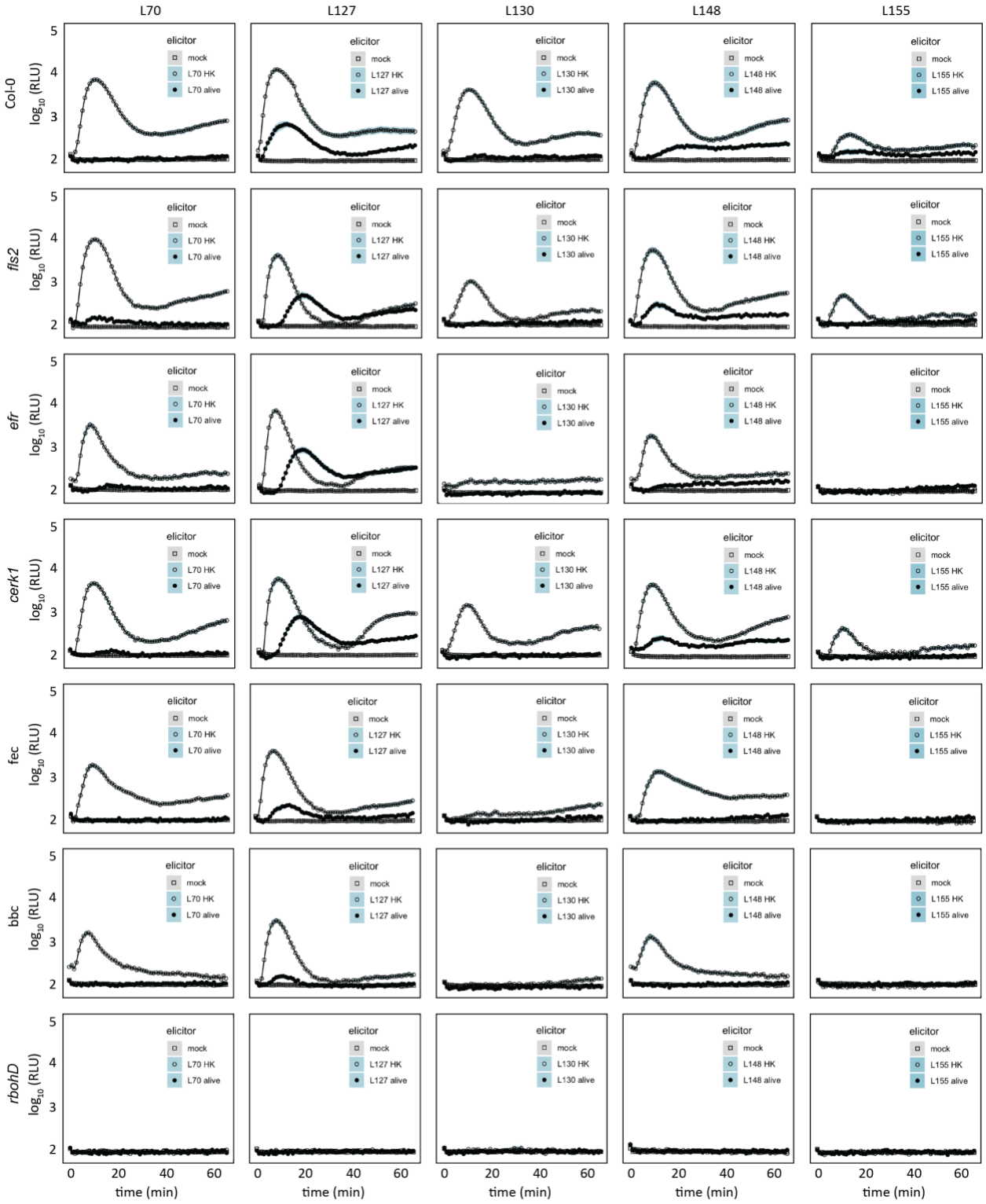
L70
L127
L130
L148
L155
Col-0
fls2
efr
cerk1
fec
bbc
rbohD
log10(RLU)
elicitor
mock
L70 HK
L70 alive
L127 HK
L127 alive
L130 HK
L130 alive
L148 HK
L148 alive
L155 HK
L155 alive
time (min)

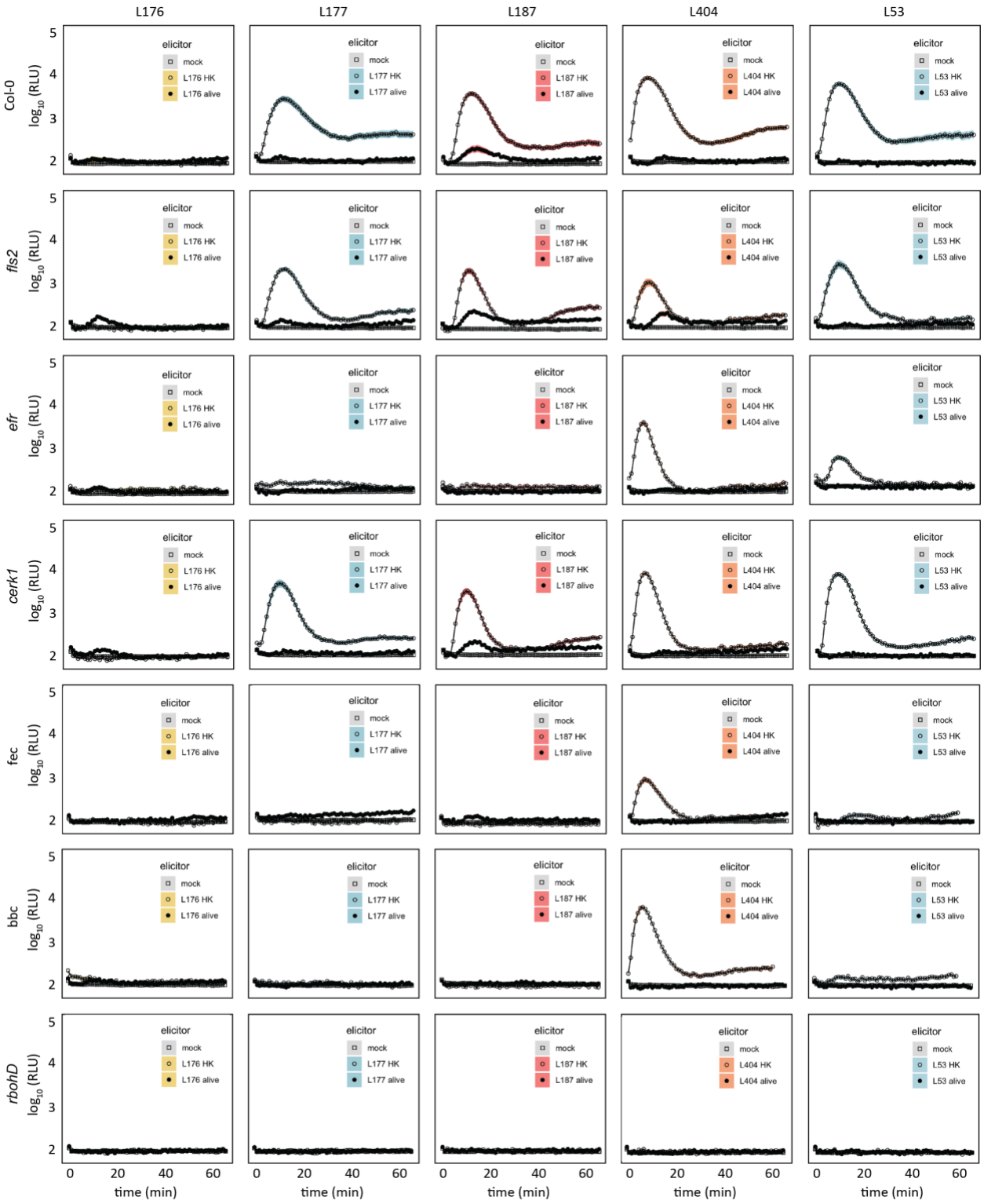
L176
L177
L187
L404
L53
Col-0
fls2
efr
cerk1
fec
bbc
rbohD
log10 (RLU)
elicitor
mock
L176 HK
L176 alive
L177 HK
L177 alive
L187 HK
L187 alive
L404 HK
L404 alive
L53 HK
L53 alive
time (min)

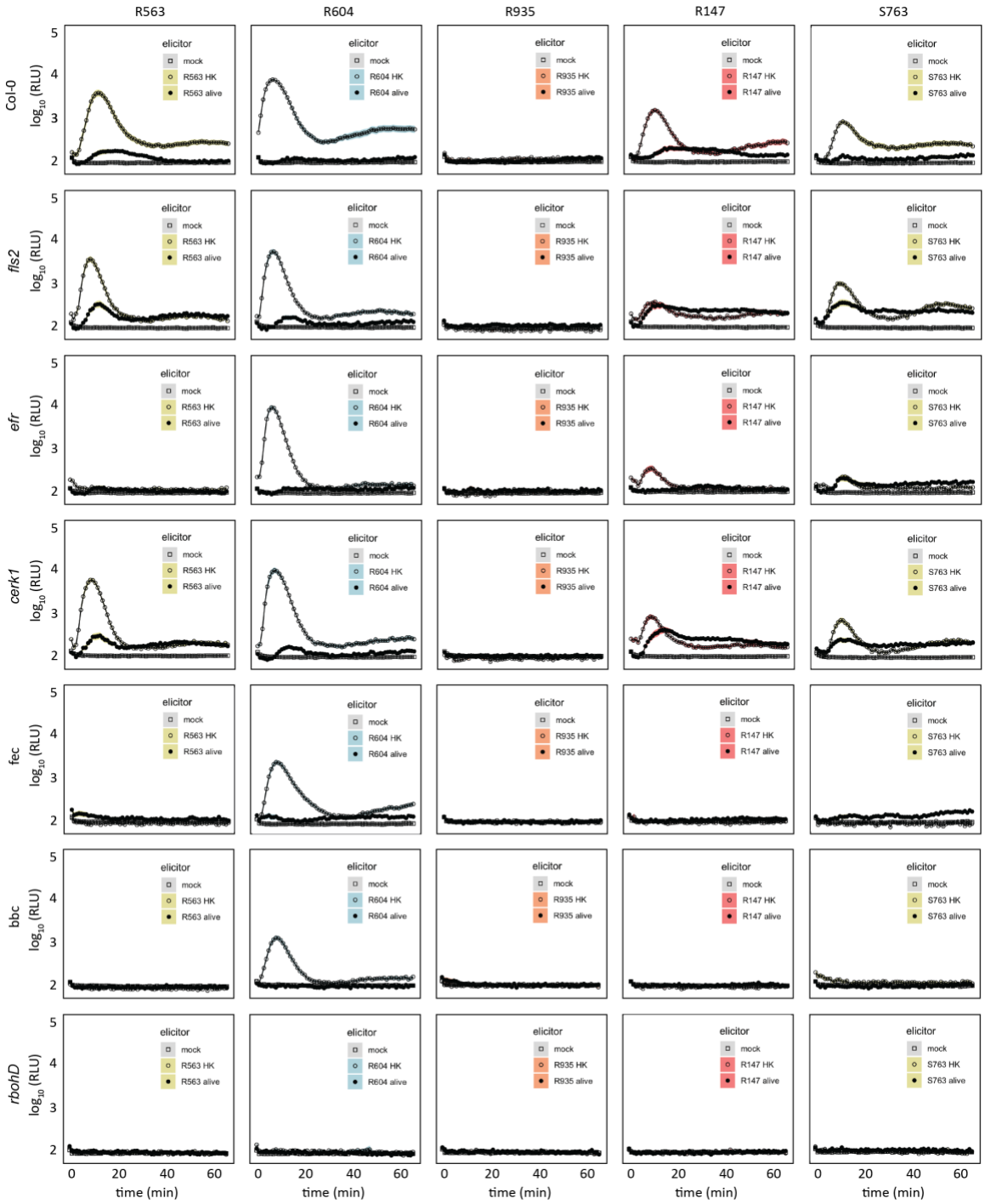

Supplementary Figure S2. ROS burst profile of immune-compromised mutants and Col-0 wild-type plants with commensal bacteria. Leaf discs from 5-to-6-week-old plants were inoculated with live or heat-killed microbiota strains (OD_{600}=0.5) in mono-associations for ROS burst assays. Data from at least 2 independent experiments each with 8 biological replicates were used. This figure was adopted from Entila et al, (*in preparation*).

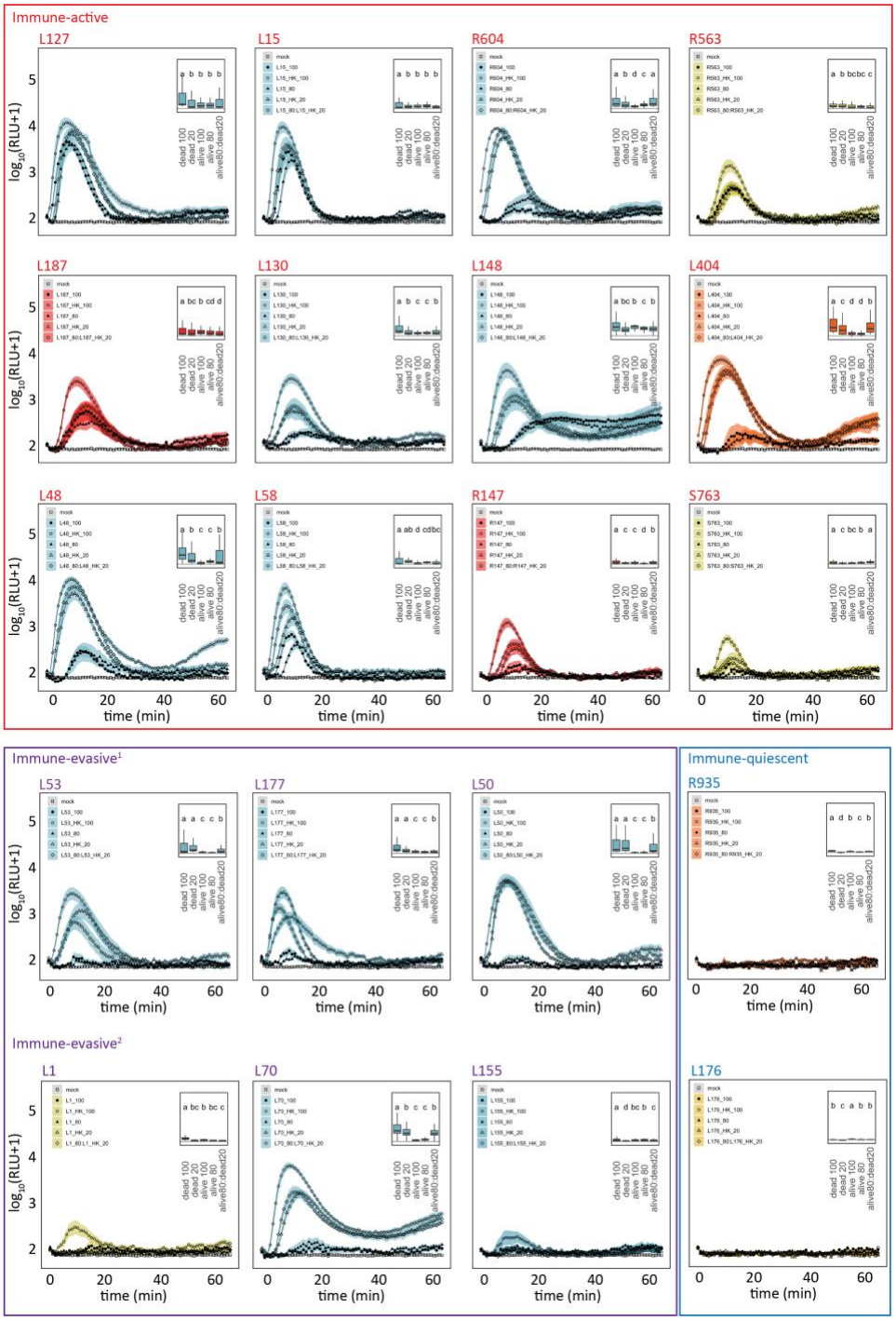

Supplementary Figure S3. ROS burst profile of microbiota members with evasion signatures. Leaf discs from 5-to-6-week-old plants were induced with live (100% or 80%), heat-killed (100% or 20%) or live:heat-killed (80:20) microbiota strains (OD_{600}=0.5) in mono-associations for ROS burst assays. Data from at least 2 independent experiments each with 8 biological replicates were used. Microbiota members can be broadly classified as immune-active, immune-evasive[1], immune-evasive[2], or immune-quiescent.

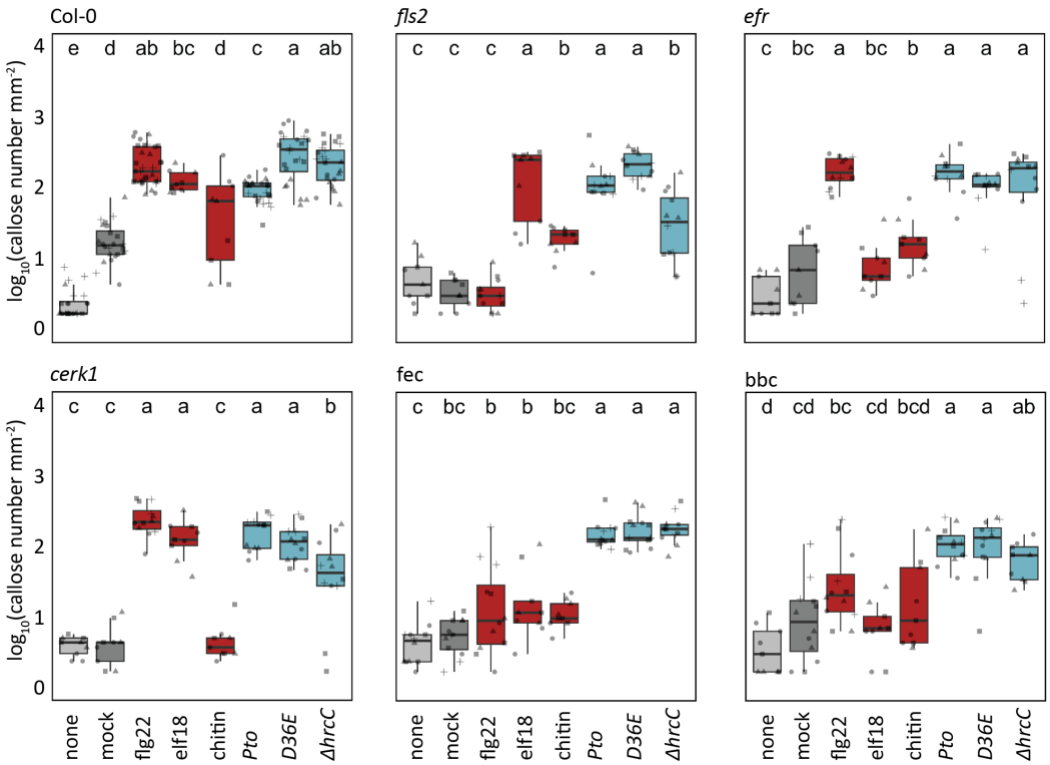

Supplementary Figure S4. Callose deposition in immune-compromised mutants and Col-0 wildtype plants with MAMPs and foliar pathogens. Leaves from 5-to-6-week-old plants were hand-infiltrated with 1 µM of MAMPs, flg22, elf18, and chitin or pathogenic *Pto* wild-type and avirulent *Pto* Δ*hrcC and D36E* (OD_{600}=0.2), and harvested for callose staining 18-20 dpi. The immune-compromised mutant *fls2* lacks the receptor recognizing flg22, *efr* lacks the receptor for elf18, and *cerk1* lacks the co-receptor for chitinDP7; *fec* (*fls2 efr, cerk1*) and *bbc* (*bak1 bkk1 cerk1*) are triple mutants lacking the MAMP (co) receptor. Data from at least 2 independent experiments each with 2-3 biological replicates were used**.** Different letters indicate statistically significant differences (ANOVA with *post hoc* Tukey's test, $P \leq 0.05$). Results are depicted as box plots with the boxes spanning the interquartile range (IQR, 25th to 75th percentiles), the mid-line indicates the median, and the whiskers cover the minimum and maximum values not extending beyond 1.5x of the IQR.

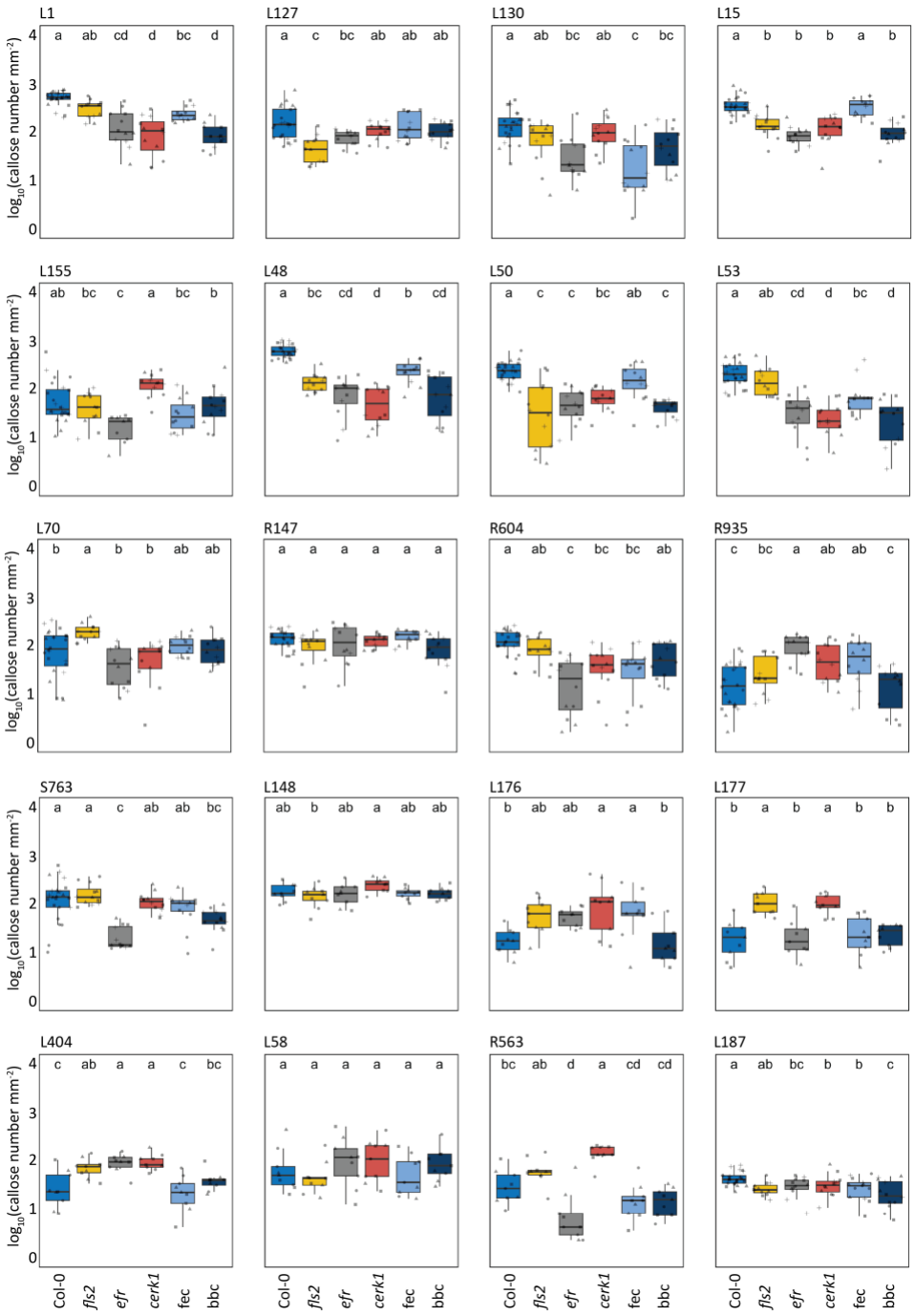

Supplementary Figure S5. Callose deposition in immune-compromised mutants and Col-0 wildtype plants with the microbiota members. Leaves from 5-to-6-week-old plants were hand-infiltrated with microbiota members in mono-associations (OD_{600}=0.2), and harvested for callose staining 18-20 dpi. Data from at least 2 independent experiments each with 2-3 biological replicates were used**.** Different letters indicate statistically significant differences (ANOVA with *post hoc* Tukey's test, $P \leq 0.05$). Results are depicted as box plots with the boxes spanning the interquartile range (IQR, 25th to 75th percentiles), the mid-line indicates the median, and the whiskers cover the minimum and maximum values not extending beyond 1.5x of the IQR.

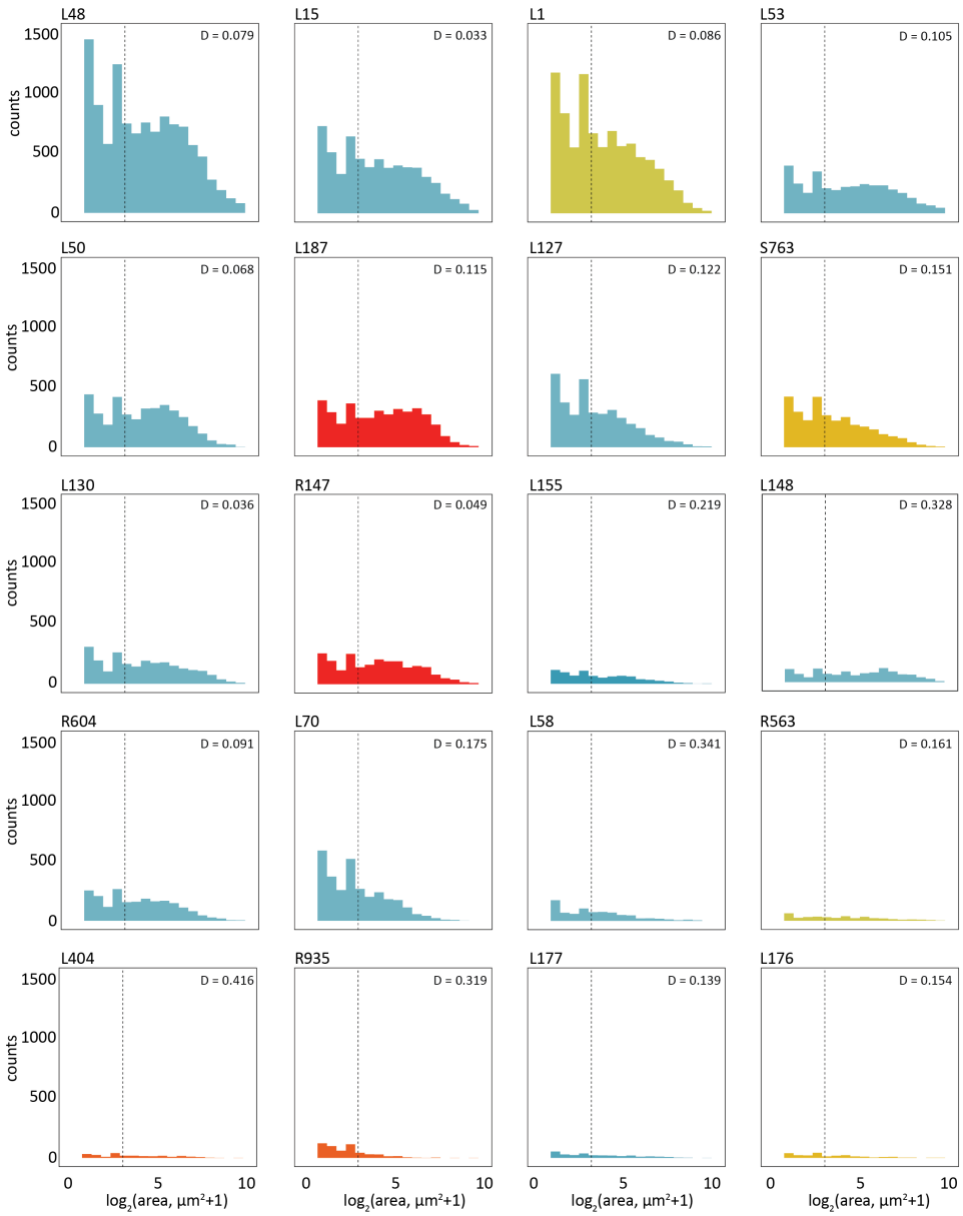

Supplementary Figure S6. Callose profile of microbiota members upon inoculation to the wild-type Col-0 leaves. Leaves from 5-to-6-week-old plants were hand-infiltrated with microbiota members in mono-associations (OD_{600}=0.2), and harvested for callose staining 18-20 dpi. Data from at least 2 independent experiments each with 2-3 biological replicates were used**.** Histogram depicting callose size distributions, and compared against the callose distribution of the avirulent *Pto D36E* (Kolmogorov-Smirnov statistics D, if value approaches 1, indicates very similar distributions). Dotted vertical line arbitrary threshold for large callose deposits (8.3 μm^2).

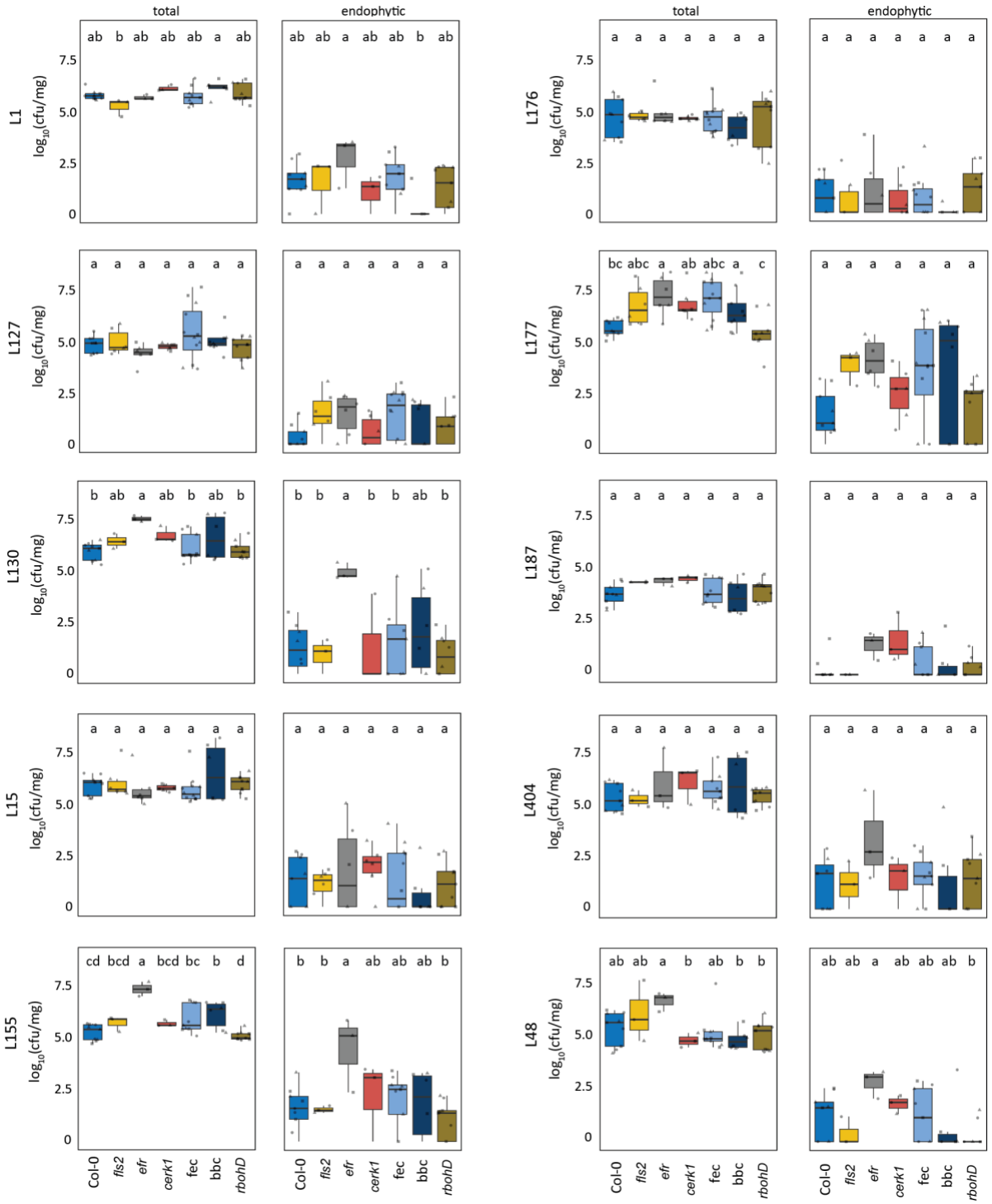
total
endophytic
L1
L127
L130
L15
L155
L176
L177
L187
L404
L48
log10(cfu/mg)
0
2.5
5.0
7.5
Col-0
fls2
efr
cerk1
fec
bbc
rbohD

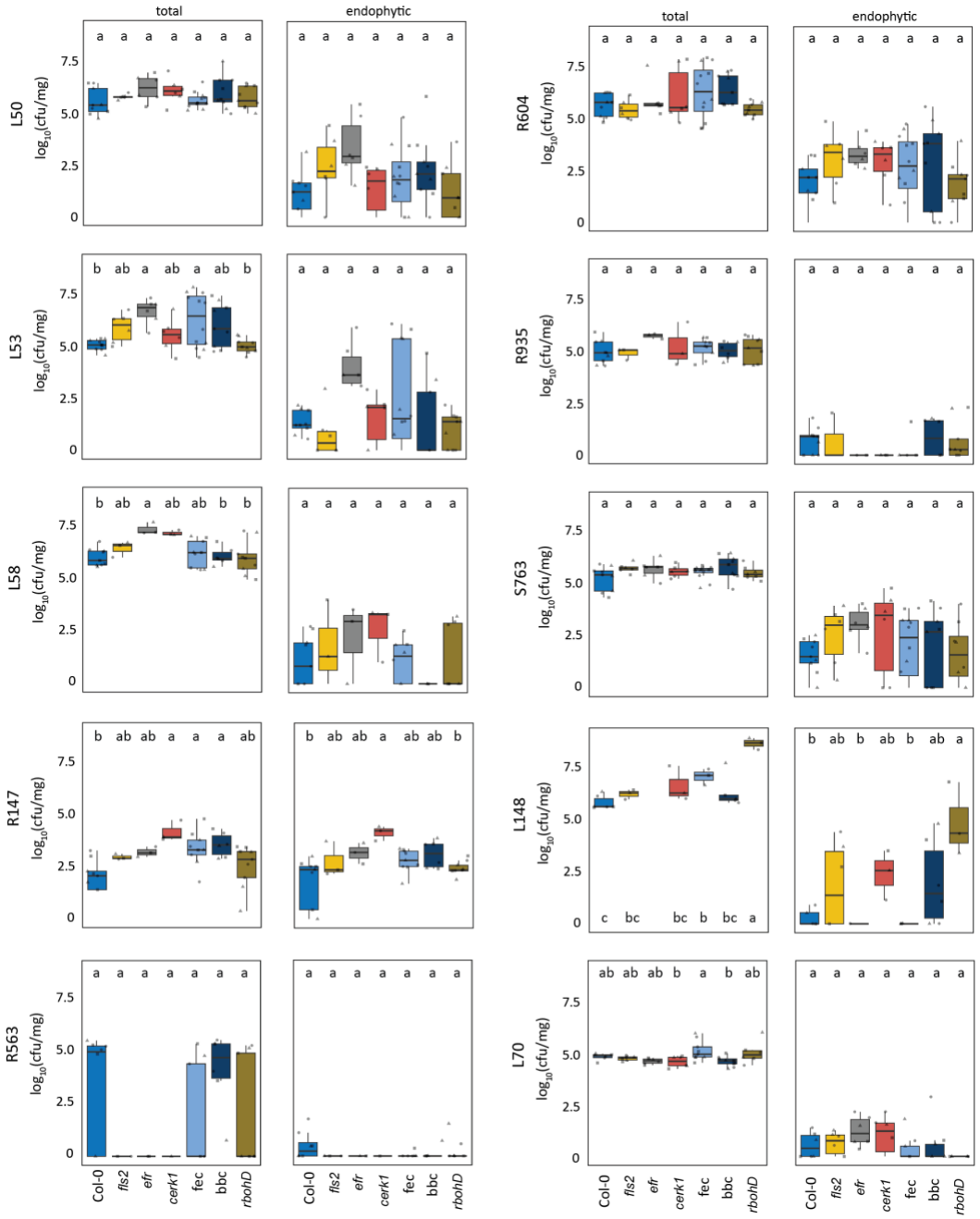

Supplementary Figure S7. Leaf colonization capacities of commensal bacteria on immune-compromised mutants and Col-0 wildtype plants. Two-week-old axenic plants were flood-inoculated with microbiota strains (OD_{600}=0.005) and were plated for colony counts for the total and endophytic leaf compartments at 5 dpi. Data from at least 2 independent experiments each with 8 biological replicates were used. Different letters indicate statistically significant differences (ANOVA with *post hoc* Tukey's test, $P \leq 0.05$). Results are depicted as box plots with the boxes spanning the interquartile range (IQR, 25th to 75th percentiles), the mid-line indicates the median, and the whiskers cover the minimum and maximum values not extending beyond 1.5x of the IQR. This figure was adopted from Entila et al, (*in preparation*).

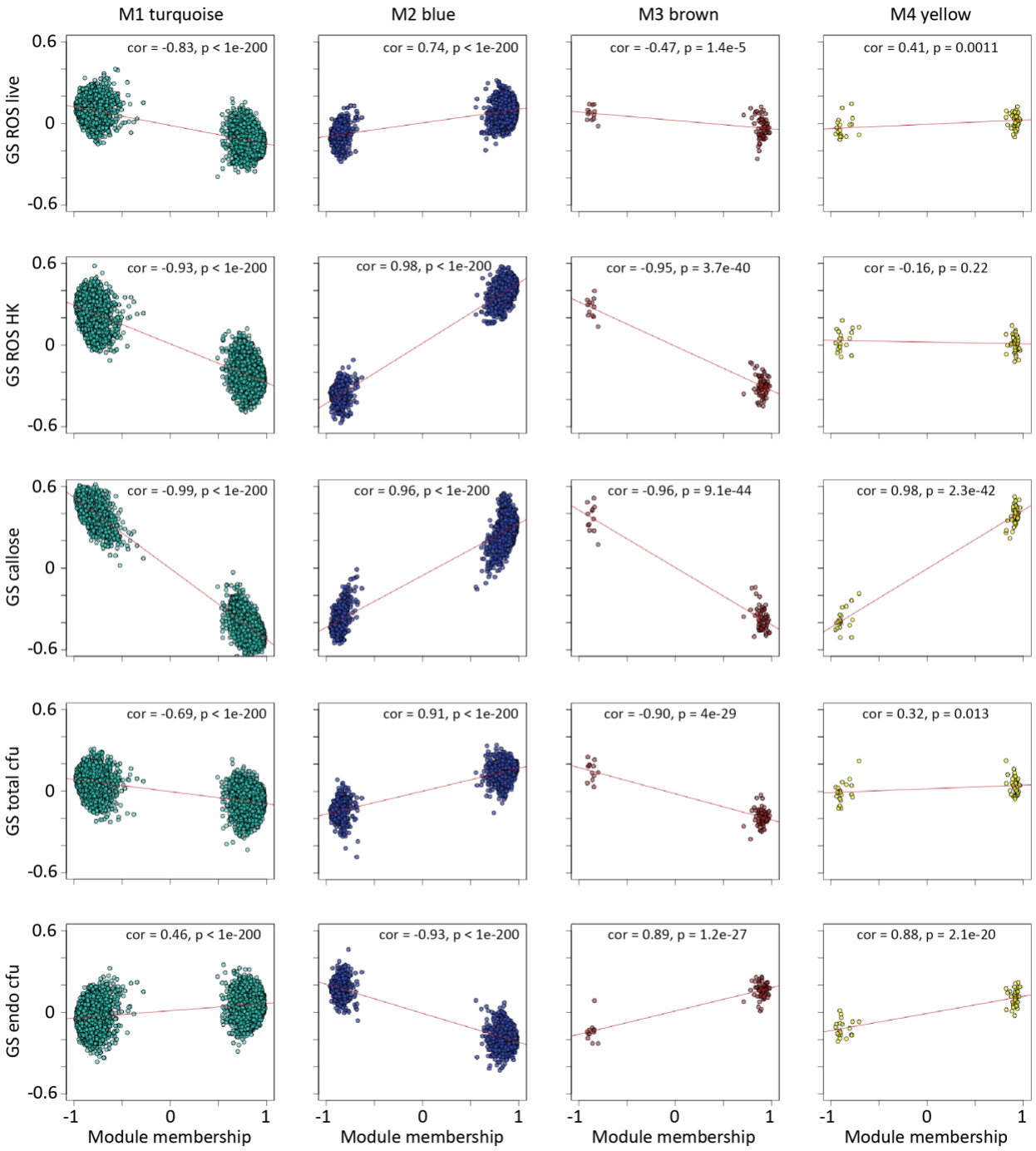

Supplementary Figure S8. WGCNA results for the plant host transcriptomic profile upon induction with microbiota members. Leaves from 5-to-6-week-old Col-0 plants were hand-infiltrated with microbiota members in mono-associations (OD_{600}=0.2), and harvested 6 hpi for plant transcriptomic profiling. The gene significance (GS) is the correlation of the gene expression profile with the PTI read-out; the module membership (MM) is the measure of connectivity of the gene within the module. Significant correlation values indicate that the module is strongly relevant to the PTI traits: ROS live and ROS HK (ROS burst with live cells and heat-killed cells respectively); callose; total cfu and endo cfu (bacterial colonization in the total and endophytic compartments, respectively).

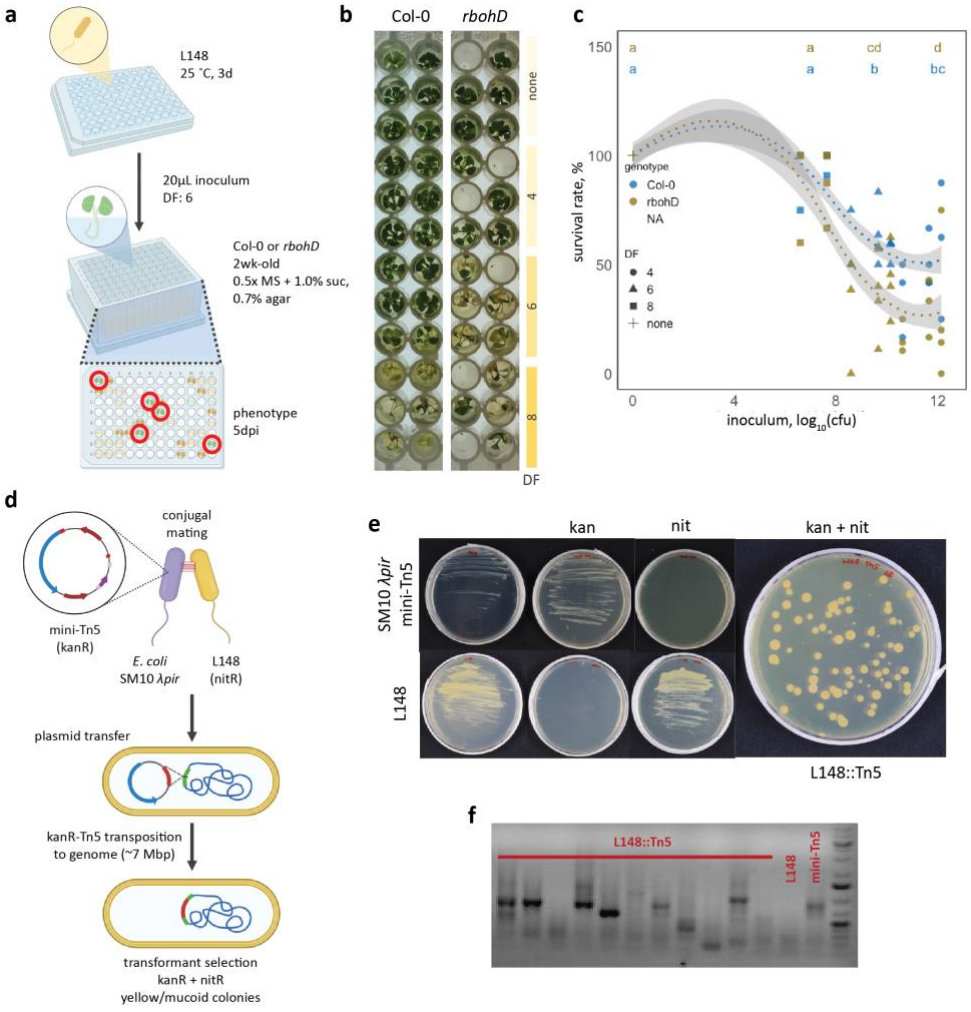

Supplementary Figure S9. Optimization of high-throughput genome-wide screening and generation of the *Xanthomonas* L148::Tn5 mutant library. a, Schematic diagram of the optimized high-throughput genetic screening for the *Xanthomonas* L148::Tn5 mutant library. Bacterial strains were inoculated onto 2-week-old *rbohD* plants followed by phenotyping at 5 dpi. Representative image of Col-0 wild-type and *rbohD* mutant plants inoculated with serially diluted *Xanthomonas* L148 suspensions in the high-throughput 96-well plate format. **b**, Representative image of Col-0 wild-type and *rbohD* mutant plants inoculated with serially diluted *Xanthomonas* L148 suspensions. The dilution factor (DF) of 6 was chosen for the best contrast between Col-0 and *rbohD*. **c,** dose curve of the *Xanthomonas* L148 with the survival rates of the wildtype Col-0 and *rbohD* mutant plants. **d,** Schematic diagram of the construction of the *Xanthomonas* L148::Tn5 mutant library via conjugation with *E. coli* harboring the mini-Tn5 plasmid. **e,** Antibiotic resistance of *Xanthomonas* L148, *E. coli* SM10λpir and the *Xanthomonas* L148::Tn5 mutants. The parental strain *Xanthomonas* L148 is resistant to nitrofurantoin (nit, 50 µg/mL in TSB medium) which was used for counter-selection for the plasmid carrier *E. coli.* The mini-Tn5 carrying *E. coli* is resistant to kanamycin (kan, 50 µg/mL in TSB medium) and was used for selecting against the wild-type *Xanthomonas* L148. *Xanthomonas* L148::Tn5 transformants are resistant to both nit and kan in TSB medium. **f**, Electrophoretogram of the genomic transposon insertion PCR validation for the randomly selected *Xanthomonas* L148::Tn5 mutant strains. PCR products were Sanger-sequenced to determine the transposon insertion site.

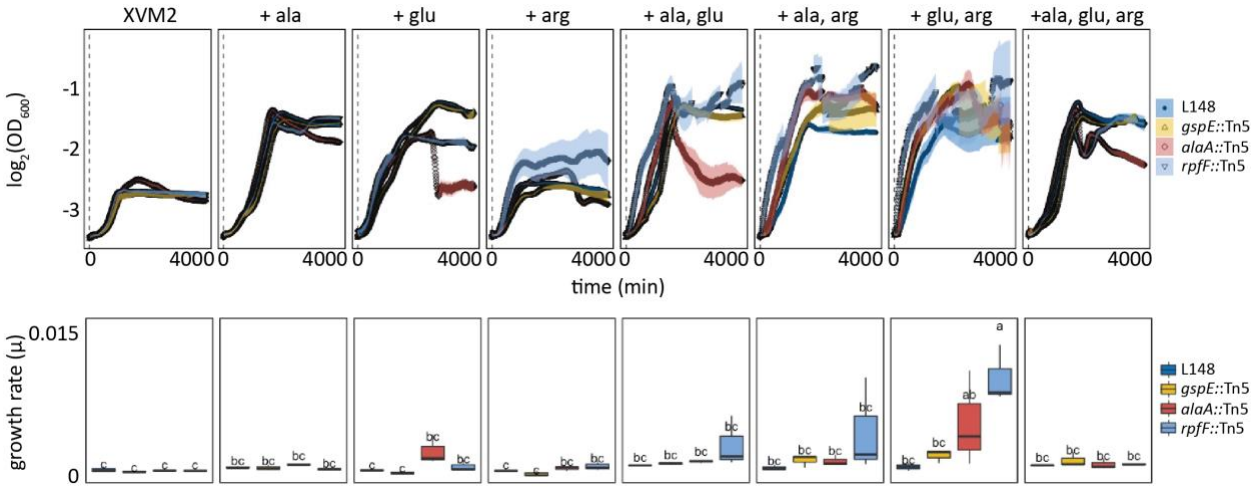

Supplementary Figure S10. The amino acid glutamic acid has a negative effect on *alaA::*Tn5 mutant growth. The *Xanthomonas* L148::Tn5 strains were grown in minimal XVM2 supplicated with each and in combinations of the following amino acids: alanine (ala), glutamic acid (glu), and arginine (arg) with final concentration of 3mM and growth was observed for 3 days. Data from 3 biological replicates were used. Different letters indicate statistically significant differences (ANOVA with *post hoc* Tukey's test, $P \leq 0.05$). Results are depicted as box plots with the boxes spanning the interquartile range (IQR, 25th to 75th percentiles), the mid-line indicates the median, and the whiskers cover the minimum and maximum values not extending beyond 1.5x of the IQR.

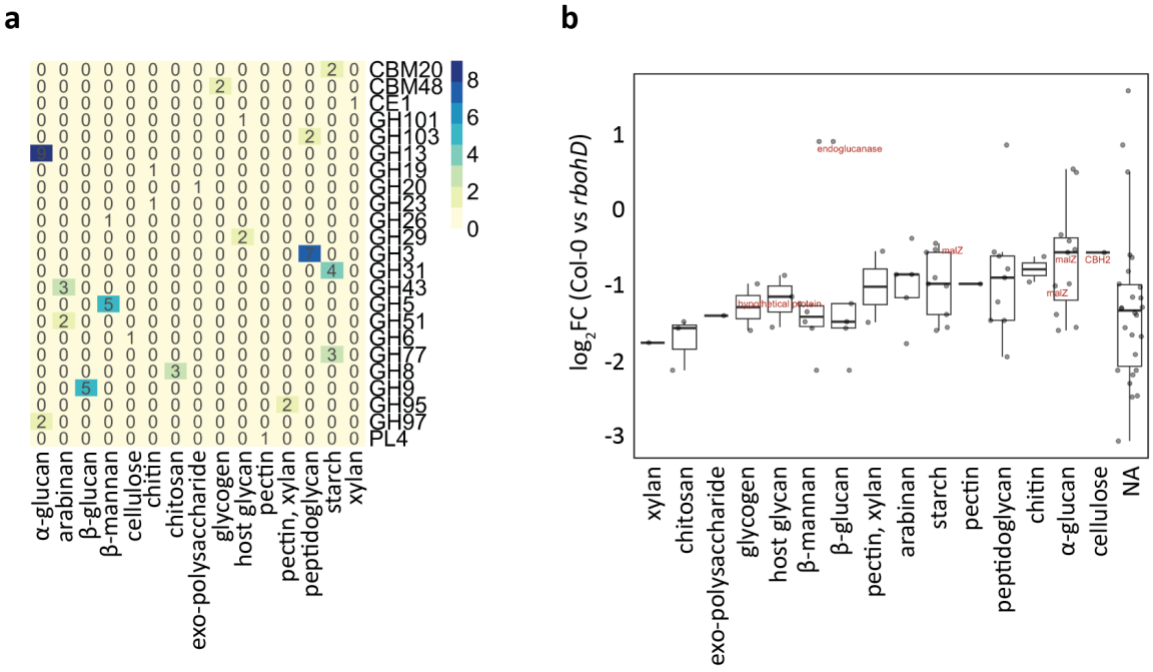

Supplementary Figure S11. Significantly down-regulated CAZymes in Col-0 can potentially degrade plant host cell wall components. **a,** Heatmap representation of the number of significantly differentially expressed CAZyme genes in *Xanthomonas* L148 (Col-0 vs. *rbohD*) with the respective potential substrates. **b**, Log_2 fold changes of the CAZyme gene expression (Col-0 vs. *rbohD*) with their respective potential substrates; *Xanthomonas* L148::Tn5 candidate genes with CAZyme annotations are labelled. Results in **b** are depicted as box plots with the boxes spanning the interquartile range (IQR, 25th to 75th percentiles), the mid-line indicates the median, and the whiskers cover the minimum and maximum values not extending beyond 1.5x of the IQR. This figure was adopted from Entila et al, (*in preparation*).

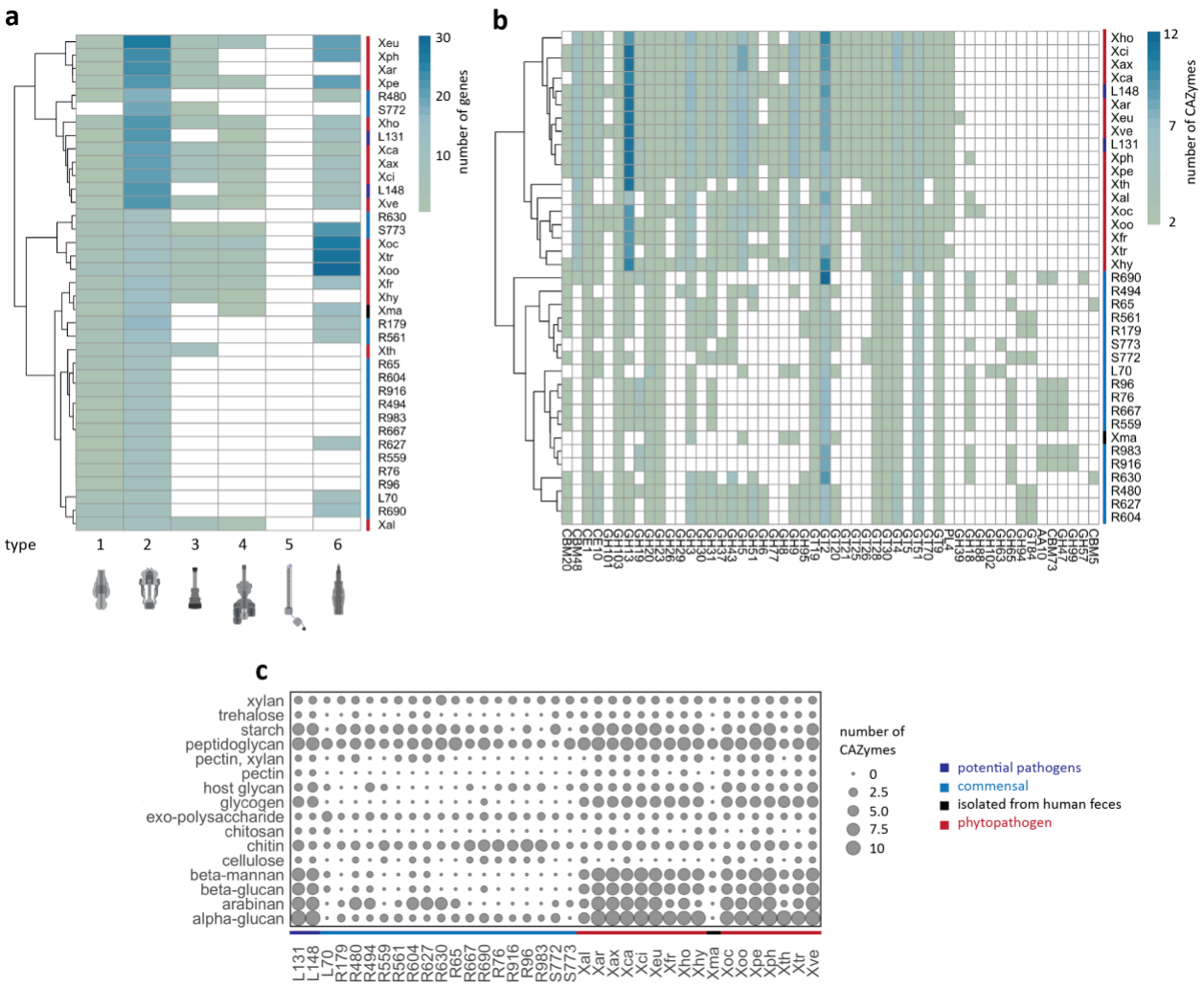

Supplementary Figure S12. Secretion systems and CAZyme repertoire of Xanthomonadales clade. **a-b,** genomic examination of Xanthomonadales members of *A. thaliana* microbiota (20, Bai et al, 2015) and pathogenic *Xanthomonas* strains (17): Xal, = *X. albineans*; Xar = *X. arboricola;* Xax = *X. axonopodis*; Xca = *X. campestris;* Xci = *X. citri;* Xeu = *X. euvesicatoria;* Xfr = *X. fragariae;* Xho = *X. hortorum;* Xhy = *X. hyacinthi;* Xoc = *X. oryzae* pv. *oryzicola*; Xoo = *X. oryzae* pv. *oryzae;* Xpe = *X. perforans;* Xph = *X. phaseoli;* Xth = *X. theicola;* Xtr = *X. translucens;* Xve = *X. vesicatoria;* Xma = *X. massiliensis* is non-pathogenic strain isolated from human feces; L148 (in this study) and L131 (Pfeilmeier et al, 2021) are potentially pathogenic. **a,** occurrence of type 1 to 6 secretion systems. **b,** CAZyme repertoire of the Xanthomonadales. **c,** potential substrates of the genome encoded CAZymes. Some illustrations created in BioRender. This figure was adopted from Entila et al, (*in preparation*).

List of Supplementary Tables and Datasets

Supplementary Table S1. List of *Arabidopsis thaliana* wild-type and mutants used in this study.
Supplementary Table S2. List of bacterial strains used and generated in this study.
Supplementary Table S3. List of primers and PCR profiles used in this study.

Supplementary Dataset S1. Results of the weighted gene network co-expression analysis of the Col-0 plant transcriptome upon mono-infiltration with microbiota members 6 hpi.
Supplementary Dataset S2. GO term enrichment analysis for the gene modules in the plant transcriptome.
Supplementary Dataset S3. List of genes within modules relevant to PTI readouts determined through support vector machine with recursive feature elimination.
Supplementary Dataset S4. List of *Xanthomonas* L148::Tn5 mutant candidates with loss-of-mortality in *rbohD* phenotypes using the high-throughput screening.
Supplementary Dataset S5. Top table of the DEGs for *in planta Xanthomonas* L148 transcriptome Col-0 vs. *rbohD* colonized plants.
Supplementary Dataset S6. Clustering membership of the DEGs and the GO term enrichment analysis for the gene clusters.

All the supplementary tables and datasets are deposited in EDMOND and can be accessed through the following link:

https://edmond.mpdl.mpg.de/privateurl.xhtml?token=01e73ff1-67c0-4072-91a7-e747bfc4e143

9. AUTHOR CONTRIBUTIONS

The **CHAPTER 2** of this thesis will be included in a manuscript for a publication and is authored by the following:

Frederickson Entila[1,2], Xiaowei Han[1,3,4], Akira Mine[5,6], Paul Schulze-Lefert[2], Kenichi Tsuda[1,2,3,4*]

[1]State Key Laboratory of Agricultural Microbiology, Hubei Hongshan Laboratory, Hubei Key Lab of Plant Pathology, College of Plant Science and Technology, Huazhong Agricultural University, Wuhan 430070, China.

[2]Department of Plant Microbe Interactions, Max Planck Institute for Plant Breeding Research, Carl-von-Linne-Weg 10, Cologne 50829, Germany

[3]Shenzhen Institute of Nutrition and Health, Huazhong Agricultural University, Wuhan 430070, China.

[4]Shenzhen Branch, Guangdong Laboratory of Lingnan Modern Agriculture, Genome Analysis Laboratory of the Ministry of Agriculture and Rural Affairs, Agricultural Genomics Institute at Shenzhen, Chinese Academy of Agricultural Sciences, Shenzhen, Guangdong 518120, China

[5]JST PRESTO, Kawaguchi-shi, Saitama 332-0012, Japan

[6]Laboratory of Plant Pathology, Graduate School of Agriculture, Kyoto University, Kyoto 606-8502, Japan

F.E. and K.T. **conceived the research**. **F.E.,** X.H., P.S.-L, and K.T. **designed the research**. A.M. designed and constructed *Pto* lux. **F.E. performed all of the experimental work and the analysis of the data. F.E.** and K.T. **wrote the manuscript with input from all the authors**.

10. REFERENCES

1 Agler MT, Ruhe J, Kroll S, Morhenn C, Kim S-T, Weigel D, et al. (2016) Microbial Hub Taxa Link Host and Abiotic Factors to Plant Microbiome Variation. PLoS Biol 14(1): e1002352. https://doi.org/10.1371/journal.pbio.1002352

2 Ahan Dalal, Ziv Attia, & Menachem Moshelion. (2021). Flagellin triggers mesophyll dehydration: An early PTI defense against bacterial establishment in intercellular spaces. BioRxiv, 2020.12.31.424953. https://doi.org/10.1101/2020.12.31.424953

3 Antolín-Llovera, M., Petutsching, E. K., Ried, M. K., Lipka, V., Nürnberger, T., Robatzek, S., & Parniske, M. (2014). Knowing your friends and foes--plant receptor-like kinases as initiators of symbiosis or defence. The New phytologist, 204(4), 791–802. https://doi.org/10.1111/nph.13117

4 Arvizu-Gómez, J. L., Hernández-Morales, A., Juárez-Navarro, R. A., Paredes-Tadeo, J. D., Campos-Guillén, J., Pacheco-Aguilar, J. R., Martínez-Rizo, A. B., & González-Reyes, C. (2022). OxyR Positively Influences Phaseolotoxin Synthesis and Pyoverdin Production in Pseudomonas savastanoi pv. phaseolicola NPS3121. Microorganisms, 10(11), 2123. https://doi.org/10.3390/microorganisms10112123

5 Asano, T., Nguyen, T. H., Yasuda, M., Sidiq, Y., Nishimura, K., Nakashita, H., & Nishiuchi, T. (2020). Arabidopsis MAPKKK δ-1 is required for full immunity against bacterial and fungal infection. *Journal of experimental botany*, *71*(6), 2085–2097. https://doi.org/10.1093/jxb/erz556

6 Ayumi Matsumoto, Titus Schlüter, Katharina Melkonian, Atsushi Takeda, Hirofumi Nakagami, Akira Mine. (2022). A versatile Tn7 transposon-based bioluminescence tagging tool for quantitative and spatial detection of bacteria in plants, Plant Communications, Volume 3, Issue 1, 2022, 100227, ISSN 2590-3462, https://doi.org/10.1016/j.xplc.2021.100227.

7 Bacete, L., Mélida, H., Miedes, E., & Molina, A. (2018). Plant cell wall-mediated immunity: cell wall changes trigger disease resistance responses. The Plant journal : for cell and molecular biology, 93(4), 614–636. https://doi.org/10.1111/tpj.13807

8 Bai, Y., Müller, D., Srinivas, G. et al. (2015). Functional overlap of the Arabidopsis leaf and root microbiota. Nature 528, 364–369, https://doi.org/10.1038/nature16192

9 Bais, H. P., Weir, T. L., Perry, L. G., Gilroy, S., & Vivanco, J. M. (2006). The role of root exudates in rhizosphere interactions with plants and other organisms. Annual review of plant biology, 57, 233–266. https://doi.org/10.1146/annurev.arplant.57.032905.105159

10 Bao, Z., Wei, H. L., Ma, X., & Swingle, B. (2020). Pseudomonas syringae AlgU Downregulates Flagellin Gene Expression, Helping Evade Plant Immunity. Journal of bacteriology, 202(4), e00418-19. https://doi.org/10.1128/JB.00418-19
11 Barbosa, V.A.A., Lery, L.M.S. Insights into Klebsiella pneumoniae type VI secretion system transcriptional regulation. BMC Genomics 20, 506 (2019). https://doi.org/10.1186/s12864-019-5885-9
12 Bartsev, A. V., Deakin, W. J., Boukli, N. M., McAlvin, C. B., Stacey, G., Malnoë, P., Broughton, W. J., & Staehelin, C. (2004). NopL, an effector protein of Rhizobium sp. NGR234, thwarts activation of plant defense reactions. Plant physiology, 134(2), 871–879. https://doi.org/10.1104/pp.103.031740
13 Bastide, P., Solís-Lemus, C., Kriebel, R., William Sparks, K., & Ané, C. (2018). Phylogenetic Comparative Methods on Phylogenetic Networks with Reticulations. Systematic biology, 67(5), 800–820. https://doi.org/10.1093/sysbio/syy033
14 Bebber, D., Ramotowski, M. & Gurr, S. Crop pests and pathogens move polewards in a warming world. Nature Clim Change 3, 985–988 (2013). https://doi.org/10.1038/nclimate1990
15 Beckers, B., Op De Beeck, M., Weyens, N., Van Acker, R., Van Montagu, M., Boerjan, W., & Vangronsveld, J. (2016). Lignin engineering in field-grown poplar trees affects the endosphere bacterial microbiome. Proceedings of the National Academy of Sciences of the United States of America, 113(8), 2312–2317. https://doi.org/10.1073/pnas.1523264113
16 Beketov, M. A., Kefford, B. J., Schäfer, R. B., & Liess, M. (2013). Pesticides reduce regional biodiversity of stream invertebrates. Proceedings of the National Academy of Sciences of the United States of America, 110(27), 11039–11043. https://doi.org/10.1073/pnas.1305618110
17 Bergelson, J., Mittelstrass, J., & Horton, M. W. (2019). Characterizing both bacteria and fungi improves understanding of the Arabidopsis root microbiome. Scientific reports, 9(1), 24. https://doi.org/10.1038/s41598-018-37208-z
18 Bigeard, J., Colcombet, J., & Hirt, H. (2015). Signaling mechanisms in pattern-triggered immunity (PTI). Molecular plant, 8(4), 521–539. https://doi.org/10.1016/j.molp.2014.12.022
19 Birkenbihl, R. P., Kracher, B., Ross, A., Kramer, K., Finkemeier, I., & Somssich, I. E. (2018). Principles and characteristics of the Arabidopsis WRKY regulatory network during early MAMP-triggered immunity. *The Plant journal : for cell and molecular biology*, *96*(3), 487–502. https://doi.org/10.1111/tpj.14043
20 Blume, B., Nürnberger, T., Nass, N., & Scheel, D. (2000). Receptor-mediated increase in cytoplasmic free calcium required for activation of pathogen defense in parsley. The Plant cell, 12(8), 1425–1440. https://doi.org/10.1105/tpc.12.8.1425
21 Bodenhausen, N., Bortfeld-Miller, M., Ackermann, M., & Vorholt, J. A. (2014). A synthetic community approach reveals plant genotypes affecting the phyllosphere microbiota. PLoS genetics, 10(4), e1004283. https://doi.org/10.1371/journal.pgen.1004283
22 Boller, T., & Felix, G. (2009). A renaissance of elicitors: perception of microbe-associated molecular patterns and danger signals by pattern-recognition receptors. Annual review of plant biology, 60, 379–406. https://doi.org/10.1146/annurev.arplant.57.032905.105346
23 Bozsoki, Z., Gysel, K., Hansen, S. B., Lironi, D., Krönauer, C., Feng, F., de Jong, N., Vinther, M., Kamble, M., Thygesen, M. B., Engholm, E., Kofoed, C., Fort, S., Sullivan, J. T., Ronson, C. W., Jensen, K. J., Blaise, M., Oldroyd, G., Stougaard, J., Andersen, K. R., … Radutoiu, S. (2020). Ligand-recognizing motifs in plant LysM receptors are major determinants of specificity. Science (New York, N.Y.), 369(6504), 663–670. https://doi.org/10.1126/science.abb3377
24 Brown, S. P., Cornforth, D. M., & Mideo, N. (2012). Evolution of virulence in opportunistic pathogens: generalism, plasticity, and control. Trends in microbiology, 20(7), 336–342. https://doi.org/10.1016/j.tim.2012.04.005
25 Bulgarelli, D., Rott, M., Schlaeppi, K., Ver Loren van Themaat, E., Ahmadinejad, N., Assenza, F., Rauf, P., Huettel, B., Reinhardt, R., Schmelzer, E., Peplies, J., Gloeckner, F. O., Amann, R., Eickhorst, T., & Schulze-Lefert, P. (2012). Revealing structure and assembly cues for Arabidopsis root-inhabiting bacterial microbiota. Nature, 488(7409), 91–95.
26 Bulgarelli, D., Schlaeppi, K., Spaepen, S., Ver Loren van Themaat, E., & Schulze-Lefert, P. (2013). Structure and functions of the bacterial microbiota of plants. Annual review of plant biology, 64, 807–838. https://doi.org/10.1146/annurev-arplant-050312-120106

27 Buscaill, P., Chandrasekar, B., Sanguankiattichai, N., Kourelis, J., Kaschani, F., Thomas, E. L., Morimoto, K., Kaiser, M., Preston, G. M., Ichinose, Y., & van der Hoorn, R. A. L. (2019). Glycosidase and glycan polymorphism control hydrolytic release of immunogenic flagellin peptides. Science (New York, N.Y.), 364(6436), eaav0748. https://doi.org/10.1126/science.aav0748
28 Cantalapiedra, C. P., Hernández-Plaza, A., Letunic, I., Bork, P., & Huerta-Cepas, J. (2021). eggNOG-mapper v2: Functional Annotation, Orthology Assignments, and Domain Prediction at the Metagenomic Scale. Molecular biology and evolution, 38(12), 5825–5829. https://doi.org/10.1093/molbev/msab293
29 Carlström, C. I., Field, C. M., Bortfeld-Miller, M., Müller, B., Sunagawa, S., & Vorholt, J. A. (2019). Synthetic microbiota reveal priority effects and keystone strains in the Arabidopsis phyllosphere. Nature ecology & evolution, 3(10), 1445–1454. https://doi.org/10.1038/s41559-019-0994-z
30 Caruso, R., Mathes, T., Martens, E. C., Kamada, N., Nusrat, A., Inohara, N., & Núñez, G. (2019). A specific gene-microbe interaction drives the development of Crohn's disease-like colitis in mice. Science immunology, 4(34), eaaw4341. https://doi.org/10.1126/sciimmunol.aaw4341
31 Castillo-Ruiz, A., Mosley, M., George, A. J., Mussaji, L. F., Fullerton, E. F., Ruszkowski, E. M., Jacobs, A. J., Gewirtz, A. T., Chassaing, B., & Forger, N. G. (2018). The microbiota influences cell death and microglial colonization in the perinatal mouse brain. Brain, behavior, and immunity, 67, 218–229. https://doi.org/10.1016/j.bbi.2017.08.027
32 Castrillo, G., Teixeira, P. J., Paredes, S. H., Law, T. F., de Lorenzo, L., Feltcher, M. E., Finkel, O. M., Breakfield, N. W., Mieczkowski, P., Jones, C. D., Paz-Ares, J., & Dangl, J. L. (2017). Root microbiota drive direct integration of phosphate stress and immunity. Nature, 543(7646), 513–518. https://doi.org/10.1038/nature21417
33 Charrad, M., Ghazzali, . N., Boiteau, V., & Niknafs, A. (2014). NbClust: An R Package for Determining the Relevant Number of Clusters in a Data Set. Journal of Statistical Software, 61(6), 1–36. https://doi.org/10.18637/jss.v061.i06
34 Chase, J. M., & Myers, J. A. (2011). Disentangling the importance of ecological niches from stochastic processes across scales. Philosophical transactions of the Royal Society of London. Series B, Biological sciences, 366(1576), 2351–2363. https://doi.org/10.1098/rstb.2011.0063
35 Chen, T., Nomura, K., Wang, X. et al. A plant genetic network for preventing dysbiosis in the phyllosphere. Nature 580, 653–657 (2020). https://doi.org/10.1038/s41586-020-2185-0
36 Cheng, J. H. T., Bredow, M., Monaghan, J., & diCenzo, G. C. (2021). Proteobacteria Contain Diverse flg22 Epitopes That Elicit Varying Immune Responses in Arabidopsis thaliana. Molecular plant-microbe interactions : MPMI, 34(5), 504–510. https://doi.org/10.1094/MPMI-11-20-0314-SC
37 Chin, K. H., Lee, Y. C., Tu, Z. L., Chen, C. H., Tseng, Y. H., Yang, J. M., Ryan, R. P., McCarthy, Y., Dow, J. M., Wang, A. H., & Chou, S. H. (2010). The cAMP receptor-like protein CLP is a novel c-di-GMP receptor linking cell-cell signaling to virulence gene expression in Xanthomonas campestris. Journal of molecular biology, 396(3), 646–662. https://doi.org/10.1016/j.jmb.2009.11.076
38 Chisholm, S. T., Coaker, G., Day, B., & Staskawicz, B. J. (2006). Host-microbe interactions: shaping the evolution of the plant immune response. Cell, 124(4), 803–814. https://doi.org/10.1016/j.cell.2006.02.008
39 Chow, J., & Mazmanian, S. K. (2010). A pathobiont of the microbiota balances host colonization and intestinal inflammation. Cell host & microbe, 7(4), 265–276. https://doi.org/10.1016/j.chom.2010.03.004
40 Christman, M. F., Storz, G., & Ames, B. N. (1989). OxyR, a positive regulator of hydrogen peroxide-inducible genes in Escherichia coli and Salmonella typhimurium, is homologous to a family of bacterial regulatory proteins. Proceedings of the National Academy of Sciences of the United States of America, 86(10), 3484–3488.
41 Cianciotto N. P. (2005). Type II secretion: a protein secretion system for all seasons. Trends in microbiology, 13(12), 581–588. https://doi.org/10.1016/j.tim.2005.09.005
42 Clasen, S. J., Bell, M. E. W., Borbón, A., Lee, D. H., Henseler, Z. M., de la Cuesta-Zuluaga, J., Parys, K., Zou, J., Wang, Y., Altmannova, V., Youngblut, N. D., Weir, J. R., Gewirtz, A. T.,

Belkhadir, Y., & Ley, R. E. (2023). Silent recognition of flagellins from human gut commensal bacteria by Toll-like receptor 5. Science immunology, 8(79), eabq7001. https://doi.org/10.1126/sciimmunol.abq7001
43 Clay, N. K., Adio, A. M., Denoux, C., Jander, G., & Ausubel, F. M. (2009). Glucosinolate metabolites required for an Arabidopsis innate immune response. Science (New York, N.Y.), 323(5910), 95–101. https://doi.org/10.1126/science.1164627
44 Colaianni, N. R., Parys, K., Lee, H. S., Conway, J. M., Kim, N. H., Edelbacher, N., Mucyn, T. S., Madalinski, M., Law, T. F., Jones, C. D., Belkhadir, Y., & Dangl, J. L. (2021). A complex immune response to flagellin epitope variation in commensal communities. Cell host & microbe, 29(4), 635–649.e9. https://doi.org/10.1016/j.chom.2021.02.006
45 Coleman-Derr, D., Desgarennes, D., Fonseca-Garcia, C., Gross, S., Clingenpeel, S., Woyke, T., North, G., Visel, A., Partida-Martinez, L. P., & Tringe, S. G. (2016). Plant compartment and biogeography affect microbiome composition in cultivated and native Agave species. The New phytologist, 209(2), 798–811. https://doi.org/10.1111/nph.13697
46 Conway, J.M., Walton, W.G., Salas-González, I. et al. Diverse MarR bacterial regulators of auxin catabolism in the plant microbiome. Nat Microbiol 7, 1817–1833 (2022). https://doi.org/10.1038/s41564-022-01244-3
47 Cosgrove, D. Growth of the plant cell wall. Nat Rev Mol Cell Biol 6, 850–861 (2005). https://doi.org/10.1038/nrm1746
48 Csardi G, Nepusz T (2006). “The igraph software package for complex network research.” InterJournal, Complex Systems, 1695. https://igraph.org.
49 Danne, C., Ryzhakov, G., Martínez-López, M., Ilott, N. E., Franchini, F., Cuskin, F., Lowe, E. C., Bullers, S. J., Arthur, J. S. C., & Powrie, F. (2017). A Large Polysaccharide Produced by Helicobacter hepaticus Induces an Anti-inflammatory Gene Signature in Macrophages. Cell host & microbe, 22(6), 733–745.e5. https://doi.org/10.1016/j.chom.2017.11.002
50 de Jonge, R., van Esse, H. P., Kombrink, A., Shinya, T., Desaki, Y., Bours, R., van der Krol, S., Shibuya, N., Joosten, M. H., & Thomma, B. P. (2010). Conserved fungal LysM effector Ecp6 prevents chitin-triggered immunity in plants. Science (New York, N.Y.), 329(5994), 953–955. https://doi.org/10.1126/science.1190859
51 De Lorenzo, G., Ferrari, S., Cervone, F., & Okun, E. (2018). Extracellular DAMPs in Plants and Mammals: Immunity, Tissue Damage and Repair. Trends in immunology, 39(11), 937–950. https://doi.org/10.1016/j.it.2018.09.006
52 Denness, L., McKenna, J. F., Segonzac, C., Wormit, A., Madhou, P., Bennett, M., Mansfield, J., Zipfel, C., & Hamann, T. (2011). Cell wall damage-induced lignin biosynthesis is regulated by a reactive oxygen species- and jasmonic acid-dependent process in Arabidopsis. Plant physiology, 156(3), 1364–1374. https://doi.org/10.1104/pp.111.175737
53 Dodds, P. N., & Rathjen, J. P. (2010). Plant immunity: towards an integrated view of plant-pathogen interactions. Nature reviews. Genetics, 11(8), 539–548. https://doi.org/10.1038/nrg2812
54 Doke, N. (1985). NADPH-dependent O2− generation in membrane fractions isolated from wounded potato tubers inoculated with Phytophthora infestans. Physiological Plant Pathology, 27(3), 311-322.
55 Dombrowski, N., Schlaeppi, K., Agler, M. T., Hacquard, S., Kemen, E., Garrido-Oter, R., Wunder, J., Coupland, G., & Schulze-Lefert, P. (2017). Root microbiota dynamics of perennial Arabis alpina are dependent on soil residence time but independent of flowering time. The ISME journal, 11(1), 43–55. https://doi.org/10.1038/ismej.2016.109
56 Drew, G.C., Stevens, E.J. & King, K.C. Microbial evolution and transitions along the parasite–mutualist continuum. Nat Rev Microbiol 19, 623–638 (2021). https://doi.org/10.1038/s41579-021-00550-7
57 Drula, E., Garron, M. L., Dogan, S., Lombard, V., Henrissat, B., & Terrapon, N. (2022). The carbohydrate-active enzyme database: functions and literature. Nucleic acids research, 50(D1), D571–D577. https://doi.org/10.1093/nar/gkab1045
58 Dudek, C. A., & Jahn, D. (2022). PRODORIC: state-of-the-art database of prokaryotic gene regulation. Nucleic acids research, 50(D1), D295–D302. https://doi.org/10.1093/nar/gkab1110

59 Durán, P., Thiergart, T., Garrido-Oter, R., Agler, M., Kemen, E., Schulze-Lefert, P., & Hacquard, S. (2018). Microbial Interkingdom Interactions in Roots Promote Arabidopsis Survival. Cell, 175(4), 973–983.e14. https://doi.org/10.1016/j.cell.2018.10.020
60 Edwards, J., Johnson, C., Santos-Medellín, C., Lurie, E., Podishetty, N. K., Bhatnagar, S., Eisen, J. A., & Sundaresan, V. (2015). Structure, variation, and assembly of the root-associated microbiomes of rice. Proceedings of the National Academy of Sciences of the United States of America, 112(8), E911–E920. https://doi.org/10.1073/pnas.1414592112
61 Emonet, A., Zhou, F., Vacheron, J., Heiman, C. M., Dénervaud Tendon, V., Ma, K. W., Schulze-Lefert, P., Keel, C., & Geldner, N. (2021). Spatially Restricted Immune Responses Are Required for Maintaining Root Meristematic Activity upon Detection of Bacteria. Current biology : CB, 31(5), 1012–1028.e7. https://doi.org/10.1016/j.cub.2020.12.048
62 Erisman, J., Sutton, M., Galloway, J. et al. How a century of ammonia synthesis changed the world. Nature Geosci 1, 636–639 (2008). https://doi.org/10.1038/ngeo325
63 Expert, D., Patrit, O., Shevchik, V. E., Perino, C., Boucher, V., Creze, C., Wenes, E., & Fagard, M. (2018). Dickeya dadantii pectic enzymes necessary for virulence are also responsible for activation of the Arabidopsis thaliana innate immune system. Molecular plant pathology, 19(2), 313–327. https://doi.org/10.1111/mpp.12522
64 Farber C. R. (2013). Systems-level analysis of genome-wide association data. G3 (Bethesda, Md.), 3(1), 119–129. https://doi.org/10.1534/g3.112.004788
65 Feng, F., Sun, J., Radhakrishnan, G. V., Lee, T., Bozsóki, Z., Fort, S., Gavrin, A., Gysel, K., Thygesen, M. B., Andersen, K. R., Radutoiu, S., Stougaard, J., & Oldroyd, G. E. D. (2019). A combination of chitooligosaccharide and lipochitooligosaccharide recognition promotes arbuscular mycorrhizal associations in Medicago truncatula. Nature communications, 10(1), 5047. https://doi.org/10.1038/s41467-019-12999-5
66 Finkel, O.M., Salas-González, I., Castrillo, G. et al. A single bacterial genus maintains root growth in a complex microbiome. Nature 587, 103–108 (2020). https://doi.org/10.1038/s41586-020-2778-7
67 Fitzpatrick, C. R., Copeland, J., Wang, P. W., Guttman, D. S., Kotanen, P. M., & Johnson, M. T. J. (2018). Assembly and ecological function of the root microbiome across angiosperm plant species. Proceedings of the National Academy of Sciences of the United States of America, 115(6), E1157–E1165. https://doi.org/10.1073/pnas.1717617115
68 Flores-Cruz, Z., & Allen, C. (2011). Necessity of OxyR for the hydrogen peroxide stress response and full virulence in Ralstonia solanacearum. Applied and environmental microbiology, 77(18), 6426–6432. https://doi.org/10.1128/AEM.05813-11
69 Foley, J., Ramankutty, N., Brauman, K. et al. Solutions for a cultivated planet. Nature 478, 337–342 (2011). https://doi.org/10.1038/nature10452
70 Fonseca, J. P., Lakshmanan, V., Boschiero, C., & Mysore, K. S. (2022). The Pattern Recognition Receptor FLS2 Can Shape the Arabidopsis Rhizosphere Microbiome β-Diversity but Not EFR1 and CERK1. Plants (Basel, Switzerland), 11(10), 1323. https://doi.org/10.3390/plants11101323
71 Fujita, S., De Bellis, D., Edel, K. H., Köster, P., Andersen, T. G., Schmid-Siegert, E., Dénervaud Tendon, V., Pfister, A., Marhavý, P., Ursache, R., Doblas, V. G., Barberon, M., Daraspe, J., Creff, A., Ingram, G., Kudla, J., & Geldner, N. (2020). SCHENGEN receptor module drives localized ROS production and lignification in plant roots. The EMBO journal, 39(9), e103894. https://doi.org/10.15252/embj.2019103894
72 Furukawa, T., Inagaki, H., Takai, R., Hirai, H., & Che, F. S. (2014). Two distinct EF-Tu epitopes induce immune responses in rice and Arabidopsis. Molecular plant-microbe interactions : MPMI, 27(2), 113–124. https://doi.org/10.1094/MPMI-10-13-0304-R
73 Gámez-Arjona, F. M., Vitale, S., Voxeur, A., Dora, S., Müller, S., Sancho-Andrés, G., Montesinos, J. C., Di Pietro, A., & Sánchez-Rodríguez, C. (2022). Impairment of the cellulose degradation machinery enhances Fusarium oxysporum virulence but limits its reproductive fitness. Science advances, 8(16), eabl9734. https://doi.org/10.1126/sciadv.abl9734
74 Gano-Cohen, K. A., Wendlandt, C. E., Stokes, P. J., Blanton, M. A., Quides, K. W., Zomorrodian, A., Adinata, E. S., & Sachs, J. L. (2019). Interspecific conflict and the evolution of ineffective rhizobia. Ecology letters, 22(6), 914–924. https://doi.org/10.1111/ele.13247

75 Gao, F., Zhang, B. S., Zhao, J. H., Huang, J. F., Jia, P. S., Wang, S., Zhang, J., Zhou, J. M., & Guo, H. S. (2019). Deacetylation of chitin oligomers increases virulence in soil-borne fungal pathogens. Nature plants, 5(11), 1167–1176. https://doi.org/10.1038/s41477-019-0527-4
76 Garrido-Oter, R., Nakano, R. T., Dombrowski, N., Ma, K. W., AgBiome Team, McHardy, A. C., & Schulze-Lefert, P. (2018). Modular Traits of the Rhizobiales Root Microbiota and Their Evolutionary Relationship with Symbiotic Rhizobia. Cell host & microbe, 24(1), 155–167.e5. https://doi.org/10.1016/j.chom.2018
77 Gauthier, A. E., Chandler, C. E., Poli, V., Gardner, F. M., Tekiau, A., Smith, R., Bonham, K. S., Cordes, E. E., Shank, T. M., Zanoni, I., Goodlett, D. R., Biller, S. J., Ernst, R. K., Rotjan, R. D., & Kagan, J. C. (2021). Deep-sea microbes as tools to refine the rules of innate immune pattern recognition. Science immunology, 6(57), eabe0531. https://doi.org/10.1126/sciimmunol.abe0531
78 Ge, Y. Y., Xiang, Q. W., Wagner, C., Zhang, D., Xie, Z. P., & Staehelin, C. (2016). The type 3 effector NopL of Sinorhizobium sp. strain NGR234 is a mitogen-activated protein kinase substrate. Journal of experimental botany, 67(8), 2483–2494. https://doi.org/10.1093/jxb/erw065
79 Getzke, F., Hassani, M. A., Crüsemann, M., Malisic, M., Zhang, P., Ishigaki, Y., Böhringer, N., Jiménez Fernández, A., Wang, L., Ordon, J., Ma, K. W., Thiergart, T., Harbort, C. J., Wesseler, H., Miyauchi, S., Garrido-Oter, R., Shirasu, K., Schäberle, T. F., Hacquard, S., & Schulze-Lefert, P. (2023). Cofunctioning of bacterial exometabolites drives root microbiota establishment. Proceedings of the National Academy of Sciences of the United States of America, 120(15), e2221508120. https://doi.org/10.1073/pnas.2221508120
80 Gibson, D. G., Young, L., Chuang, R. Y., Venter, J. C., Hutchison, C. A., 3rd, & Smith, H. O. (2009). Enzymatic assembly of DNA molecules up to several hundred kilobases. Nature methods, 6(5), 343–345. https://doi.org/10.1038/nmeth.1318
81 Giuseppe P., Bonfim, I., Murakami, M. (2023). Enzymatic systems for carbohydrate utilization and biosynthesis in Xanthomonas and their role in pathogenesis and tissue specificity. Essays Biochem; 67 (3): 455–470. doi: https://doi.org/10.1042/EBC20220128
82 Godfray, H. C., Beddington, J. R., Crute, I. R., Haddad, L., Lawrence, D., Muir, J. F., Pretty, J., Robinson, S., Thomas, S. M., & Toulmin, C. (2010). Food security: the challenge of feeding 9 billion people. Science (New York, N.Y.), 327(5967), 812–818. https://doi.org/10.1126/science.1185383
83 Göhre, V., Spallek, T., Häweker, H., Mersmann, S., Mentzel, T., Boller, T., de Torres, M., Mansfield, J. W., & Robatzek, S. (2008). Plant pattern-recognition receptor FLS2 is directed for degradation by the bacterial ubiquitin ligase AvrPtoB. Current biology : CB, 18(23), 1824–1832. https://doi.org/10.1016/j.cub.2008.10.063
84 Gómez-Gómez, L., & Boller, T. (2000). FLS2: an LRR receptor-like kinase involved in the perception of the bacterial elicitor flagellin in Arabidopsis. Molecular cell, 5(6), 1003–1011. https://doi.org/10.1016/s1097-2765(00)80265-8
85 Gómez-Gómez, L., Felix, G., & Boller, T. (1999). A single locus determines sensitivity to bacterial flagellin in Arabidopsis thaliana. The Plant journal : for cell and molecular biology, 18(3), 277–284. https://doi.org/10.1046/j.1365-313x.1999.00451.x
86 González-Chávez, M. C., Carrillo-González, R., Wright, S. F., & Nichols, K. A. (2004). The role of glomalin, a protein produced by arbuscular mycorrhizal fungi, in sequestering potentially toxic elements. Environmental pollution (Barking, Essex : 1987), 130(3), 317–323. https://doi.org/10.1016/j.envpol.2004.01.004
87 González-Flecha, B., & Demple, B. (1997). Transcriptional regulation of the Escherichia coli oxyR gene as a function of cell growth. Journal of bacteriology, 179(19), 6181–6186. https://doi.org/10.1128/jb.179.19.6181-6186.1997
88 Gourion, B., Berrabah, F., Ratet, P., & Stacey, G. (2015). Rhizobium-legume symbioses: the crucial role of plant immunity. Trends in plant science, 20(3), 186–194. https://doi.org/10.1016/j.tplants.2014.11.008
89 Gronnier, J., Franck, C. M., Stegmann, M., DeFalco, T. A., Abarca, A., von Arx, M., Dünser, K., Lin, W., Yang, Z., Kleine-Vehn, J., Ringli, C., & Zipfel, C. (2022). Regulation of immune receptor kinase plasma membrane nanoscale organization by a plant peptide hormone and its receptors. eLife, 11, e74162. https://doi.org/10.7554/eLife.74162

90 Gu Z (2022). “Complex Heatmap Visualization.” iMeta. doi: 10.1002/imt2.43
91 Gui, Y. J., Chen, J. Y., Zhang, D. D., Li, N. Y., Li, T. G., Zhang, W. Q., Wang, X. Y., Short, D. P. G., Li, L., Guo, W., Kong, Z. Q., Bao, Y. M., Subbarao, K. V., & Dai, X. F. (2017). Verticillium dahliae manipulates plant immunity by glycoside hydrolase 12 proteins in conjunction with carbohydrate-binding module 1. Environmental microbiology, 19(5), 1914–1932. https://doi.org/10.1111/1462-2920.13695
92 Hackenberg, T., Juul, T., Auzina, A., Gwizdz, S., Malolepszy, A., Van Der Kelen, K., Dam, S., Bressendorff, S., Lorentzen, A., Roepstorff, P., Lehmann Nielsen, K., Jørgensen, J. E., Hofius, D., Van Breusegem, F., Petersen, M., & Andersen, S. U. (2013). Catalase and NO CATALASE ACTIVITY1 promote autophagy-dependent cell death in Arabidopsis. The Plant cell, 25(11), 4616–4626. https://doi.org/10.1105/tpc.113.117192
93 Hacquard, S., Spaepen, S., Garrido-Oter, R., & Schulze-Lefert, P. (2017). Interplay Between Innate Immunity and the Plant Microbiota. Annual review of phytopathology, 55, 565–589. https://doi.org/10.1146/annurev-phyto-080516-035623
94 Hacquard, S., Kracher, B., Hiruma, K. et al. Survival trade-offs in plant roots during colonization by closely related beneficial and pathogenic fungi. Nat Commun 7, 11362 (2016). https://doi.org/10.1038/ncomms11362
95 Ham, J. H., Kim, M. G., Lee, S. Y., & Mackey, D. (2007). Layered basal defenses underlie non-host resistance of Arabidopsis to Pseudomonas syringae pv. phaseolicola. The Plant journal : for cell and molecular biology, 51(4), 604–616. https://doi.org/10.1111/j.1365-313X.2007.03165.x
96 Hamonts, K., Trivedi, P., Garg, A., Janitz, C., Grinyer, J., Holford, P., Botha, F. C., Anderson, I. C., & Singh, B. K. (2018). Field study reveals core plant microbiota and relative importance of their drivers. Environmental microbiology, 20(1), 124–140. https://doi.org/10.1111/1462-2920.14031
97 Harbort, C. J., Hashimoto, M., Inoue, H., Niu, Y., Guan, R., Rombolà, A. D., Kopriva, S., Voges, M. J. E. E. E., Sattely, E. S., Garrido-Oter, R., & Schulze-Lefert, P. (2020). Root-Secreted Coumarins and the Microbiota Interact to Improve Iron Nutrition in Arabidopsis. Cell host & microbe, 28(6), 825–837.e6. https://doi.org/10.1016/j.chom.2020.09.006
98 Hayes, K. S., Bancroft, A. J., Goldrick, M., Portsmouth, C., Roberts, I. S., & Grencis, R. K. (2010). Exploitation of the intestinal microflora by the parasitic nematode Trichuris muris. Science (New York, N.Y.), 328(5984), 1391–1394. https://doi.org/10.1126/science.1187703
99 He, D., Singh, S.K., Peng, L. et al. Flavonoid-attracted Aeromonas sp. from the Arabidopsis root microbiome enhances plant dehydration resistance. ISME J 16, 2622–2632 (2022). https://doi.org/10.1038/s41396-022-01288-7
100 Heinz Körner, Heidi J. Sofia, Walter G. Zumft, Phylogeny of the bacterial superfamily of Crp-Fnr transcription regulators: exploiting the metabolic spectrum by controlling alternative gene programs, FEMS Microbiology Reviews, Volume 27, Issue 5, December 2003, Pages 559–592, https://doi.org/10.1016/S0168-6445(03)00066-4
101 Herp, S., Brugiroux, S., Garzetti, D., Ring, D., Jochum, L. M., Beutler, M., Eberl, C., Hussain, S., Walter, S., Gerlach, R. G., Ruscheweyh, H. J., Huson, D., Sellin, M. E., Slack, E., Hanson, B., Loy, A., Baines, J. F., Rausch, P., Basic, M., Bleich, A., … Stecher, B. (2019). Mucispirillum schaedleri Antagonizes Salmonella Virulence to Protect Mice against Colitis. Cell host & microbe, 25(5), 681–694.e8. https://doi.org/10.1016/j.chom.2019.03.004
102 Hiruma, K., Gerlach, N., Sacristán, S., Nakano, R. T., Hacquard, S., Kracher, B., Neumann, U., Ramírez, D., Bucher, M., O'Connell, R. J., & Schulze-Lefert, P. (2016). Root Endophyte Colletotrichum tofieldiae Confers Plant Fitness Benefits that Are Phosphate Status Dependent. Cell, 165(2), 464–474. https://doi.org/10.1016/j.cell.2016.02.028
103 Holmes, A., Pritchard, L., Hedley, P., Morris, J., McAteer, S. P., Gally, D. L., & Holden, N. J. (2020). A high-throughput genomic screen identifies a role for the plasmid-borne type II secretion system of Escherichia coli O157:H7 (Sakai) in plant-microbe interactions. Genomics, 112(6), 4242–4253. https://doi.org/10.1016/j.ygeno.2020.07.021
104 Horton, M. W., Bodenhausen, N., Beilsmith, K., Meng, D., Muegge, B. D., Subramanian, S., Vetter, M. M., Vilhjálmsson, B. J., Nordborg, M., Gordon, J. I., & Bergelson, J. (2014).

Genome-wide association study of Arabidopsis thaliana leaf microbial community. Nature communications, 5, 5320. https://doi.org/10.1038/ncomms6320
105 Hou, S., Thiergart, T., Vannier, N. et al. A microbiota–root–shoot circuit favours Arabidopsis growth over defence under suboptimal light. Nat. Plants 7, 1078–1092 (2021). https://doi.org/10.1038/s41477-021-00956-4
106 Howden, S. M., Soussana, J. F., Tubiello, F. N., Chhetri, N., Dunlop, M., & Meinke, H. (2007). Adapting agriculture to climate change. Proceedings of the National Academy of Sciences of the United States of America, 104(50), 19691–19696. https://doi.org/10.1073/pnas.0701890104
107 Hu, L., Robert, C.A.M., Cadot, S. et al. Root exudate metabolites drive plant-soil feedbacks on growth and defense by shaping the rhizosphere microbiota. Nat Commun 9, 2738 (2018). https://doi.org/10.1038/s41467-018-05122-7
108 Huang, A. C., Jiang, T., Liu, Y. X., Bai, Y. C., Reed, J., Qu, B., Goossens, A., Nützmann, H. W., Bai, Y., & Osbourn, A. (2019). A specialized metabolic network selectively modulates Arabidopsis root microbiota. Science (New York, N.Y.), 364(6440), eaau6389. https://doi.org/10.1126/science.aau6389
109 Huang, S., Jia, A., Song, W., Hessler, G., Meng, Y., Sun, Y., Xu, L., Laessle, H., Jirschitzka, J., Ma, S., Xiao, Y., Yu, D., Hou, J., Liu, R., Sun, H., Liu, X., Han, Z., Chang, J., Parker, J. E., & Chai, J. (2022). Identification and receptor mechanism of TIR-catalyzed small molecules in plant immunity. Science (New York, N.Y.), 377(6605), eabq3297. https://doi.org/10.1126/science.abq3297
110 Huchelmann, A., Boutry, M., & Hachez, C. (2017). Plant Glandular Trichomes: Natural Cell Factories of High Biotechnological Interest. Plant physiology, 175(1), 6–22. https://doi.org/10.1104/pp.17.00727
111 Hugouvieux, V., Barber, C. E., & Daniels, M. J. (1998). Entry of Xanthomonas campestris pv. campestris into hydathodes of Arabidopsis thaliana leaves: a system for studying early infection events in bacterial pathogenesis. Molecular plant-microbe interactions : MPMI, 11(6), 537–543. https://doi.org/10.1094/MPMI.1998.11.6.537
112 Jacobs, S., Zechmann, B., Molitor, A., Trujillo, M., Petutschnig, E., Lipka, V., Kogel, K. H., & Schäfer, P. (2011). Broad-spectrum suppression of innate immunity is required for colonization of Arabidopsis roots by the fungus Piriformospora indica. Plant physiology, 156(2), 726–740. https://doi.org/10.1104/pp.111.176446
113 Jakob, K., Goss, E. M., Araki, H., Van, T., Kreitman, M., & Bergelson, J. (2002). Pseudomonas viridiflava and P. syringae--natural pathogens of Arabidopsis thaliana. Molecular plant-microbe interactions : MPMI, 15(12), 1195–1203. https://doi.org/10.1094/MPMI.2002.15.12.1195
114 Jashni, M. K., Dols, I. H., Iida, Y., Boeren, S., Beenen, H. G., Mehrabi, R., Collemare, J., & de Wit, P. J. (2015). Synergistic Action of a Metalloprotease and a Serine Protease from Fusarium oxysporum f. sp. lycopersici Cleaves Chitin-Binding Tomato Chitinases, Reduces Their Antifungal Activity, and Enhances Fungal Virulence. Molecular plant-microbe interactions : MPMI, 28(9), 996–1008. https://doi.org/10.1094/MPMI-04-15-0074-R
115 Jia, A., Huang, S., Song, W., Wang, J., Meng, Y., Sun, Y., Xu, L., Laessle, H., Jirschitzka, J., Hou, J., Zhang, T., Yu, W., Hessler, G., Li, E., Ma, S., Yu, D., Gebauer, J., Baumann, U., Liu, X., Han, Z., … Chai, J. (2022). TIR-catalyzed ADP-ribosylation reactions produce signaling molecules for plant immunity. Science (New York, N.Y.), 377(6605), eabq8180. https://doi.org/10.1126/science.abq8180
116 Jin, L., & Mackey, D. M. (2017). Measuring Callose Deposition, an Indicator of Cell Wall Reinforcement, During Bacterial Infection in Arabidopsis. Methods in molecular biology (Clifton, N.J.), 1578, 195–205. https://doi.org/10.1007/978-1-4939-6859-6_16
117 Jochum, L., & Stecher, B. (2020). Label or Concept - What Is a Pathobiont?. Trends in microbiology, 28(10), 789–792. https://doi.org/10.1016/j.tim.2020.04.011
118 Jones, D.L., Nguyen, C. & Finlay, R.D. Carbon flow in the rhizosphere: carbon trading at the soil–root interface. Plant Soil 321, 5–33 (2009). https://doi.org/10.1007/s11104-009-9925-0
119 Jones, J. D., & Dangl, J. L. (2006). The plant immune system. Nature, 444(7117), 323–329. https://doi.org/10.1038/nature05286
120 Kadota, Y., Sklenar, J., Derbyshire, P., Stransfeld, L., Asai, S., Ntoukakis, V., Jones, J. D., Shirasu, K., Menke, F., Jones, A., & Zipfel, C. (2014). Direct regulation of the NADPH oxidase

RBOHD by the PRR-associated kinase BIK1 during plant immunity. Molecular cell, 54(1), 43–55. https://doi.org/10.1016/j.molcel.2014.02.021

121 Kannenberg, E. L., & Carlson, R. W. (2001). Lipid A and O-chain modifications cause Rhizobium lipopolysaccharides to become hydrophobic during bacteroid development. Molecular microbiology, 39(2), 379–391. https://doi.org/10.1046/j.1365-2958.2001.02225.x

122 Karasov, T. L., Almario, J., Friedemann, C., Ding, W., Giolai, M., Heavens, D., Kersten, S., Lundberg, D. S., Neumann, M., Regalado, J., Neher, R. A., Kemen, E., & Weigel, D. (2018). Arabidopsis thaliana and Pseudomonas Pathogens Exhibit Stable Associations over Evolutionary Timescales. Cell host & microbe, 24(1), 168–179.e4. https://doi.org/10.1016/j.chom.2018.06.011

123 Kessler, B., V. de Lorenzo, and K. N. Timmis. (1992). A general system to integrate lacZ fusions into the chromosomes of gram-negative eubacteria: regulation of the Pm-promotor of the Tol-plasmid studied with all controlling elements in monocopy. Mol. Gen. Genet. 233:293-301.

124 Khabbazian, M., Kriebel, R., Rohe, K. and Ané, C. (2016), Fast and accurate detection of evolutionary shifts in Ornstein–Uhlenbeck models. Methods Ecol Evol, 7: 811-824. https://doi.org/10.1111/2041-210X.12534

125 Kiers, E., Rousseau, R., West, S. et al. Host sanctions and the legume–rhizobium mutualism. Nature 425, 78–81 (2003). https://doi.org/10.1038/nature01931

126 Koo, M. S., Lee, J. H., Rah, S. Y., Yeo, W. S., Lee, J. W., Lee, K. L., Koh, Y. S., Kang, S. O., & Roe, J. H. (2003). A reducing system of the superoxide sensor SoxR in Escherichia coli. The EMBO journal, 22(11), 2614–2622. https://doi.org/10.1093/emboj/cdg252

127 Kour, D., Kaur, T., Devi, R., Yadav, A., Singh, M., Joshi, D., Singh, J., Suyal, D. C., Kumar, A., Rajput, V. D., Yadav, A. N., Singh, K., Singh, J., Sayyed, R. Z., Arora, N. K., & Saxena, A. K. (2021). Beneficial microbiomes for bioremediation of diverse contaminated environments for environmental sustainability: present status and future challenges. Environmental science and pollution research international, 28(20), 24917–24939. https://doi.org/10.1007/s11356-021-13252-7

128 Kuhn, M. (2008). Caret package. Journal of Statistical Software, 28(5)

129 Kusstatscher, P., Wicaksono, W. A., Bergna, A., Cernava, T., Bergau, N., Tissier, A., Hause, B., & Berg, G. (2020). Trichomes form genotype-specific microbial hotspots in the phyllosphere of tomato. Environmental microbiome, 15(1), 17. https://doi.org/10.1186/s40793-020-00364-9

130 Kvitko, B. H., & Collmer, A. (2011). Construction of Pseudomonas syringae pv. tomato DC3000 mutant and polymutant strains. Methods in molecular biology (Clifton, N.J.), 712, 109–128. https://doi.org/10.1007/978-1-61737-998-7_10

131 Kwak, J. M., Mori, I. C., Pei, Z. M., Leonhardt, N., Torres, M. A., Dangl, J. L., Bloom, R. E., Bodde, S., Jones, J. D., & Schroeder, J. I. (2003). NADPH oxidase AtrbohD and AtrbohF genes function in ROS-dependent ABA signaling in Arabidopsis. The EMBO journal, 22(11), 2623–2633. https://doi.org/10.1093/emboj/cdg277

132 Kwak, MJ., Kong, H., Choi, K. et al. Rhizosphere microbiome structure alters to enable wilt resistance in tomato. Nat Biotechnol 36, 1100–1109 (2018). https://doi.org/10.1038/nbt.4232

133 Lacombe, S., Rougon-Cardoso, A., Sherwood, E., Peeters, N., Dahlbeck, D., van Esse, H. P., Smoker, M., Rallapalli, G., Thomma, B. P., Staskawicz, B., Jones, J. D., & Zipfel, C. (2010). Interfamily transfer of a plant pattern-recognition receptor confers broad-spectrum bacterial resistance. Nature biotechnology, 28(4), 365–369. https://doi.org/10.1038/nbt.1613

134 Langfelder, P., & Horvath, S. (2008). WGCNA: an R package for weighted correlation network analysis. BMC bioinformatics, 9, 559. https://doi.org/10.1186/1471-2105-9-559

135 Lebeis, S. L., Paredes, S. H., Lundberg, D. S., Breakfield, N., Gehring, J., McDonald, M., Malfatti, S., Glavina del Rio, T., Jones, C. D., Tringe, S. G., & Dangl, J. L. (2015). PLANT MICROBIOME. Salicylic acid modulates colonization of the root microbiome by specific bacterial taxa. Science (New York, N.Y.), 349(6250), 860–864. https://doi.org/10.1126/science.aaa8764

136 Leduc, J. L., & Roberts, G. P. (2009). Cyclic di-GMP allosterically inhibits the CRP-like protein (Clp) of Xanthomonas axonopodis pv. citri. Journal of bacteriology, 191(22), 7121–7122. https://doi.org/10.1128/JB.00845-09
137 Lee, B., Park, Y. S., Lee, S., Song, G. C., & Ryu, C. M. (2016). Bacterial RNAs activate innate immunity in Arabidopsis. *The New phytologist*, *209*(2), 785–797. https://doi.org/10.1111/nph.13717
138 Lengfelder, I., Sava, I. G., Hansen, J. J., Kleigrewe, K., Herzog, J., Neuhaus, K., Hofmann, T., Sartor, R. B., & Haller, D. (2019). Complex Bacterial Consortia Reprogram the Colitogenic Activity of Enterococcus faecalis in a Gnotobiotic Mouse Model of Chronic, Immune-Mediated Colitis. Frontiers in immunology, 10, 1420. https://doi.org/10.3389/fimmu.2019.01420
139 Levy, M., Kolodziejczyk, A., Thaiss, C. et al. Dysbiosis and the immune system. Nat Rev Immunol 17, 219–232 (2017). https://doi.org/10.1038/nri.2017.7
140 Li, X., Rui, J., Xiong, J., Li, J., He, Z., Zhou, J., Yannarell, A. C., & Mackie, R. I. (2014). Functional potential of soil microbial communities in the maize rhizosphere. PloS one, 9(11), e112609. https://doi.org/10.1371/journal.pone.0112609
141 Li, Y., Kabbage, M., Liu, W., & Dickman, M. B. (2016). Aspartyl Protease-Mediated Cleavage of BAG6 Is Necessary for Autophagy and Fungal Resistance in Plants. The Plant cell, 28(1), 233–247. https://doi.org/10.1105/tpc.15.00626
142 Liao Y, Smyth GK, Shi W (2019). “The R package Rsubread is easier, faster, cheaper and better for alignment and quantification of RNA sequencing reads.” Nucleic Acids Research, 47, e47. doi: 10.1093/nar/gkz114
143 Libault, M., Wan, J., Czechowski, T., Udvardi, M., & Stacey, G. (2007). Identification of 118 Arabidopsis transcription factor and 30 ubiquitin-ligase genes responding to chitin, a plant-defense elicitor. Molecular plant-microbe interactions : MPMI, 20(8), 900–911. https://doi.org/10.1094/MPMI-20-8-0900
144 Lindsey, B. E., 3rd, Rivero, L., Calhoun, C. S., Grotewold, E., & Brkljacic, J. (2017). Standardized Method for High-throughput Sterilization of Arabidopsis Seeds. Journal of visualized experiments : JoVE, (128), 56587. https://doi.org/10.3791/56587
145 Liu, H., Li, J., Carvalhais, L. C., Percy, C. D., Prakash Verma, J., Schenk, P. M., & Singh, B. K. (2021). Evidence for the plant recruitment of beneficial microbes to suppress soil-borne pathogens. The New phytologist, 229(5), 2873–2885. https://doi.org/10.1111/nph.17057
146 Liu, L., Song, W., Huang, S., Jiang, K., Moriwaki, Y., Wang, Y., Men, Y., Zhang, D., Wen, X., Han, Z., Chai, J., & Guo, H. (2022). Extracellular pH sensing by plant cell-surface peptide-receptor complexes. Cell, 185(18), 3341–3355.e13. https://doi.org/10.1016/j.cell.2022.07.012
147 Liu, Y., Wilson, A. J., Han, J., Hui, A., O'Sullivan, L., Huan, T., & Haney, C. H. (2023). Amino Acid Availability Determines Plant Immune Homeostasis in the Rhizosphere Microbiome. mBio, e0342422. Advance online publication. https://doi.org/10.1128/mbio.03424-22
148 Liu, Z., Beskrovnaya, P., Melnyk, R. A., Hossain, S. S., Khorasani, S., O'Sullivan, L. R., Wiesmann, C. L., Bush, J., Richard, J. D., & Haney, C. H. (2018). A Genome-Wide Screen Identifies Genes in Rhizosphere-Associated Pseudomonas Required to Evade Plant Defenses. mBio, 9(6), e00433-18. https://doi.org/10.1128/mBio.00433-18
149 Love MI, Huber W, Anders S (2014). “Moderated estimation of fold change and dispersion for RNA-seq data with DESeq2.” Genome Biology, 15, 550. doi: 10.1186/s13059-014-0550-8.
150 Lundberg, D. S., Lebeis, S. L., Paredes, S. H., Yourstone, S., Gehring, J., Malfatti, S., Tremblay, J., Engelbrektson, A., Kunin, V., Del Rio, T. G., Edgar, R. C., Eickhorst, T., Ley, R. E., Hugenholtz, P., Tringe, S. G., & Dangl, J. L. (2012). Defining the core Arabidopsis thaliana root microbiome. Nature, 488(7409), 86–90. https://doi.org/10.1038/nature11237
151 Ma, KW., Niu, Y., Jia, Y. et al. Coordination of microbe–host homeostasis by crosstalk with plant innate immunity. Nat. Plants 7, 814–825 (2021). https://doi.org/10.1038/s41477-021-00920-2
152 Ma, Z., Song, T., Zhu, L., Ye, W., Wang, Y., Shao, Y., Dong, S., Zhang, Z., Dou, D., Zheng, X., Tyler, B. M., & Wang, Y. (2015). A Phytophthora sojae Glycoside Hydrolase 12 Protein Is a Major Virulence Factor during Soybean Infection and Is Recognized as a PAMP. The Plant cell, 27(7), 2057–2072. https://doi.org/10.1105/tpc.15.00390
153 Macho, A. P., Schwessinger, B., Ntoukakis, V., Brutus, A., Segonzac, C., Roy, S., Kadota, Y., Oh, M. H., Sklenar, J., Derbyshire, P., Lozano-Durán, R., Malinovsky, F. G., Monaghan, J.,

Menke, F. L., Huber, S. C., He, S. Y., & Zipfel, C. (2014). A bacterial tyrosine phosphatase inhibits plant pattern recognition receptor activation. Science (New York, N.Y.), 343(6178), 1509–1512. https://doi.org/10.1126/science.1248849
154 Maier, B.A., Kiefer, P., Field, C.M. et al. A general non-self response as part of plant immunity. Nat. Plants 7, 696–705 (2021). https://doi.org/10.1038/s41477-021-00913-1
155 Mancuso, G., Gambuzza, M., Midiri, A., Biondo, C., Papasergi, S., Akira, S., Teti, G., & Beninati, C. (2009). Bacterial recognition by TLR7 in the lysosomes of conventional dendritic cells. Nature immunology, 10(6), 587–594. https://doi.org/10.1038/ni.1733
156 Martinez, J., Ok, S., Smith, S., Snoeck, K., Day, J. P., & Jiggins, F. M. (2015). Should Symbionts Be Nice or Selfish? Antiviral Effects of Wolbachia Are Costly but Reproductive Parasitism Is Not. PLoS pathogens, 11(7), e1005021. https://doi.org/10.1371/journal.ppat.1005021
157 Matsumura, M., Nomoto, M., Itaya, T., Aratani, Y., Iwamoto, M., Matsuura, T., Hayashi, Y., Mori, T., Skelly, M. J., Yamamoto, Y. Y., Kinoshita, T., Mori, I. C., Suzuki, T., Betsuyaku, S., Spoel, S. H., Toyota, M., & Tada, Y. (2022). Mechanosensory trichome cells evoke a mechanical stimuli-induced immune response in Arabidopsis thaliana. Nature communications, 13(1), 1216. https://doi.org/10.1038/s41467-022-28813-8
158 Mazmanian, S., Round, J. & Kasper, D. A microbial symbiosis factor prevents intestinal inflammatory disease. Nature 453, 620–625 (2008). https://doi.org/10.1038/nature07008
159 Melotto, M., Underwood, W., Koczan, J., Nomura, K., & He, S. Y. (2006). Plant stomata function in innate immunity against bacterial invasion. Cell, 126(5), 969–980. https://doi.org/10.1016/j.cell.2006.06.054
160 Mendes, R., Kruijt, M., de Bruijn, I., Dekkers, E., van der Voort, M., Schneider, J. H., Piceno, Y. M., DeSantis, T. Z., Andersen, G. L., Bakker, P. A., & Raaijmakers, J. M. (2011). Deciphering the rhizosphere microbiome for disease-suppressive bacteria. Science (New York, N.Y.), 332(6033), 1097–1100. https://doi.org/10.1126/science.1203980
161 Mendiburu F and Yaseen M. (2020). agricolae: Statistical Procedures for Agricultural Research. R package version 1.4.0 ,https://myaseen208.github.io/agricolae/https://cran.r-project.org/package=agricolae.
162 Merrell, D. S., Hava, D. L., & Camilli, A. (2002). Identification of novel factors involved in colonization and acid tolerance of Vibrio cholerae. Molecular microbiology, 43(6), 1471–1491. https://doi.org/10.1046/j.1365-2958.2002.02857.x
163 Mesny, F., Miyauchi, S., Thiergart, T. et al. Genetic determinants of endophytism in the Arabidopsis root mycobiome. Nat Commun 12, 7227 (2021). https://doi.org/10.1038/s41467-021-27479-y
164 Mi, H., Muruganujan, A., Casagrande, J. T., & Thomas, P. D. (2013). Large-scale gene function analysis with the PANTHER classification system. Nature protocols, 8(8), 1551–1566. https://doi.org/10.1038/nprot.2013.092
165 Miller, B. M., Liou, M. J., Zhang, L. F., Nguyen, H., Litvak, Y., Schorr, E. M., Jang, K. K., Tiffany, C. R., Butler, B. P., & Bäumler, A. J. (2020). Anaerobic Respiration of NOX1-Derived Hydrogen Peroxide Licenses Bacterial Growth at the Colonic Surface. Cell host & microbe, 28(6), 789–797.e5. https://doi.org/10.1016/j.chom.2020.10.009
166 Miller, G., Schlauch, K., Tam, R., Cortes, D., Torres, M. A., Shulaev, V., Dangl, J. L., & Mittler, R. (2009). The plant NADPH oxidase RBOHD mediates rapid systemic signaling in response to diverse stimuli. Science signaling, 2(84), ra45. https://doi.org/10.1126/scisignal.2000448
167 Millet, Y. A., Danna, C. H., Clay, N. K., Songnuan, W., Simon, M. D., Werck-Reichhart, D., & Ausubel, F. M. (2010). Innate immune responses activated in Arabidopsis roots by microbe-associated molecular patterns. The Plant cell, 22(3), 973–990. https://doi.org/10.1105/tpc.109.069658
168 Mino, Y., Matsushita, Y., & Sakai, R. (1987). Effect of coronatine on stomatal opening in leaves of broadbean and Italian ryegrass. Japanese Journal of Phytopathology, 53(1), 53-55.
169 Miya, A., Albert, P., Shinya, T., Desaki, Y., Ichimura, K., Shirasu, K., Narusaka, Y., Kawakami, N., Kaku, H., & Shibuya, N. (2007). CERK1, a LysM receptor kinase, is essential for chitin elicitor signaling in Arabidopsis. Proceedings of the National Academy of Sciences of the United States of America, 104(49), 19613–19618. https://doi.org/10.1073/pnas.0705147104

170 Molina, A., Miedes, E., Bacete, L., Rodríguez, T., Mélida, H., Denancé, N., Sánchez-Vallet, A., Rivière, M. P., López, G., Freydier, A., Barlet, X., Pattathil, S., Hahn, M., & Goffner, D. (2021). Arabidopsis cell wall composition determines disease resistance specificity and fitness. Proceedings of the National Academy of Sciences of the United States of America, 118(5), e2010243118. https://doi.org/10.1073/pnas.2010243118
171 Moore, J.P.; Waldron, M.; Lindsey, G.G.; Farrant, J.M.; Brandt, W.F. An ultrastructural investigation of the surface microbiota present on the leaves and reproductive structures of the resurrection plant Myrothamnus flabellifolia. S. Afr. J. Bot. 2011, 77, 485–491.
172 Morello, J. E., & Collmer, A. (2009). Pseudomonas syringae HrpP Is a type III secretion substrate specificity switch domain protein that is translocated into plant cells but functions atypically for a substrate-switching protein. Journal of bacteriology, 191(9), 3120–3131. https://doi.org/10.1128/JB.01623-08
173 Naylor, D., DeGraaf, S., Purdom, E. et al. Drought and host selection influence bacterial community dynamics in the grass root microbiome. ISME J 11, 2691–2704 (2017). https://doi.org/10.1038/ismej.2017.118
174 Ngou, B. P. M., Ding, P., & Jones, J. D. G. (2022). Thirty years of resistance: Zig-zag through the plant immune system. The Plant cell, 34(5), 1447–1478. https://doi.org/10.1093/plcell/koac041
175 Nicaise, V., Joe, A., Jeong, B. R., Korneli, C., Boutrot, F., Westedt, I., Staiger, D., Alfano, J. R., & Zipfel, C. (2013). Pseudomonas HopU1 modulates plant immune receptor levels by blocking the interaction of their mRNAs with GRP7. The EMBO journal, 32(5), 701–712. https://doi.org/10.1038/emboj.2013.15
176 Nobori, T., & Tsuda, K. (2018). In planta Transcriptome Analysis of Pseudomonas syringae. Bio-protocol, 8(17), e2987. https://doi.org/10.21769/BioProtoc.2987
177 Nobori, T., Cao, Y., Entila, F., Dahms, E., Tsuda, Y., Garrido-Oter, R., & Tsuda, K. (2022). Dissecting the cotranscriptome landscape of plants and their microbiota. EMBO reports, 23(12), e55380. https://doi.org/10.15252/embr.202255380
178 Nobori, T., Velásquez, A. C., Wu, J., Kvitko, B. H., Kremer, J. M., Wang, Y., He, S. Y., & Tsuda, K. (2018). Transcriptome landscape of a bacterial pathogen under plant immunity. Proceedings of the National Academy of Sciences of the United States of America, 115(13), E3055–E3064. https://doi.org/10.1073/pnas.1800529115
179 Nobori, T., Wang, Y., Wu, J. et al. Multidimensional gene regulatory landscape of a bacterial pathogen in plants. Nat. Plants 6, 883–896 (2020). https://doi.org/10.1038/s41477-020-0690-7
180 Nühse, T. S., Bottrill, A. R., Jones, A. M., & Peck, S. C. (2007). Quantitative phosphoproteomic analysis of plasma membrane proteins reveals regulatory mechanisms of plant innate immune responses. The Plant journal : for cell and molecular biology, 51(5), 931–940. https://doi.org/10.1111/j.1365-313X.2007.03192.x
181 Nühse, T. S., Peck, S. C., Hirt, H., & Boller, T. (2000). Microbial elicitors induce activation and dual phosphorylation of the Arabidopsis thaliana MAPK 6. The Journal of biological chemistry, 275(11), 7521–7526. https://doi.org/10.1074/jbc.275.11.7521
182 Nürnberger, T., Brunner, F., Kemmerling, B., & Piater, L. (2004). Innate immunity in plants and animals: striking similarities and obvious differences. Immunological reviews, 198, 249–266. https://doi.org/10.1111/j.0105-2896.2004.0119.x
183 Ofek-Lalzar, M., Sela, N., Goldman-Voronov, M. et al. Niche and host-associated functional signatures of the root surface microbiome. Nat Commun 5, 4950 (2014). https://doi.org/10.1038/ncomms5950
184 Oliveira-Garcia, E., & Deising, H. B. (2016). Attenuation of PAMP-triggered immunity in maize requires down-regulation of the key β-1,6-glucan synthesis genes KRE5 and KRE6 in biotrophic hyphae of Colletotrichum graminicola. The Plant journal : for cell and molecular biology, 87(4), 355–375. https://doi.org/10.1111/tpj.13205
185 Ost, K. S., O'Meara, T. R., Stephens, W. Z., Chiaro, T., Zhou, H., Penman, J., Bell, R., Catanzaro, J. R., Song, D., Singh, S., Call, D. H., Hwang-Wong, E., Hanson, K. E., Valentine, J. F., Christensen, K. A., O'Connell, R. M., Cormack, B., Ibrahim, A. S., Palm, N. W., Noble, S. M., … Round, J. L. (2021). Adaptive immunity induces mutualism between commensal eukaryotes. Nature, 596(7870), 114–118. https://doi.org/10.1038/s41586-021-03722-w

186 Paauw, M., van Hulten, M., Chatterjee, S., Berg, J. A., Taks, N. W., Giesbers, M., Richard, M. M. S., & van den Burg, H. A. (2023). Hydathode immunity protects the Arabidopsis leaf vasculature against colonization by bacterial pathogens. Current biology : CB, 33(4), 697–710.e6. https://doi.org/10.1016/j.cub.2023.01.013
187 Parys, K., Colaianni, N. R., Lee, H.-S., Hohmann, U., Edelbacher, N., Trgovcevic, A., Blahovska, Z., Lee, D., Mechtler, A., Muhari-Portik, Z., Madalinski, M., Schandry, N., Rodríguez-Arévalo, I., Becker, C., Sonnleitner, E., Korte, A., Bläsi, U., Geldner, N., Hothorn, M., … Belkhadir, Y. (2021). Signatures of antagonistic pleiotropy in a bacterial flagellin epitope. Cell Host & Microbe, 29(4), 620-634.e9. https://doi.org/10.1016/j.chom.2021.02.008
188 Pascale, A., Proietti, S., Pantelides, I. S., & Stringlis, I. A. (2020). Modulation of the Root Microbiome by Plant Molecules: The Basis for Targeted Disease Suppression and Plant Growth Promotion. Frontiers in plant science, 10, 1741. https://doi.org/10.3389/fpls.2019.01741
189 Pel, M. J., van Dijken, A. J., Bardoel, B. W., Seidl, M. F., van der Ent, S., van Strijp, J. A., & Pieterse, C. M. (2014). Pseudomonas syringae evades host immunity by degrading flagellin monomers with alkaline protease AprA. Molecular plant-microbe interactions : MPMI, 27(7), 603–610. https://doi.org/10.1094/MPMI-02-14-0032-R
190 Pfeilmeier, S., Petti, G. C., Bortfeld-Miller, M., Daniel, B., Field, C. M., Sunagawa, S., & Vorholt, J. A. (2021). The plant NADPH oxidase RBOHD is required for microbiota homeostasis in leaves. Nature microbiology, 6(7), 852–864. https://doi.org/10.1038/s41564-021-00929-5
191 Pfeilmeier, S., Saur, I. M., Rathjen, J. P., Zipfel, C., & Malone, J. G. (2016). High levels of cyclic-di-GMP in plant-associated Pseudomonas correlate with evasion of plant immunity. Molecular plant pathology, 17(4), 521–531. https://doi.org/10.1111/mpp.12297
192 R Core Team (2013). R: A language and environment for statistical computing. R Foundation for Statistical Computing, Vienna, Austria. ISBN 3-900051-07-0, http://www.R-project.org/
193 Raaijmakers, J. M., & Mazzola, M. (2016). Soil immune responses. Science, 352(6292), 1392-1393.
194 Reisberg, E. E., Hildebrandt, U., Riederer, M., & Hentschel, U. (2012). Phyllosphere bacterial communities of trichome-bearing and trichomeless Arabidopsis thaliana leaves. Antonie van Leeuwenhoek, 101(3), 551–560. https://doi.org/10.1007/s10482-011-9669-8
195 Reisberg, E. E., Hildebrandt, U., Riederer, M., & Hentschel, U. (2013). Distinct phyllosphere bacterial communities on Arabidopsis wax mutant leaves. PloS one, 8(11), e78613. https://doi.org/10.1371/journal.pone.0078613
196 Remus-Emsermann, M. N., Lücker, S., Müller, D. B., Potthoff, E., Daims, H., & Vorholt, J. A. (2014). Spatial distribution analyses of natural phyllosphere-colonizing bacteria on Arabidopsis thaliana revealed by fluorescence in situ hybridization. Environmental microbiology, 16(7), 2329–2340. https://doi.org/10.1111/1462-2920.12482
197 Reverchon, S., Expert, D., Robert-Baudouy, J., & Nasser, W. (1997). The cyclic AMP receptor protein is the main activator of pectinolysis genes in Erwinia chrysanthemi. Journal of bacteriology, 179(11), 3500–3508. https://doi.org/10.1128/jb.179.11.3500-3508.1997
198 Reynolds, L. A., Smith, K. A., Filbey, K. J., Harcus, Y., Hewitson, J. P., Redpath, S. A., Valdez, Y., Yebra, M. J., Finlay, B. B., & Maizels, R. M. (2014). Commensal-pathogen interactions in the intestinal tract: lactobacilli promote infection with, and are promoted by, helminth parasites. Gut microbes, 5(4), 522–532. https://doi.org/10.4161/gmic.32155
199 Rimbach, K., Kaiser, S., Helm, M., Dalpke, A. H., & Eigenbrod, T. (2015). 2'-O-Methylation within Bacterial RNA Acts as Suppressor of TLR7/TLR8 Activation in Human Innate Immune Cells. Journal of innate immunity, 7(5), 482–493. https://doi.org/10.1159/000375460
200 Ritchie ME, Phipson B, Wu D, Hu Y, Law CW, Shi W, Smyth GK (2015). “limma powers differential expression analyses for RNA-sequencing and microarray studies.” Nucleic Acids Research, 43(7), e47. doi: 10.1093/nar/gkv007.
201 Ritpitakphong, U., Falquet, L., Vimoltust, A., Berger, A., Métraux, J. P., & L'Haridon, F. (2016). The microbiome of the leaf surface of Arabidopsis protects against a fungal pathogen. The New phytologist, 210(3), 1033–1043. https://doi.org/10.1111/nph.13808
202 Roux, M., Schwessinger, B., Albrecht, C., Chinchilla, D., Jones, A., Holton, N., Malinovsky, F. G., Tör, M., de Vries, S., & Zipfel, C. (2011). The Arabidopsis leucine-rich repeat receptor-like kinases BAK1/SERK3 and BKK1/SERK4 are required for innate immunity to hemibiotrophic

and biotrophic pathogens. The Plant cell, 23(6), 2440–2455. https://doi.org/10.1105/tpc.111.084301
203 Rudrappa, T., Czymmek, K. J., Paré, P. W., & Bais, H. P. (2008). Root-secreted malic acid recruits beneficial soil bacteria. Plant physiology, 148(3), 1547–1556. https://doi.org/10.1104/pp.108.127613
204 Sachs, J. L., Ehinger, M. O., & Simms, E. L. (2010). Origins of cheating and loss of symbiosis in wild Bradyrhizobium. Journal of evolutionary biology, 23(5), 1075–1089. https://doi.org/10.1111/j.1420-9101.2010.01980.x
205 Salas-González, I., Reyt, G., Flis, P., Custódio, V., Gopaulchan, D., Bakhoum, N., Dew, T. P., Suresh, K., Franke, R. B., Dangl, J. L., Salt, D. E., & Castrillo, G. (2021). Coordination between microbiota and root endodermis supports plant mineral nutrient homeostasis. Science (New York, N.Y.), 371(6525), eabd0695. https://doi.org/10.1126/science.abd0695
206 Salmond, G. P. (1994). Secretion of extracellular virulence factors by plant pathogenic bacteria. Annual review of phytopathology, 32(1), 181-200.
207 Sayers, E. W., Bolton, E. E., Brister, J. R., Canese, K., Chan, J., Comeau, D. C., Connor, R., Funk, K., Kelly, C., Kim, S., Madej, T., Marchler-Bauer, A., Lanczycki, C., Lathrop, S., Lu, Z., Thibaud-Nissen, F., Murphy, T., Phan, L., Skripchenko, Y., Tse, T., … Sherry, S. T. (2022). Database resources of the national center for biotechnology information. Nucleic acids research, 50(D1), D20–D26. https://doi.org/10.1093/nar/gkab1112
208 Schellenberg, B., Ramel, C., & Dudler, R. (2010). Pseudomonas syringae virulence factor syringolin A counteracts stomatal immunity by proteasome inhibition. Molecular plant-microbe interactions : MPMI, 23(10), 1287–1293. https://doi.org/10.1094/MPMI-04-10-0094
209 Schlechter, R. O., Miebach, M., & Remus-Emsermann, M. N. P. (2019). Driving factors of epiphytic bacterial communities: A review. Journal of advanced research, 19, 57–65. https://doi.org/10.1016/j.jare.2019.03.003
210 Schmitz, L., Yan, Z., Schneijderberg, M. et al. Synthetic bacterial community derived from a desert rhizosphere confers salt stress resilience to tomato in the presence of a soil microbiome. ISME J 16, 1907–1920 (2022). https://doi.org/10.1038/s41396-022-01238-3
211 Shalev, O., Karasov, T.L., Lundberg, D.S. et al. Commensal Pseudomonas strains facilitate protective response against pathogens in the host plant. Nat Ecol Evol 6, 383–396 (2022). https://doi.org/10.1038/s41559-022-01673-7
212 Si, M., Zhao, C., Burkinshaw, B., Zhang, B., Wei, D., Wang, Y., Dong, T. G., & Shen, X. (2017). Manganese scavenging and oxidative stress response mediated by type VI secretion system in Burkholderia thailandensis. Proceedings of the National Academy of Sciences of the United States of America, 114(11), E2233–E2242. https://doi.org/10.1073/pnas.1614902114
213 Sieber, M., Pita, L., Weiland-Bräuer, N., Dirksen, P., Wang, J., Mortzfeld, B., Franzenburg, S., Schmitz, R. A., Baines, J. F., Fraune, S., Hentschel, U., Schulenburg, H., Bosch, T. C. G., & Traulsen, A. (2019). Neutrality in the Metaorganism. PLoS biology, 17(6), e3000298. https://doi.org/10.1371/journal.pbio.3000298
214 Sierla, M., Waszczak, C., Vahisalu, T., & Kangasjärvi, J. (2016). Reactive Oxygen Species in the Regulation of Stomatal Movements. Plant physiology, 171(3), 1569–1580. https://doi.org/10.1104/pp.16.00328
215 Smets, W., Chock, M., Walsh, C., et al. (2022). Leaf side determines the relative importance of dispersal versus host filtering in the phyllosphere microbiome. BioRvix. 2022.08.16.504148; doi: https://doi.org/10.1101/2022.08.16.504148
216 Smith, J.M., Heese, A. (2014). Rapid bioassay to measure early reactive oxygen species production in Arabidopsis leave tissue in response to living Pseudomonas syringae. Plant Methods 10, 6 . https://doi.org/10.1186/1746-4811-10-6
217 Song, Y., Wilson, A. J., Zhang, X. C., Thoms, D., Sohrabi, R., Song, S., Geissmann, Q., Liu, Y., Walgren, L., He, S. Y., & Haney, C. H. (2021). FERONIA restricts Pseudomonas in the rhizosphere microbiome via regulation of reactive oxygen species. Nature plants, 7(5), 644–654. https://doi.org/10.1038/s41477-021-00914-0
218 Spanu, P., Grosskopf, D. G., Felix, G., & Boller, T. (1994). The Apparent Turnover of 1-Aminocyclopropane-1-Carboxylate Synthase in Tomato Cells Is Regulated by Protein Phosphorylation and Dephosphorylation. Plant physiology, 106(2), 529–535. https://doi.org/10.1104/pp.106.2.529

219 Spindler, M. P., Siu, S., Mogno, I., Li, Z., Yang, C., Mehandru, S., Britton, G. J., & Faith, J. J. (2022). Human gut microbiota stimulate defined innate immune responses that vary from phylum to strain. Cell host & microbe, 30(10), 1481–1498.e5. https://doi.org/10.1016/j.chom.2022.08.009
220 Stegen, J. C., Lin, X., Konopka, A. E., & Fredrickson, J. K. (2012). Stochastic and deterministic assembly processes in subsurface microbial communities. The ISME journal, 6(9), 1653–1664. https://doi.org/10.1038/ismej.2012.22
221 Stehle, S., & Schulz, R. (2015). Agricultural insecticides threaten surface waters at the global scale. Proceedings of the National Academy of Sciences of the United States of America, 112(18), 5750–5755. https://doi.org/10.1073/pnas.1500232112
222 Stevens, E. J., Bates, K. A., & King, K. C. (2021). Host microbiota can facilitate pathogen infection. PLoS pathogens, 17(5), e1009514. https://doi.org/10.1371/journal.ppat.1009514
223 Storey JD, Bass AJ, Dabney A, Robinson D (2022). qvalue: Q-value estimation for false discovery rate control. R package version 2.30.0, http://github.com/jdstorey/qvalue.
224 Stringlis, I. A., Proietti, S., Hickman, R., Van Verk, M. C., Zamioudis, C., & Pieterse, C. M. J. (2018). Root transcriptional dynamics induced by beneficial rhizobacteria and microbial immune elicitors reveal signatures of adaptation to mutualists. The Plant journal : for cell and molecular biology, 93(1), 166–180. https://doi.org/10.1111/tpj.13741
225 Stringlis, I. A., Yu, K., Feussner, K., de Jonge, R., Van Bentum, S., Van Verk, M. C., Berendsen, R. L., Bakker, P. A. H. M., Feussner, I., & Pieterse, C. M. J. (2018). MYB72-dependent coumarin exudation shapes root microbiome assembly to promote plant health. Proceedings of the National Academy of Sciences of the United States of America, 115(22), E5213–E5222. https://doi.org/10.1073/pnas.1722335115
226 Struyf A, Hubert M, Rousseeuw P (1997). “Clustering in an Object-Oriented Environment.” Journal of Statistical Software. doi:10.18637/jss.v001.i04.
227 Takahashi, F., Mizoguchi, T., Yoshida, R., Ichimura, K., & Shinozaki, K. (2011). Calmodulin-dependent activation of MAP kinase for ROS homeostasis in Arabidopsis. *Molecular cell*, *41*(6), 649–660. https://doi.org/10.1016/j.molcel.2011.02.029
228 Tao, K., Makino, K., Yonei, S., Nakata, A., & Shinagawa, H. (1991). Purification and characterization of the Escherichia coli OxyR protein, the positive regulator for a hydrogen peroxide-inducible regulon. Journal of biochemistry, 109(2), 262–266.
229 Tateda, C., Zhang, Z., Shrestha, J., Jelenska, J., Chinchilla, D., & Greenberg, J. T. (2014). Salicylic acid regulates Arabidopsis microbial pattern receptor kinase levels and signaling. The Plant cell, 26(10), 4171–4187. https://doi.org/10.1105/tpc.114.131938
230 Teixeira, P. J. P. L., Colaianni, N. R., Law, T. F., Conway, J. M., Gilbert, S., Li, H., Salas-González, I., Panda, D., Del Risco, N. M., Finkel, O. M., Castrillo, G., Mieczkowski, P., Jones, C. D., & Dangl, J. L. (2021). Specific modulation of the root immune system by a community of commensal bacteria. Proceedings of the National Academy of Sciences of the United States of America, 118(16), e2100678118. https://doi.org/10.1073/pnas.2100678118
231 Teixeira, P. J. P., Colaianni, N. R., Fitzpatrick, C. R., & Dangl, J. L. (2019). Beyond pathogens: microbiota interactions with the plant immune system. Current opinion in microbiology, 49, 7–17. https://doi.org/10.1016/j.mib.2019.08.003
232 Theis, K. R., Dheilly, N. M., Klassen, J. L., Brucker, R. M., Baines, J. F., Bosch, T. C., Cryan, J. F., Gilbert, S. F., Goodnight, C. J., Lloyd, E. A., Sapp, J., Vandenkoornhuyse, P., Zilber-Rosenberg, I., Rosenberg, E., & Bordenstein, S. R. (2016). Getting the Hologenome Concept Right: an Eco-Evolutionary Framework for Hosts and Their Microbiomes. mSystems, 1(2), e00028-16. https://doi.org/10.1128/mSystems.00028-16
233 Thiergart, T., Durán, P., Ellis, T., Vannier, N., Garrido-Oter, R., Kemen, E., Roux, F., Alonso-Blanco, C., Ågren, J., Schulze-Lefert, P., & Hacquard, S. (2020). Root microbiota assembly and adaptive differentiation among European Arabidopsis populations. Nature ecology & evolution, 4(1), 122–131. https://doi.org/10.1038/s41559-019-1063-3
234 Thoms, D., Chen, M., Liu, Y., Moreeira, Z., Luo, Y., Song, S., Wang, N., Haney, C. (2023). Innate immunity can distinguish beneficial from pathogenic rhizosphere microbiota. BioRvix. 2023.01.07.523123; doi: https://doi.org/10.1101/2023.01.07.523123
235 Tierens, K. F. J., Thomma, B. P., Brouwer, M., Schmidt, J., Kistner, K., Porzel, A., ... & Broekaert, W. F. (2001). Study of the role of antimicrobial glucosinolate-derived

isothiocyanates in resistance of Arabidopsis to microbial pathogens. Plant physiology, 125(4), 1688-1699.
236 Tintelnot, J., Xu, Y., Lesker, T.R. et al. Microbiota-derived 3-IAA influences chemotherapy efficacy in pancreatic cancer. Nature 615, 168–174 (2023). https://doi.org/10.1038/s41586-023-05728-y
237 Toledano, M. B., Kullik, I., Trinh, F., Baird, P. T., Schneider, T. D., & Storz, G. (1994). Redox-dependent shift of OxyR-DNA contacts along an extended DNA-binding site: a mechanism for differential promoter selection. Cell, 78(5), 897–909. https://doi.org/10.1016/s0092-8674(94)90702-1
238 Ton, J., Jakab, G., Toquin, V., Flors, V., Iavicoli, A., Maeder, M. N., Métraux, J. P., & Mauch-Mani, B. (2005). Dissecting the beta-aminobutyric acid-induced priming phenomenon in Arabidopsis. The Plant cell, 17(3), 987–999. https://doi.org/10.1105/tpc.104.029728
239 Torres, M. A., Dangl, J. L., & Jones, J. D. (2002). Arabidopsis gp91phox homologues AtrbohD and AtrbohF are required for accumulation of reactive oxygen intermediates in the plant defense response. Proceedings of the National Academy of Sciences of the United States of America, 99(1), 517–522. https://doi.org/10.1073/pnas.012452499
240 Tripathi, M., Munot, H.P., Shouche, Y. et al. Isolation and Functional Characterization of Siderophore-Producing Lead- and Cadmium-Resistant Pseudomonas putida KNP9. Curr Microbiol 50, 233–237 (2005). https://doi.org/10.1007/s00284-004-4459-4
241 Trivedi, P., Leach, J.E., Tringe, S.G. et al. Plant–microbiome interactions: from community assembly to plant health. Nat Rev Microbiol 18, 607–621 (2020). https://doi.org/10.1038/s41579-020-0412-1
242 Turner, N. C., & Graniti, A. (1969). Fusicoccin: a fungal toxin that opens stomata. Nature, 223(5210), 1070-1071.
243 Tzipilevich, E., Russ, D., Dangl, J. L., & Benfey, P. N. (2021). Plant immune system activation is necessary for efficient root colonization by auxin-secreting beneficial bacteria. Cell host & microbe, 29(10), 1507–1520.e4. https://doi.org/10.1016/j.chom.2021.09.005
244 Vatanen, T., Kostic, A. D., d'Hennezel, E., Siljander, H., Franzosa, E. A., Yassour, M., Kolde, R., Vlamakis, H., Arthur, T. D., Hämäläinen, A. M., Peet, A., Tillmann, V., Uibo, R., Mokurov, S., Dorshakova, N., Ilonen, J., Virtanen, S. M., Szabo, S. J., Porter, J. A., Lähdesmäki, H., … Xavier, R. J. (2016). Variation in Microbiome LPS Immunogenicity Contributes to Autoimmunity in Humans. Cell, 165(4), 842–853. https://doi.org/10.1016/j.cell.2016.04.007
245 Vellend M. (2010). Conceptual synthesis in community ecology. The Quarterly review of biology, 85(2), 183–206. https://doi.org/10.1086/652373
246 Veluchamy, S., Hind, S. R., Dunham, D. M., Martin, G. B., & Panthee, D. R. (2014). Natural variation for responsiveness to flg22, flgII-28, and csp22 and Pseudomonas syringae pv. tomato in heirloom tomatoes. PloS one, 9(9), e106119. https://doi.org/10.1371/journal.pone.0106119
247 Vetter, M., Karasov, T. L., & Bergelson, J. (2016). Differentiation between MAMP Triggered Defenses in Arabidopsis thaliana. PLoS genetics, 12(6), e1006068. https://doi.org/10.1371/journal.pgen.1006068
248 Vogel, C., Bodenhausen, N., Gruissem, W., & Vorholt, J. A. (2016). The Arabidopsis leaf transcriptome reveals distinct but also overlapping responses to colonization by phyllosphere commensals and pathogen infection with impact on plant health. The New phytologist, 212(1), 192–207. https://doi.org/10.1111/nph.14036
249 Vogel, C.M., Potthoff, D.B., Schäfer, M. et al. Protective role of the Arabidopsis leaf microbiota against a bacterial pathogen. Nat Microbiol 6, 1537–1548 (2021). https://doi.org/10.1038/s41564-021-00997-7
250 Vorburger, C., & Gouskov, A. (2011). Only helpful when required: a longevity cost of harbouring defensive symbionts. Journal of evolutionary biology, 24(7), 1611–1617. https://doi.org/10.1111/j.1420-9101.2011.02292.x
251 Wan, L., Essuman, K., Anderson, R. G., Sasaki, Y., Monteiro, F., Chung, E. H., Osborne Nishimura, E., DiAntonio, A., Milbrandt, J., Dangl, J. L., & Nishimura, M. T. (2019). TIR domains of plant immune receptors are NAD+-cleaving enzymes that promote cell death. Science (New York, N.Y.), 365(6455), 799–803. https://doi.org/10.1126/science.aax1771

252 Wang, B., Li, K., Wu, G., Xu, Z., Hou, R., Guo, B., Zhao, Y., & Liu, F. (2022). Sulforaphane, a secondary metabolite in crucifers, inhibits the oxidative stress adaptation and virulence of Xanthomonas by directly targeting OxyR. Molecular plant pathology, 23(10), 1508–1523. https://doi.org/10.1111/mpp.13245
253 Wang, J., Liu, J., Zhao, Y., Sun, M., Yu, G., Fan, J., Tian, Y., & Hu, B. (2022). OxyR contributes to virulence of Acidovorax citrulli by regulating anti-oxidative stress and expression of flagellin FliC and type IV pili PilA. Frontiers in microbiology, 13, 977281. https://doi.org/10.3389/fmicb.2022.977281
254 Wang, T., Si, M., Song, Y., Zhu, W., Gao, F., Wang, Y., Zhang, L., Zhang, W., Wei, G., Luo, Z. Q., & Shen, X. (2015). Type VI Secretion System Transports Zn2+ to Combat Multiple Stresses and Host Immunity. PLoS pathogens, 11(7), e1005020. https://doi.org/10.1371/journal.ppat.1005020
255 Wang, W., Yang, J., Zhang, J., Liu, Y. X., Tian, C., Qu, B., Gao, C., Xin, P., Cheng, S., Zhang, W., Miao, P., Li, L., Zhang, X., Chu, J., Zuo, J., Li, J., Bai, Y., Lei, X., & Zhou, J. M. (2020). An Arabidopsis Secondary Metabolite Directly Targets Expression of the Bacterial Type III Secretion System to Inhibit Bacterial Virulence. Cell host & microbe, 27(4), 601–613.e7. https://doi.org/10.1016/j.chom.2020.03.004
256 Wang, Y., Garrido-Oter, R., Wu, J. et al. Site-specific cleavage of bacterial MucD by secreted proteases mediates antibacterial resistance in Arabidopsis. Nat Commun 10, 2853 (2019). https://doi.org/10.1038/s41467-019-10793-x
257 Wang, Y., Pruitt, R. N., Nürnberger, T., & Wang, Y. (2022). Evasion of plant immunity by microbial pathogens. Nature reviews. Microbiology, 20(8), 449–464. https://doi.org/10.1038/s41579-022-00710-3
258 Wang, Y., Xu, Y., Sun, Y., Wang, H., Qi, J., Wan, B., Ye, W., Lin, Y., Shao, Y., Dong, S., Tyler, B. M., & Wang, Y. (2018). Leucine-rich repeat receptor-like gene screen reveals that Nicotiana RXEG1 regulates glycoside hydrolase 12 MAMP detection. Nature communications, 9(1), 594. https://doi.org/10.1038/s41467-018-03010-8
259 Wei, H. L., & Collmer, A. (2018). Defining essential processes in plant pathogenesis with Pseudomonas syringae pv. tomato DC3000 disarmed polymutants and a subset of key type III effectors. Molecular plant pathology, 19(7), 1779–1794. https://doi.org/10.1111/mpp.12655
260 Wei, Y., Balaceanu, A., Rufian, J.S. et al. An immune receptor complex evolved in soybean to perceive a polymorphic bacterial flagellin. Nat Commun 11, 3763 (2020). https://doi.org/10.1038/s41467-020-17573-y
261 Wei, Y., Caceres-Moreno, C., Jimenez-Gongora, T., Wang, K., Sang, Y., Lozano-Duran, R., & Macho, A. P. (2018). The Ralstonia solanacearum csp22 peptide, but not flagellin-derived peptides, is perceived by plants from the Solanaceae family. Plant biotechnology journal, 16(7), 1349–1362. https://doi.org/10.1111/pbi.12874
262 Wengelnik, K., Marie, C., Russel, M., & Bonas, U. (1996). Expression and localization of HrpA1, a protein of Xanthomonas campestris pv. vesicatoria essential for pathogenicity and induction ofthe hypersensitive reaction. Journal of bacteriology, 178(4), 1061–1069. https://doi.org/10.1128/jb.178.4.1061-1069.1996
263 Westhoek, A., Clark, L. J., Culbert, M., Dalchau, N., Griffiths, M., Jorrin, B., Karunakaran, R., Ledermann, R., Tkacz, A., Webb, I., James, E. K., Poole, P. S., & Turnbull, L. A. (2021). Conditional sanctioning in a legume-Rhizobium mutualism. Proceedings of the National Academy of Sciences of the United States of America, 118(19), e2025760118. https://doi.org/10.1073/pnas.2025760118
264 Whiteley, A.T., Eaglesham, J.B., de Oliveira Mann, C.C. et al. Bacterial cGAS-like enzymes synthesize diverse nucleotide signals. Nature 567, 194–199 (2019). https://doi.org/10.1038/s41586-019-0953-5
265 Wickham, H. (2016). ggplot2: Elegant Graphics for Data Analysis. Springer-Verlag New York. Retrieved from https://ggplot2.tidyverse.org
266 Wippel, K., Tao, K., Niu, Y. et al. Host preference and invasiveness of commensal bacteria in the Lotus and Arabidopsis root microbiota. Nat Microbiol 6, 1150–1162 (2021). https://doi.org/10.1038/s41564-021-00941-9
267 Wolinska, K. W., Vannier, N., Thiergart, T., Pickel, B., Gremmen, S., Piasecka, A., Piślewska-Bednarek, M., Nakano, R. T., Belkhadir, Y., Bednarek, P., & Hacquard, S. (2021). Tryptophan

metabolism and bacterial commensals prevent fungal dysbiosis in Arabidopsis roots. Proceedings of the National Academy of Sciences of the United States of America, 118(49), e2111521118. https://doi.org/10.1073/pnas.2111521118
268 Wu T, Hu E, Xu S, Chen M, Guo P, Dai Z, Feng T, Zhou L, Tang W, Zhan L, Fu x, Liu S, Bo X, Yu G (2021). “clusterProfiler 4.0: A universal enrichment tool for interpreting omics data.” The Innovation, 2(3), 100141. doi: 10.1016/j.xinn.2021.100141
269 Xin, X. F., Nomura, K., Aung, K., Velásquez, A. C., Yao, J., Boutrot, F., Chang, J. H., Zipfel, C., & He, S. Y. (2016). Bacteria establish an aqueous living space in plants crucial for virulence. Nature, 539(7630), 524–529. https://doi.org/10.1038/nature20166
270 Xu, L., Naylor, D., Dong, Z., Simmons, T., Pierroz, G., Hixson, K. K., Kim, Y. M., Zink, E. M., Engbrecht, K. M., Wang, Y., Gao, C., DeGraaf, S., Madera, M. A., Sievert, J. A., Hollingsworth, J., Birdseye, D., Scheller, H. V., Hutmacher, R., Dahlberg, J., Jansson, C., … Coleman-Derr, D. (2018). Drought delays development of the sorghum root microbiome and enriches for monoderm bacteria. Proceedings of the National Academy of Sciences of the United States of America, 115(18), E4284–E4293. https://doi.org/10.1073/pnas.1717308115
271 Xu, Z., Takizawa, F., Casadei, E., Shibasaki, Y., Ding, Y., Sauters, T. J. C., Yu, Y., Salinas, I., & Sunyer, J. O. (2020). Specialization of mucosal immunoglobulins in pathogen control and microbiota homeostasis occurred early in vertebrate evolution. Science immunology, 5(44), eaay3254. https://doi.org/10.1126/sciimmunol.aay3254
272 Yamaguchi, Y., Huffaker, A., Bryan, A. C., Tax, F. E., & Ryan, C. A. (2010). PEPR2 is a second receptor for the Pep1 and Pep2 peptides and contributes to defense responses in Arabidopsis. The Plant cell, 22(2), 508–522. https://doi.org/10.1105/tpc.109.068874
273 Yardeni, T., Tanes, C. E., Bittinger, K., Mattei, L. M., Schaefer, P. M., Singh, L. N., Wu, G. D., Murdock, D. G., & Wallace, D. C. (2019). Host mitochondria influence gut microbiome diversity: A role for ROS. Science signaling, 12(588), eaaw3159. https://doi.org/10.1126/scisignal.aaw3159
274 Yi, S. Y., Shirasu, K., Moon, J. S., Lee, S. G., & Kwon, S. Y. (2014). The activated SA and JA signaling pathways have an influence on flg22-triggered oxidative burst and callose deposition. PloS one, 9(2), e88951. https://doi.org/10.1371/journal.pone.0088951
275 Yu, C., Wang, N., Wu, M., Tian, F., Chen, H., Yang, F., Yuan, X., Yang, C. H., & He, C. (2016). OxyR-regulated catalase CatB promotes the virulence in rice via detoxifying hydrogen peroxide in Xanthomonas oryzae pv. oryzae. BMC microbiology, 16(1), 269. https://doi.org/10.1186/s12866-016-0887-0
276 Yu, D., Song, W., Tan, E. Y. J., Liu, L., Cao, Y., Jirschitzka, J., Li, E., Logemann, E., Xu, C., Huang, S., Jia, A., Chang, X., Han, Z., Wu, B., Schulze-Lefert, P., & Chai, J. (2022). TIR domains of plant immune receptors are 2',3'-cAMP/cGMP synthetases mediating cell death. Cell, 185(13), 2370–2386.e18. https://doi.org/10.1016/j.cell.2022.04.032
277 Yu, K., Liu, Y., Tichelaar, R., Savant, N., Lagendijk, E., van Kuijk, S. J. L., Stringlis, I. A., van Dijken, A. J. H., Pieterse, C. M. J., Bakker, P. A. H. M., Haney, C. H., & Berendsen, R. L. (2019). Rhizosphere-Associated Pseudomonas Suppress Local Root Immune Responses by Gluconic Acid-Mediated Lowering of Environmental pH. Current biology : CB, 29(22), 3913–3920.e4. https://doi.org/10.1016/j.cub.2019.09.015
278 Yu, L.CH. Microbiota dysbiosis and barrier dysfunction in inflammatory bowel disease and colorectal cancers: exploring a common ground hypothesis. J Biomed Sci 25, 79 (2018). https://doi.org/10.1186/s12929-018-0483-8
279 Yu, P., He, X., Baer, M. et al. Plant flavones enrich rhizosphere Oxalobacteraceae to improve maize performance under nitrogen deprivation. Nat. Plants 7, 481–499 (2021). https://doi.org/10.1038/s41477-021-00897-y
280 Zablackis, E., Huang, J., Müller, B., Darvill, A. G., & Albersheim, P. (1995). Characterization of the cell-wall polysaccharides of Arabidopsis thaliana leaves. Plant physiology, 107(4), 1129–1138. https://doi.org/10.1104/pp.107.4.1129
281 Zeng, J., Hong, Y., Zhao, N., Liu, Q., Zhu, W., Xiao, L., Wang, W., Chen, M., Hong, S., Wu, L., Xue, Y., Wang, D., Niu, J., Drlica, K., & Zhao, X. (2022). A broadly applicable, stress-mediated bacterial death pathway regulated by the phosphotransferase system (PTS) and the cAMP-Crp cascade. Proceedings of the National Academy of Sciences of the United States of America, 119(23), e2118566119. https://doi.org/10.1073/pnas.2118566119

282 Zhao, Z., Liu, H., Wang, C. et al. Erratum to: Comparative analysis of fungal genomes reveals different plant cell wall degrading capacity in fungi. BMC Genomics 15, 6 (2014). https://doi.org/10.1186/1471-2164-15-6
283 Zhou, F., Emonet, A., Dénervaud Tendon, V., Marhavy, P., Wu, D., Lahaye, T., & Geldner, N. (2020). Co-incidence of Damage and Microbial Patterns Controls Localized Immune Responses in Roots. Cell, 180(3), 440–453.e18. https://doi.org/10.1016/j.cell.2020.01.013
284 Zipfel, C., & Oldroyd, G. E. (2017). Plant signalling in symbiosis and immunity. Nature, 543(7645), 328–336. https://doi.org/10.1038/nature22009
285 Zipfel, C., Kunze, G., Chinchilla, D., Caniard, A., Jones, J. D., Boller, T., & Felix, G. (2006). Perception of the bacterial PAMP EF-Tu by the receptor EFR restricts Agrobacterium-mediated transformation. Cell, 125(4), 749–760. https://doi.org/10.1016/j.cell.2006.03.037
286 Zipfel, C., Robatzek, S., Navarro, L., Oakeley, E. J., Jones, J. D., Felix, G., & Boller, T. (2004). Bacterial disease resistance in Arabidopsis through flagellin perception. Nature, 428(6984), 764–767. https://doi.org/10.1038/nature02485

11. ACKNOWLEDGEMENTS

Above all, I would like to thank me, myself, and I for enduring through this momentous and ‘sort of special’ scientific odyssey. I lose count of the times I have repeatedly doubted and criticized me, and every time it strikes, I do not let myself down, just picked myself up, the tubes, the pipettes, the weights, and everything in between, towards a better version of me. Truly, that it is only in the worsts of the situations when our fire shines the brightest. I would like to thank the unwavering support, tireless understanding, and unconditional love of my family: my mother Nita; my father Federico, who’s watching above; my twin sister Fevienette; my younger brother Fedencoprix; my nieces and nephew Jannah, Franchesca, Fieona, and Frylie. My words are cold and flat, and would never be enough to capture how thankful I am to have you in my life. I love you all.

I would also like to thank my friends for whom I have left home or have gone somewhere to chase their own dreams but never ceases to remember me from time to time. The MARS club: Ricky, Erwin, Jonas, Pao, Cely, Ann, Sha, Chuckie, Julius, Ronald, Efren, Pat, and Jerlie; KARAOKE buddy: Jed; The SHOMA and NFRH dormies: again Ricky, Harvey, Erickson, Mark, Josephine, KC, Aprille, Karen, Carolyn, Diana, Ferms, Gracious, Chaz, Ichie, Milben, JJ, Cindy; My IRRI PLANT-PHYSIO group: Meggy, Mel, Myrish, Che, Rency, Joie, Marj, Tita Vangie, Berta, Chillan, Vichelle, Yoichi, Abdel, Fannie, Elenita, Hannah, Geraldine, LaRue, and Ryan; INNER CIRCLE high-school friends: Bryan, Emma, Marco, Jonathan, Jocelyn, Lei, Percy, Kat, Allen, Anna, Arjel; BADMINTON SMASHERS: Ria, Vangie, Miel; my beloved teachers: Prof. Ana and Prof. Annalee; PEPSI QA/QC peeps: Jops, Babylyn, Nicole, Jackie, Carmen, Pao, Jet, Leo, Jonas, Tinnie, and Alvin.

I would like to thank my direct supervisor Prof. Dr. Kenichi Tsuda for the support and intellectual liberty to independently tread the unknowns, I really appreciate that you have treated me level-headedly and have helped me to immensely improve my science. I would

also like to thank my TAC members for their substantial suggestions that have shaped my research and have pruned me to the scientist that I am now: Prof. Dr. Paul Schulze-Lefert for also accepting my invitation as my reviewer; Prof. Dr. Günther Dohlemann for also taking the role as the chair for my thesis defense; and Dr. Stéphane Hacquard for accepting the role to take the minutes of my thesis defense and for open-heartedly adopting me in his group. I would like to thank Dr. Prof. Stanislav Kopriva for accepting my invitation as my thesis reviewer. Again, I thank you all for being the pillars of my scientific beginnings.

I would like to thank my supportive, extremely intelligent colleagues and new-found friends at MPIPZ: my officemate through and through, Joel, thanks for the food, your kindness, the 'coffee-breaks-turned-therapy-sessions', you are one of the great persons I have ever encountered! MCFITTIES: Noah, Pascal, Rigel, Ram, and Gauthier, the gym was more fun and bearable or "beerable" around you, thank you for making me a little sane, less robotic, and bringing some 'color' and 'spice' to my monotonous life. Jana and Felix, thanks for the cerebral conversations and generosity, it was a rare opportunity to meet such incredibly intelligent students and to scientifically grow alongside, I am very humbled. Yu, you are tremendously tenacious and committed, I am proud and thankful to have worked with the most diligent student I've ever known. I would like to thank the entire PSL Department and the Rooters, I have enjoyed the thought-storms and weathered with constructive criticisms. I would like to thank Dr. Stephan Wagner and Meagan Sierz, the MPIPZ Graduate School for assisting me with the processing of my papers, and for helping me with my PhD life in general. I am very thankful for our wonderful technicians: Dieter, Ana Lisa, and Diana; the greenhouse team; and the Genome Center. Without their help, this work would have crumbled. The Hacquard group: Guillaume, Qi, Ayu, Pris, Arpan, Stephanie, and Brigitte for making me feel welcomed in the group, I am ecstatic and excited to work with all of you. I would like to thank our secretaries: Jutta, Meagan, and Sabine for facilitating my requests and administrative stuffs. I would like to thank Lele, PJ, Peachy, Pam, and Gihanna, my refuge whenever my ear and tongue misses Tagalog, the "Marites sessions", from shallow to deep talks, about our shared aspirations and experiences. I would like to thank the MPIPZ administration, and the University of Cologne Graduate office for assisting me with the bureaucratic gymnastics.

Maraming salamat!

12. ERKLÄRUNG ZUR DISSERTATION

Erklärung zur Dissertation
gemäß der Promotionsordnung vom 12. März 2020

Diese Erklärung muss in der Dissertation enthalten sein.
(*This version must be included in the doctoral thesis*)

„Hiermit versichere ich an Eides statt, dass ich die vorliegende Dissertation selbstständig und ohne die Benutzung anderer als der angegebenen Hilfsmittel und Literatur angefertigt habe. Alle Stellen, die wörtlich oder sinngemäß aus veröffentlichten und nicht veröffentlichten Werken dem Wortlaut oder dem Sinn nach entnommen wurden, sind als solche kenntlich gemacht. Ich versichere an Eides statt, dass diese Dissertation noch keiner anderen Fakultät oder Universität zur Prüfung vorgelegen hat; dass sie - abgesehen von unten angegebenen Teilpublikationen und eingebundenen Artikeln und Manuskripten - noch nicht veröffentlicht worden ist sowie, dass ich eine Veröffentlichung der Dissertation vor Abschluss der Promotion nicht ohne Genehmigung des Promotionsausschusses vornehmen werde. Die Bestimmungen dieser Ordnung sind mir bekannt. Darüber hinaus erkläre ich hiermit, dass ich die Ordnung zur Sicherung guter wissenschaftlicher Praxis und zum Umgang mit wissenschaftlichem Fehlverhalten der Universität zu Köln gelesen und sie bei der Durchführung der Dissertation zugrundeliegenden Arbeiten und der schriftlich verfassten Dissertation beachtet habe und verpflichte mich hiermit, die dort genannten Vorgaben bei allen wissenschaftlichen Tätigkeiten zu beachten und umzusetzen. Ich versichere, dass die eingereichte elektronische Fassung der eingereichten Druckfassung vollständig entspricht."

Teilpublikationen:

2023Apr13, Frederickson D. Entila

Datum, Name und Unterschrift

Erklärung zum Gesuch um Zulassung zur Promotion
gemäß der Promotionsordnung vom 12. März 2020

1. Zugänglichkeit von Daten und Materialien

Die Dissertation beinhaltet die Gewinnung von Primärdaten oder die Analyse solcher Daten oder die Reproduzierbarkeit der in der Dissertation dargestellten Ergebnisse setzt die Verfügbarkeit von Datenanalysen, Versuchsprotokollen oder Probenmaterial voraus.

☐ Trifft nicht zu
☒ Trifft zu.
In der Dissertation ist dargelegt wie diese Daten und Materialien gesichert und zugänglich sind (entsprechend den Vorgaben des Fachgebiets beziehungsweise der Betreuerin oder des Betreuers).

2. Frühere Promotionsverfahren

Ich habe bereits einen Doktortitel erworben oder ehrenhalber verliehen bekommen.
Oder: Für mich ist an einer anderen Fakultät oder Universität ein Promotionsverfahren eröffnet worden, aber noch nicht abgeschlossen.
Oder: Ich bin in einem Promotionsverfahren gescheitert.
☒ Trifft nicht zu
☐ Zutreffend
Erläuterung:

3. Straftat

Ich bin nicht zu einer vorsätzlichen Straftat verurteilt worden, bei deren Vorbereitung oder Begehung der Status einer Doktorandin oder eines Doktoranden missbraucht wurde.

Ich versichere, alle Angaben wahrheitsgemäß gemacht zu haben.

2023Apr13	Frederickson D. Entila	
Datum	Name	Unterschrift

01-2021

Declaration for the doctoral thesis (dissertation)

according to the doctoral regulations published 12th March 2020

Non-official English translation of the "Erklärung zur Dissertation"
(*The German version must be included in the doctoral thesis*)

"I hereby declare that I have completed the present dissertation independently and without the use of any aids or literature other than those referred to. All passages that have been taken, either literally or in sense, from published and unpublished works, are marked as such. I declare that this dissertation has not been submitted to any other faculty or university; that - apart from the partial publications and included articles and manuscripts listed below - it has not yet been published, and that I will not publish the dissertation before completing my doctorate without the permission of the PhD Committee. I am aware of the terms of the doctoral regulations. In addition, I hereby declare that I am aware of the "Regulations for Safeguarding Good Scientific Practice and Dealing with Scientific Misconduct" of the University of Cologne, and that I have observed them during the work on the thesis project and the written doctoral thesis. I hereby commit myself to observe and implement the guidelines mentioned there in all scientific activities. I assure that the submitted electronic version is identical to the submitted printed version".

Partial publications of the thesis:

2023Apr13, Frederickson D. Entila
Date, name, and signature

Declaration on the application for admission to the doctoral examinations
according to the doctoral regulations published 12th March 2020

1. Accessibility of data and materials

The dissertation involves the acquisition of primary data or the analysis of such data or the reproducibility of the results presented in the dissertation requires the availability of data analyses, experimental protocols or sample material.

☐ not applicable

☒ applicable
I have described in the dissertation how these data and materials are secured and accessible (according to the specifications of the subject area or supervisor).

2. Previous doctoral examinations

I have already obtained a doctorate or been awarded an honorary doctoral degree.
Or: A doctoral examination has been opened at another faculty or university, but not yet completed.
Or: I have failed in a doctoral examination.

☒ not applicable

☐ applicable
explanatory note:

3. Criminal offense

I have not been convicted of a deliberate criminal offence in the preparation or commission of which the status as a doctoral candidate was abused.

I declare that all information provided is truthful.

2023Apr13, Frederickson D. Entila

Date Name Signature